Aircraft and Rotorcraft Pilot Couplings – Tools and Techniques for Alleviation and Detection

ACPO-GA-2010-266073

Deliverable No. D5.2
Simulation Guidelines for A/RPC Prediction

Contractual delivery date:
[04/2012]

Actual delivery date:
[10/2012]

Partner responsible for the Deliverable: TUD

Author(s):
Marilena D. Pavel, Deniz Yilmaz (TUD),
Michael Jones, Linghai Lu, Michael Jump (UoL),
Binh Dang-Vu (ONERA),
Pierangelo Masarati, Giuseppe Quaranta (POLIMI),
Hafid Smaili (NLR),
Larisa Zaichik (TsAGI)

Dissemination level		
PU	Public	X
PP	Restricted to other programme participants (including the Commission Services)	
RE	Restricted to a group specified by the consortium (including the Commission Services)	
CO	Confidential, only for members of the consortium (including the Commission Services)	

Document Information Table

Grant agreement no.	ACPO-GA-2010-266073
Project full title	ARISTOTEL – Aircraft and Rotorcraft Pilot Couplings – Tools and Techniques for Alleviation and Detection
Deliverable number	D5.2
Deliverable title	Simulation guidelines for A/RPC prediction
Nature	R[1]
Dissemination level	PU[2]
Version	1.0
Work package number	WP5
Work package leader	NLR
Partner responsible for Deliverable	TUD
Reviewer(s)	All partners

The research leading to these results has received funding from the European Community's Seventh Framework Programme (FP7/2007-2013) under grant agreement n° 266073.
The author is solely responsible for its content, it does not represent the opinion of the European Community and the Community is not responsible for any use that might be made of data appearing therein.

[1] **R**=Report, **P**=Prototype, **D**=Demonstrator, **O**=Other

[2] **PU**=Public, **PP**=Restricted to other programme participants (including the Commission Services), **RE**=Restricted to a group specified by the consortium (including the Commission Services), **CO**=Confidential, only for members of the consortium (including the Commission Services)

Revision Table

Version	Date	Modified Page/Section	Author	Comments
1.0	17-10-2013		MD Pavel	Initial issue
2.0	4-11-2013		See author lists	

Executive Summary

Flight simulators are extensively used in engineering design, development and flight training, and are an essential tool in the conceive-design-build and qualification processes of fixed- and rotary-wing aircraft. In this report, ARISTOTEL key findings and practical simulator applications during the project test campaigns are summarized for fixed-and rotary-wing flight simulators. First, the simulator settings are discussed according to the major simulator components, i.e. the visual, the motion and the control loading systems. Then simulator guidelines related to simulator settings and tasks for exposing A/RPCs are provided. The report also provides some pilot training protocols for unmasking A/RPC in the simulator.

Table of Contents

1 Introduction

One of the main objectives of the ARISTOTEL project is to provide simulator guidelines to engineers whose tasks it is to unmask A/RPCs during trials performed on flight simulators. This deliverable is issued to provide those guidelines. It also contains ideas on protocols for pilots in order to train them to avoid A/RPC events occurring in-flight or, when the A/RPC occurred, to teach the pilots to deal with them. In this sense, the present work is written from two points of view: one point of view is of the engineer that has to unmask A/RPCs in the simulator, the other point of view is of the pilot willing to avoid such instabilities or, if they happen, to tame these events. The simulator guidelines are related first to the settings of the major "hardware" components of a simulator (i.e. motion system, image generation system, control loading system). The guidelines are then related to the tasks that can be used to trigger such events. The report makes a distinction between the settings for unmasking the rigid body A/RPCs and aeroelastic RPCs. Also, guidelines related to biodynamic testing are included in this report. The document does not include (except for the fixed wing aircraft) the other major component of the simulator, i.e. the "software" mathematical model of the simulator as this part of the simulator was extensively investigated in ARISTOTEL'S deliverables of work package 2 and 3.

2 Simulator Guidelines for Rotary Wing Aircraft

2.1 Simulator Settings for rigid body RPC

2.1.1 Motion filters

The general motion base motion algorithm architectures for both the SIMONA Research Simulator (SRS) and HeliFlightR Simulator (HFR) research simulators used during the project's rigid body test campaigns are shown in Figure 1.

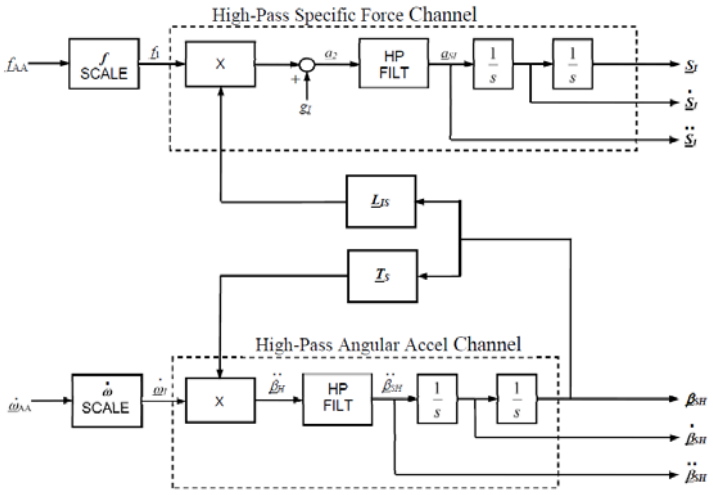

(a) Motion filter block diagram - HFR

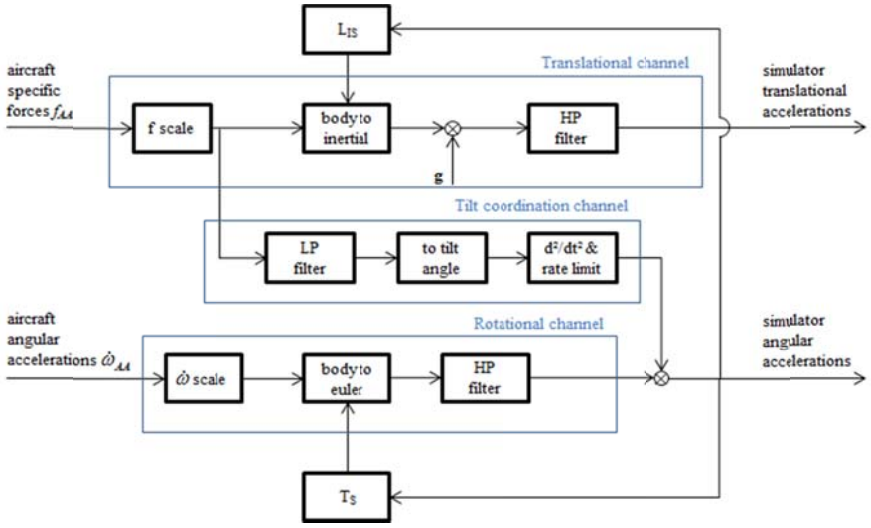

(b) Motion filter block diagram - SRS

Figure 1. Motion filter algorithms of HFR (a) and SRS(b).

It can be seen from Figure 1 that the motion filter architecture both simulators is relatively similar. Details of the simulator algorithms can be found in Refs 3 and 4. Briefly, HFR uses a third order high-pass filter for all motion channels, whereas SRS uses a third order filter only for the heave axis and utilizes a second order filter for all of the other channels. Another difference is the tilt coordination in the SRS algorithm. Tilt coordination is used to include effects of translation commands in rotational axis in order to achieve coordinated motion base response. Although it is not mandatory, benefit of applying the tilt coordination is smoother motion response during multi-axis aggressive tasks because the tilt coordination provides cross-coupled motion cues, unlike individual channel responses. However, tilt coordination uses a low pass filter, which increases the phase distortion of the resultant response around mid-frequencies. Phase distortion physically can be interpreted as the lag of the motion base in certain range of frequencies. Considering the physical specifications of the simulator motion bases, pilots commented that the resultant motion cues in both simulators were comparable. The availability of longer leg strokes for SRS provides a larger possible motion envelope, and hydraulic actuators provide a powerful motion command when compared to electric servos of HFR motion base due to the heavier weight of the SRS simulator components on the motion platform (e.g. cabinet, projection screen). The overall comparisons of motion base capabilities were presented in ref 4.

The first project rotary-wing test campaign was the first time that the SRS simulator had been used in rotorcraft mode. Thus, the choice of motion base parameters was made giving consideration to the safety of the motion base (and the simulator occupants) by using actuator position and rate limits obtained from previous fixed-wing aggressive tasks. During the first test campaign, a common set of motion base filter settings was used for all flying tasks in SRS. These settings are listed in Table 1.

All Tasks	Gain (-)	2nd order break freq (rad/s)	Damping Ratio (-)	1st order break freq (rad/s)
Roll	0.5	-	-	2.0
Pitch	0.6			1.0
Yaw	0.7			3.0
Surge	0.6	2.0	1.0	-
Sway	0.5	2.0		
Heave	0.5	2.5		0.2

Table 1. SRS motion filter settings during 1st test campaign

A first order filter was used in attitude channels of the SRS motion base, whereas translations were second order for longitudinal and lateral axes, and a third order filter was utilized for heave axis (see Table 1). A first order

filter for attitude commands was theoretically sufficient for cueing rotational acceleration commands, however some flying tasks with aggressive and coupled control (e.g. the roll-step manoeuvre) lead to noticeable simulator drifts, which drives the simulator into positions such that the new orientation is further away from the neutral position of the simulator.. As a result, washout algorithms could cause such a position drift if the high pass filters are low order Thus, it was decided to increase the filter order to second order in the expense of more phase distortion for the second test campaign.

After the first test campaign, the aim was to match the response of both motion bases as closely as possible and to tune them for each task to be undertaken. However, several factors limited the overall success of the matching process. First, both motion systems have very different physical specifications in terms of size and motion drive power sources (e.g. hydraulic and electric). This difference makes the comparisons scaled per simulators and matching chosen parameters could lead to mismatching other aspects (e.g. angular rate response matching could result in base orientation mismatch). Furthermore, the varied simulator specifications also resulted in different motion envelopes, actuator speeds and acceleration limits, all of which shaped the operational envelope of each simulator. Due to the nature of RPC scenarios, these limiting values were expected to be reached, unlike a more representative operational task. Second, the differences between software architectures and settings caused difficulties while matching the simulators. The SRS software structure is comprised of a set of in-house developed real-time codes. These provide open access to the filter shaping modules and individual adjustment for any parameter of the motion system is possible. However, HFR uses a semi-closed software structure with only selectable adaptive filters. Finally, there was not enough time for a full spectrum simulator matching process between simulator trials, due to the usage of simulators for other projects during that period.

During the second rigid body test campaign, precision hover and roll step tasks were flown and each simulator were adjusted with different motion filter settings per flying task. Task-wise motion filter settings of HFR and SRS are shown in Figure 2 and Figure 3 respectively, with highlighted high-pass filter block in the motion cue algorithm structure of each simulator.

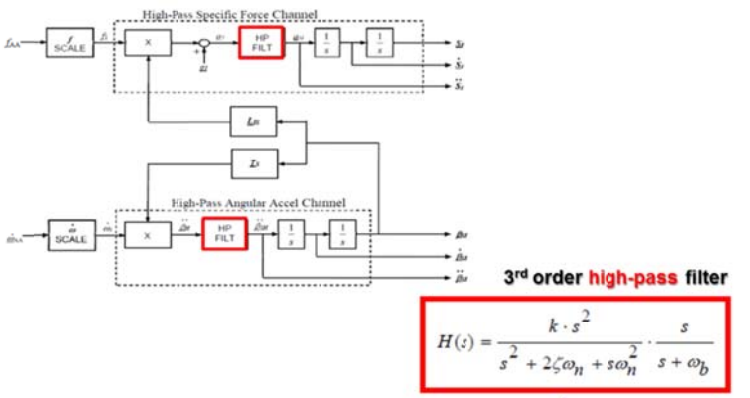

3rd order high-pass filter

$$H(s) = \frac{k \cdot s^2}{s^2 + 2\zeta\omega_n + s\omega_n^2} \cdot \frac{s}{s + \omega_b}$$

Hover	Gain (-)	High-Pass Frequency (rad/s)	Damping Ratio (-)	Break Frequency (rad/s)
Roll	0.3	0.4	0.9	0.1
Pitch	0.3	0.45		
Yaw	0.2	0.5		
Surge	0.1	2		
Sway	0.1	2		
Heave	0.1	2		

Roll Step	Gain (-)	High-Pass Frequency (rad/s)	Damping Ratio (-)	Break Frequency (rad/s)
Roll	0.2	1.4	0.9	0.15
Pitch	0.2	1.4		0.1
Yaw	0.2	1.4		
Surge	0.1	2		
Sway	0.1	2		
Heave	0.1	2		

Figure 2. Motion filter settings of HFR during2nd test campaign

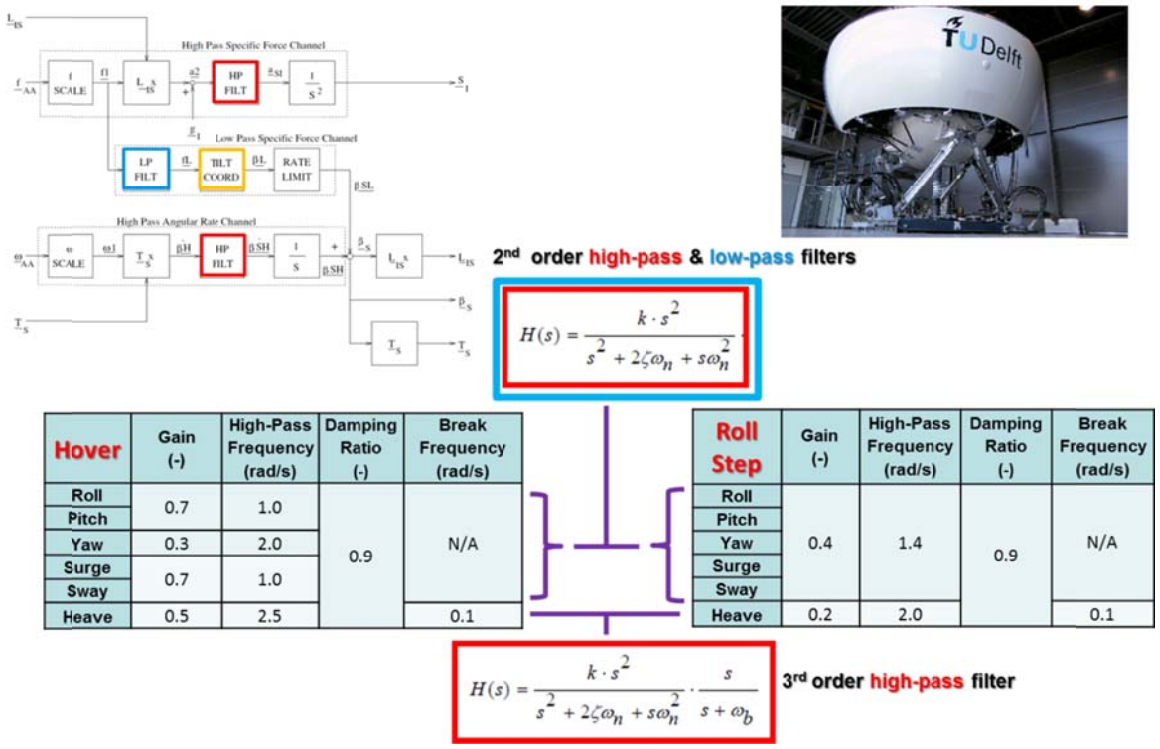

Hover	Gain (-)	High-Pass Frequency (rad/s)	Damping Ratio (-)	Break Frequency (rad/s)
Roll	0.7	1.0	0.9	N/A
Pitch				
Yaw	0.3	2.0		
Surge	0.7	1.0		
Sway				
Heave	0.5	2.5		0.1

Roll Step	Gain (-)	High-Pass Frequency (rad/s)	Damping Ratio (-)	Break Frequency (rad/s)
Roll	0.4	1.4	0.9	N/A
Pitch				
Yaw				
Surge				
Sway				
Heave	0.2	2.0		0.1

Figure 3. Motion filter settings of SRS during2nd test campaign

It can be seen from Figure 2 and Figure 3 that SRS was utilized with higher filter gains than HFR for attitude channels, with higher filter pass frequencies, due to its second order structure. The benefit of this is less motion phase distortion with a higher risk of drift. Filter gains and break frequencies suggest that HFR and SRS motion filter inputs are in different formats (SRS uses specific forces whereas HFR 'could' be using accelerations). Despite the matching efforts, the source of noticeable difference between filter values was not satisfactorily identified due to limited time. However, each simulator was efficiently functional for both test campaigns within their own limitations and they perfectly completed both test campaigns without any severe motion problems.

Figure 4 shows the comparison of motion cue ratings for two common tasks (Precision Hover and Roll Step tasks) of 1st and 2nd Rigid Body Test Campaigns (RBTC) in SRS and HFR.

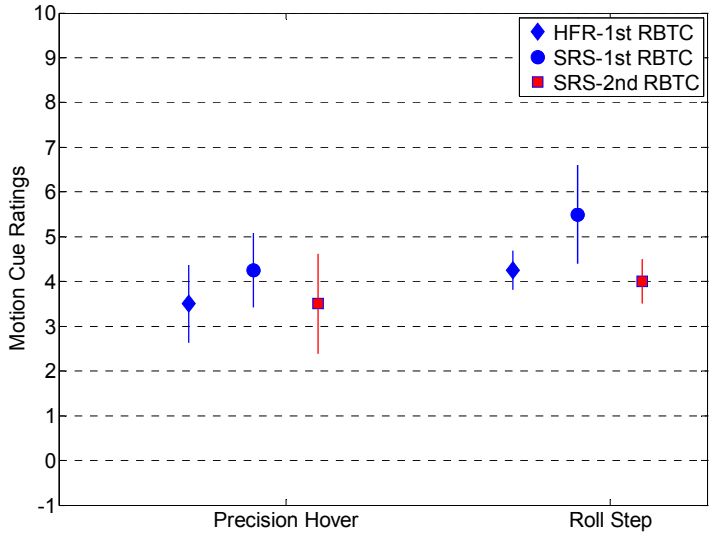

Figure 4. Motion cue ratings (mean and standard deviation bars) of Precision Hover and Roll Step tasks in HFR and SRS for 1st and 2nd Rigid Body Test Campaigns

It can be seen from Figure 4 that 2nd test campaign resulted in better motion cue ratings in SRS when compared to 1st test campaign, which were also supported by pilot comments as well. Using task-dependent motion filter settings in the 2nd RBTC has improved the motion cue capabilities of SRS with more realistic motion behaviour (according to provided Motion Cue ratings). However, there are two points to consider while interpreting Figure 4. First, the Roll Step task in the 1st RBTC in SRS was not the same as the one used in 2nd test campaign. Despite, required control and vehicle response aggressiveness were similar, as commented by the participated pilots. Second, not all pilots were participated in both simulation tasks. For example, Pilot A did not complete Precision Hover task in SRS during the first RBTC and pilot F only participated in the 2nd RBTC. Nevertheless, the means and standard deviations in Figure 4 could be used to observe the general trend of motion cue ratings deviation. Another observation from Figure 4 is the similarity of motion cue ratings between simulators. With task dependent motion filter settings of SRS in the 2nd RBTC, during which HFR used almost identical setting of the 1st RBTC with fine-tuning adjustments in HFR filter parameters, both simulators showed close motion cue ratings for both tasks. This indicates that both simulators provided similar motion cues although matching of the simulator bases was not completely accomplished.

2.1.2 Visual systems

Detailed specifications of the visual systems for both the SRS and HFR simulators are reported in Deliverable 4.6 [ref. 3]. The main difference between simulator visual systems is the field of view (FoV) capabilities of the projection screens, as shown in Figure 5.

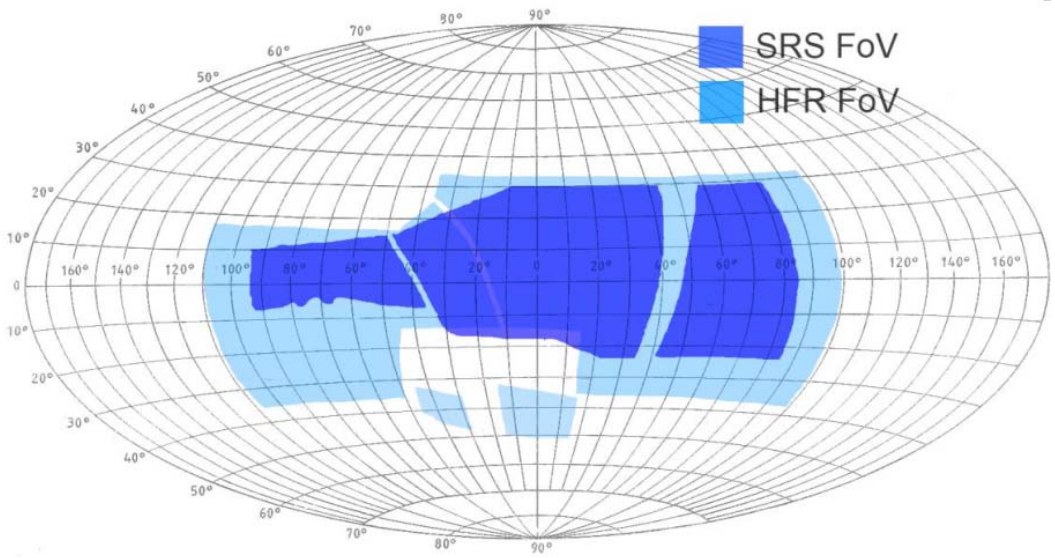

Figure 5. FoV comparison of HFR and SRS simulators

Although the difference between simulator FoVs has been discussed previously in several deliverables (e.g. Refs. 3and 4), a summary of this discussion in relation to the smaller FoV in SRS is given below:

- It leads to lower Usable Cue Environment (UCE) ratings, especially for tasks that require close ground reference cues;
- It generally resulted in worse Handling Qualities Ratings (HQRs) because pilots had difficulties in detecting the adequate and desired boundaries defined for the ADS-33 tasks;
- It generally lead to more relaxed pilot controls, which resulted in more masked RPC tendencies.

However, during the second test campaign, modifications to the task design helped to reduce the effect of visual difference between simulator setups and more consistent pilot ratings were achieved (see section on Task Guidelines).

During the first test campaign, simulators used different visual environment databases to model the same ADS-33 tasks, as illustrated in Figure 6.

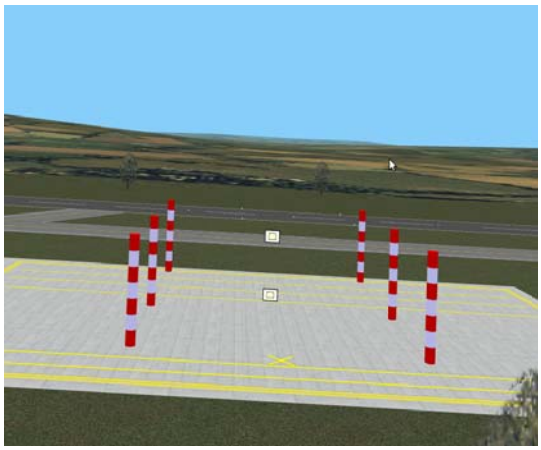

(a) SRS

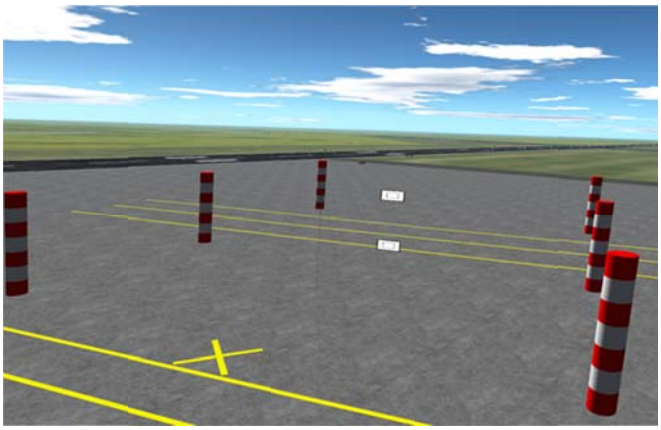

(a) HFR

Figure 6. Vertical manoeuvre visual setup in SRS (a) and HFR (b)

Although it was reported in Deliverable 4.6 that the visual differences had minor effects on the pilot's perception of the task, the second test campaign benefited from using exact the same visual database from HFR in SRS. Thus, the pilots flew the same tasks (Precision Hover and Roll Step) using exactly the same course dimensions and visual environment. This matching of the simulator outside world visual environment was implemented in order to reduce as many sources of experimental difference as possible in order to be able to compare the final effects of physical variations between the two simulators.

The option of adding a 'chin window' display to SRS was discussed. The idea here was to provide better ground texture visualisation and hence the possibility of improved visual perception during low-level manoeuvres in SRS. This was to be achieved by replacing the mid-console with display monitors. However, due to the limited time for hardware and software preparation to accomplish this adaptation, it could not be implemented.

2.1.3 Flight Control System settings

Both HFR and SRS simulators include different control loading systems, which made it difficult to match between simulators. However, the primary settings are similar and final configurations were achieved according to Bo 105 feel characteristics, as discussed in Deliverable 4.6.

During the second test campaign, the cyclic settings were varied in order to investigate the effect of this variation when trying to expose RPCs in a simulator trial. The variation of the parameters is shown in Figure 7.

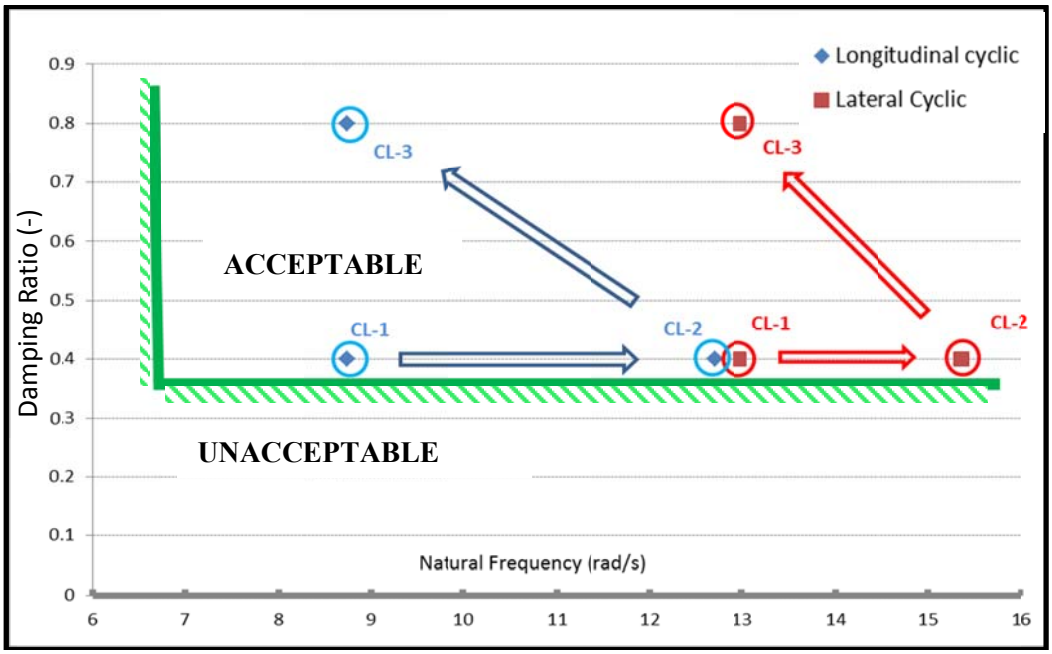

Figure 7. Variation of control loading system parameters in SRS.

It was concluded in Deliverable 4.8 that the ultimate effect of varied cyclic loading settings depends on the pilot control strategy and the task to be flown in the simulator. Pilots showed different tendencies when subjected to varied control loading settings in the presence and absence of motion as well, as illustrated in Figure 8.

N-PIOR letters

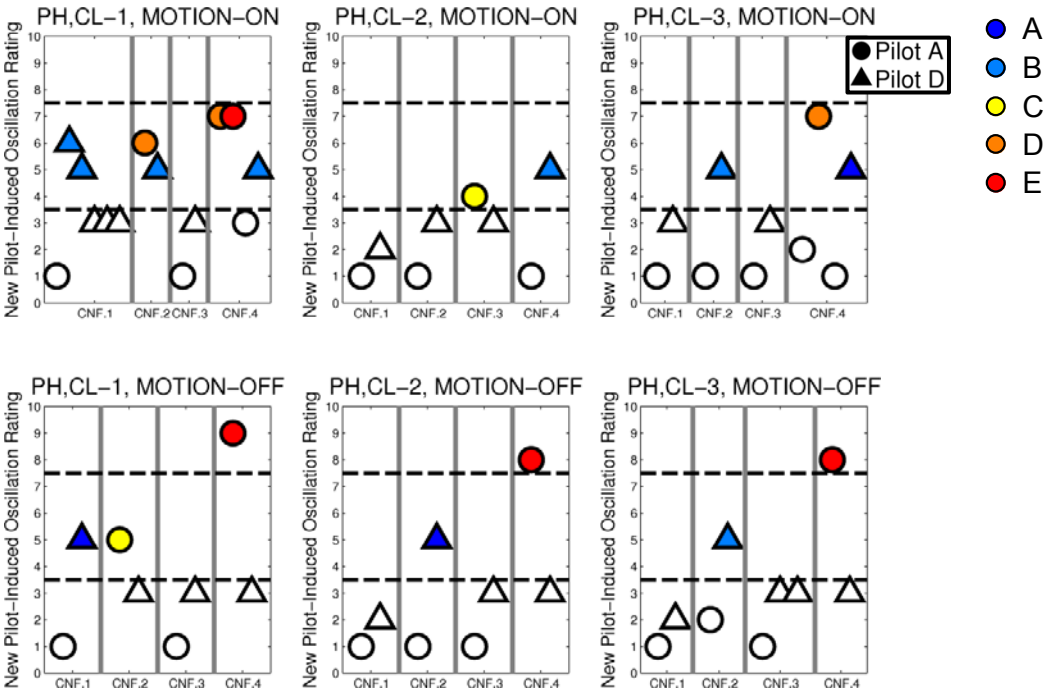

Figure 8. New Pilot-Induced oscillations ratings for various control loading settings, with and without motion during hover pole location = 20 ft.

Although there are not enough data to form definitive conclusions, it can be summarized that Pilot A favoured more resistant (higher natural frequency) and more damped (higher damping ratio) control loading settings, especially for motion on configurations, see Figure 8. In addition, he favoured motion on cases over motion off cases, regardless of the control loading settings. This suggests that for pilot A, motion cues played a supportive role for the Precision Hover PH task configuration, and secondary effects were due to varied control loading settings. Pilot D, however, preferred motion off configurations as his preference was reflected by his PIO ratings. Moreover, he did not show noticeable differences between various control loading settings. This implies that Pilot D responded dominantly to the visual cues, and motionless configurations lead him better to compensate for PIO occurrences.

Similar results were obtained for the Roll Step manoeuvre and these results are discussed in Deliverable 4.8. Finally, it can be concluded that the control loading settings have 'subjective' effects on RPC test campaigns depending on the task and the participating pilot's control strategy.

2.2 Simulator settings for Rotorcraft Aero-elastic Test Campaigns

2.2.1 Motion filters

This experiment was conducted within the UoL's HELIFLIGHT-I simulator shown in Figure 9.

Figure 9 External and internal views of HELIFLIGHT-I research simulator at the UoL

The maximum values of displacement, velocity, and acceleration in this motion system for each degree of freedom respectively are shown in the Table below.

Table 2 HELIFLIGHT-I Simulator Motion System Envelope

Axis	Displacement	Velocity	Acceleration
Surge	±0.465 [m]	±0.7 [m/s]	±0.6 [g]
Sway	±0.430 [m]	±0.7 [m/s]	±0.6 [g]
Heave	±0.250 [m]	±0.6 [m/s]	±0.6 [g]
Roll	±28 [°]	±40 [°/s]	Not specified
Pitch	-32 [°]/+34 [°]	±40 [°/s]	Not specified
Yaw	±44 [°]	±60 [°/s]	Not specified

There are eight motion digital filters (filters 0-7) implemented in the HELIFLIGHT-I Simulator (Maxcue 610-450) motion drive algorithm. The inputs to each filter may be connected to any one of six inputs to the motion drive algorithm (Host data latches 0-5) and the outputs may be connected to any one of the motion platform degrees-of-freedom (Kinematics inputs 0-5). The filters implemented in the HELIFILIGHT-I Simulator motion drive algorithm use the classical third-order washout filters of the form as shown above and the related values are shown in Table 3.

Table 3 Transfer function coefficients for the 3rd-order high-pass filters

Filter	Order	K	ζ	ω_n	ω_b
0	3HP	1.0	1.0	1.7	1.7
1	3HP	1.0	1.0	1.7	1.7
2	3HP	1.0	1.0	3.0	3.0
3	3HP	1.0	0.79	1.58	2.5
4	3HP	1.0	0.79	1.58	2.5
5	3HP	1.0	0.707	1.414	2.0
6	3LP	2.0	1.0	2.0	2.0
7	3LP	2.0	1.0	2.0	2.0

2.2.2 Visual systems

In the HELIFLIGHT-I simulator, three LCD monitor displays are collimated (Figure 10) to focus the displayed image at optical infinity giving enhanced depth perception, which is particularly important for hovering and low speed flight [96]. The displays provide a 135 (± 67.5) horizontal field-of-view by 40 deg vertical field-of-view. The vertical field-of-view is extended to 60 deg by using two flat-screen 'chin-window' displays in the cockpit foot-well. The three main displays have a resolution of 1024 x 768 pixels and a refresh rate of 60 Hz.

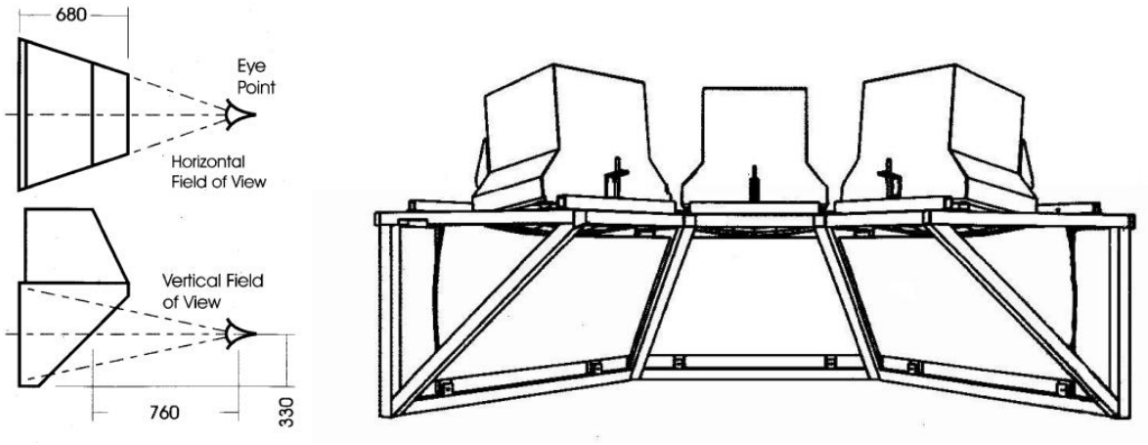

Figure 10 Collimated display system in the HELIFLIGHT-I simulator

The comparison of the outside-world field-of-view for the HELIFLIGHT-I and HELIFLIGHT-R simulators is shown in Figure 11.

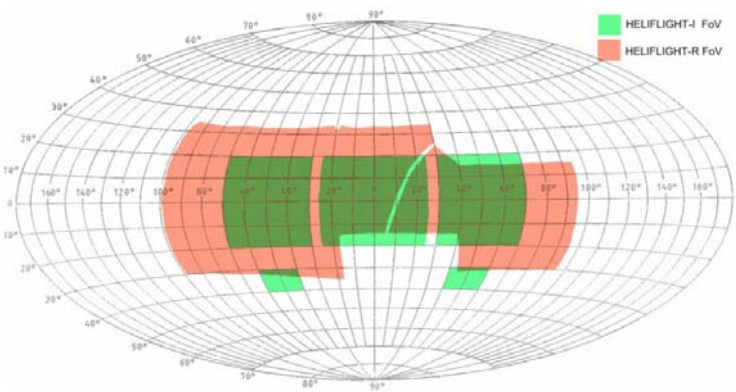

Figure 11 Comparison of field-of-view from HELIFLIGHT-I and HELIFLIGHT-R (left-hand seat) simulators

2.2.3 Flight Control System settings

A simple SCAS has been implemented on the longitudinal, lateral, and yaw control channels of the aircraft simulation model to improve its stability. The SCAS structure used in the simulation has been shown in Figure 12.

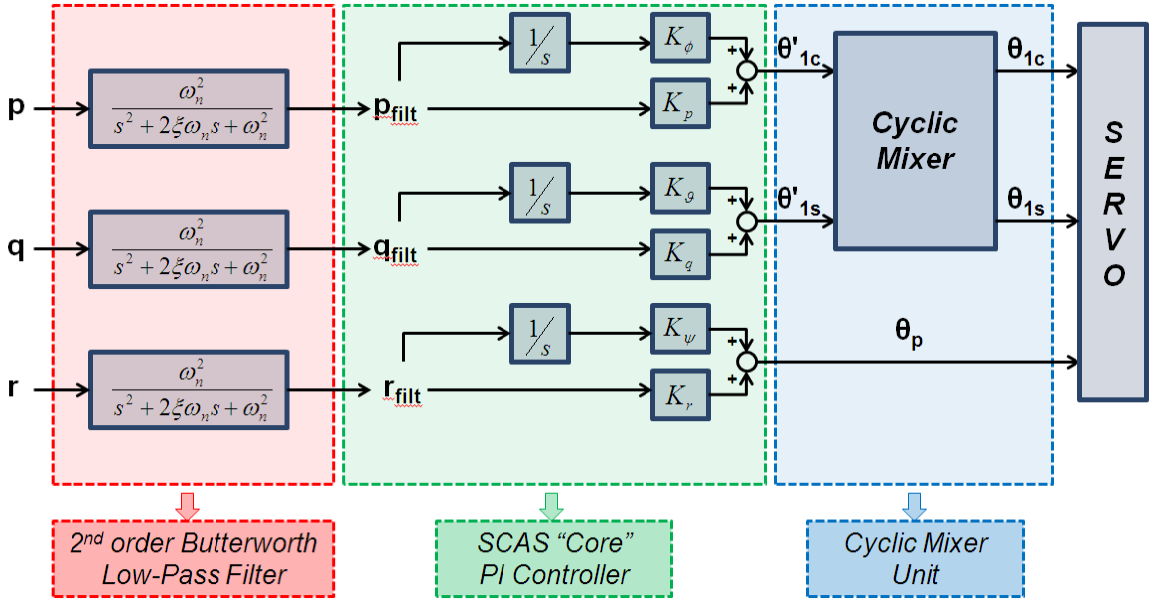

Figure 12 SCAS structure used in the experiments to improve aircraft model stability

As shown in Figure 13, the simple SCAS developed provides direct feedback between the angular rates *p*, *q*, *r* at the helicopter CG and the servo-actuator demand signals. It includes: 3 low-pass Butterworth filters, 3 proportional-integral (PI) controllers, and 1 cyclic mixing unit. The cut-off frequency of the second-order low-pass Butterworth filters is 10 Hz. Filters have been introduced to account for the dynamics of the sensors and to remove high frequency signals related to noise or external disturbances. The SCAS gains have been designed to place the flight mechanics roots inside the Level 1 boundaries. The cyclic mixing unit has been introduced to account for the swashplate phase angle effect. Moreover, the SCAS gains are not scheduled with the flight speed. The values have been selected to obtain adequate handling qualities within the complete flight envelope from hover to the maximum flight speed.

2.2.4 Real-Time Implementation of Aeroelastic Model in HELIFLIGHT-I Simulator

The related experimental set-up for the aeroelastic model to shake the pilot in the simulator is illustrated in Figure 14.

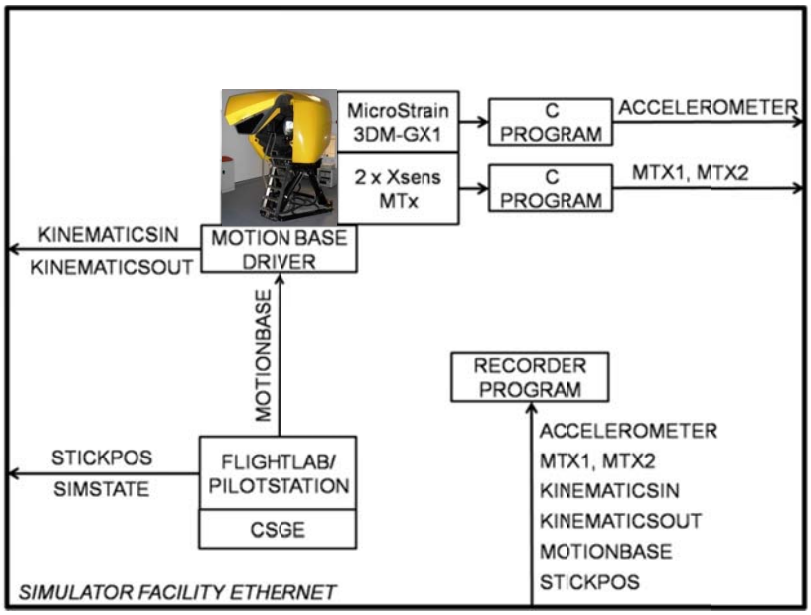

Figure 14 Schematic of biodynamic test campaign set-up

The main elements illustrated in the Figure above are described in more detail in the following Sections.

The motion base of Figure 14 is driven by proprietary software (MB-MOVE) provided by Motionbase (now part of QinetiQ). The communication process between the FLIGHTLAB flight-physics modelling software and the motion base hardware is via an is achieved using a utility (in FLIGHTLAB) that enables data blocks to be written to and read from models and enables the broadcasting of these data across a network ('flcomms'). In fact, all components shown in Figure 14 communicate with each other through this utility. A new version of this software was compiled that had the following additions made to it:

- Read in the current state of the 'model' being used to drive the motion base e.g. 'Run', 'Pause', 'Reset' etc. These states were used not only to stop/start the excitation demand being applied to the simulator motion base but also to trigger the data recording and file writing process.
- Broadcast the platform motion and actuator servo demands. These were used to validate a model of the motion base described later in this Section.

The motion base driver software in Figure 14 requires six data items as input. These are termed the 'Specific Forces' which are: 1) three linear acceleration components (surge (fore-aft), sway (left-right) and heave (up-down)) and 2) three rotational rates (pitch, roll and yaw). For the 2DOF model implemented here, the vertical acceleration that would be felt by the pilot and that is transmitted to the simulator motion system. In order to provide these to the motion base driver software, which was 'listening' on the network for a specific data block ('MOTIONBASE') containing these data, a dummy FLIGHTLAB model was created. In simple terms, this model read in the required excitation demand from a text file and then wrote it out again to the MOTIONBASE data block which was then broadcast across the simulation facility network.

Whilst the motion base modelling provided the required confidence to proceed with the testing, there was still some need for caution. The motion system contains a Motionbase proprietary safety system that is intended to protect the base from inadvertent damage. No information is available for this 'adaptive filtering' and hence could not be included in the motion base model. Whilst its exclusion from the modelling process should only have led to the conservative predictions, the actual testing was approached such that any risk to hardware or personnel was minimised as follows:

- All excitations were applied to the pod with no occupant prior to the test campaigns.
- Excitations in any given axis/combinations of axis were always applied with the lowest amplitude first.

In order to measure the actual excitation being experienced by the pod occupant, a MicroStrain® 3DM-GX1® motion sensor was procured by UoL. The sensor was mounted as shown in Figure 15 on the simulator motion base frame.

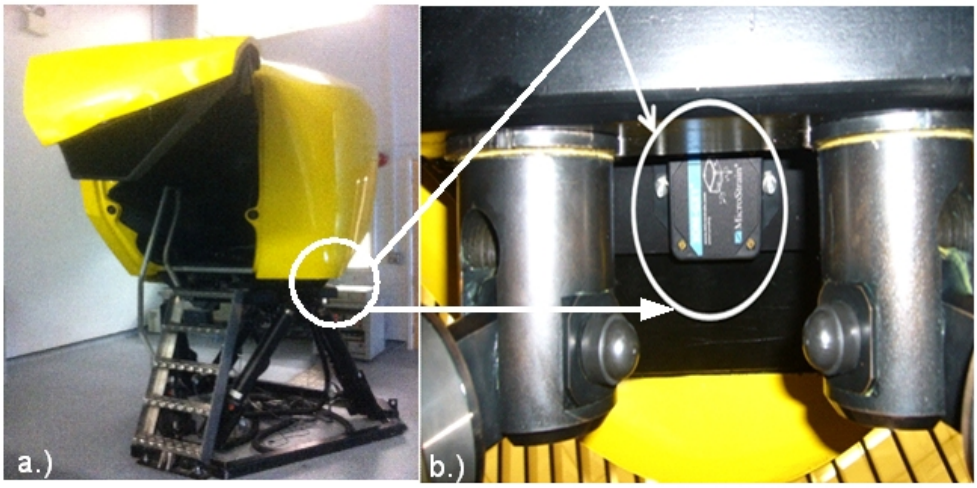

Figure 15 MicroStrain 3DM-GX1® motion sensor mounting location

Figure 15*a* indicates the sensor location which is behind, below and set back from the pilot seat in the pod. The sensor unit was bolted to a 5mm steel plate which was then fastened to the motion base using existing bolts that secure the simulator pod to the motion base frame. Figure 15b shows the 3DM-GX1® unit mounted in place. It shows the view 'looking up' from this was considered to be the most 'rigid' location that was the also the most accessible for mounting purposes.

In order that the 3DM-GX1® could be of use to the aeroelastic test, a specific program was written to request that the device output measured linear acceleration, rotational rate and angular measurement data (1 per axis so 9 data values in total). These data were then broadcast in a data block across the facility network ('ACCELEROMETER').

The requirements for the testing specified that both control inceptor and occupant arm positions be recorded for any given excitation. Because the excitation was being passed through a FLIGHTLAB model (albeit a 'dummy' one), then stick positions were automatically generated during a real-time run. These data were simply added to a data block and broadcast across the simulator network ('STICKPOS'). In addition, limb positions (wrist and above the elbow) were measured using two Xsens MTx motion sensors procured by POLIMI. The two MTx sensors were secured to the occupant using elastic fasteners, similar to those in use with the medical profession. Once again, a bespoke program was written (by POLIMI) to interrogate these devices for motion data, to write these data to data blocks and to broadcast these blocks across the simulator network ('MTX1', 'MTX2').

2.3 Simulator Guidelines to expose Rigid Body RPC

2.3.1 Task Guidelines

In the first RBTC, a detailed appraisal of task suitability to expose RPCs was conducted. Findings from this appraisal are outlined in Deliverable 4.6 [Ref. 3]. From this study, it was concluded that a number of tasks were suitable for exposing RPCs. However, it was considered that their application could be improved through modifications to task performance standards.

In the 2nd RBTC, efforts were made to design tasks suitable for RPC detection. From the tasks investigated in the 1st RBTC, the Precision Hover and Roll Step manoeuvres were found to be the most successful for exposing RPCs. This was due to the tight control elements required for the tasks, and the suitability of the tasks for use in motion-based simulation. Therefore, rather than design completely new tasks, the decision was taken to modify these existing tasks, to improve their capability to expose RPCs. The goal here was to increase pilot workload during tasks, through an increase in task bandwidth. This was to be achieved through modifications in the visual environment.

Precision Hover modifications

The PH manoeuvre, contained within ADS-33, is a multi-axis re-position stabilization task to assess low speed performance. The task assesses both the ability of the aircraft to transition from translating flight to hover, and the ability to maintain precise position. Task performance is driven by a series of visual elements, positioned within the environment. The primary height and lateral cueing is given by the `hover board'. During the 1st RBTC, during completion of the PH manoeuvre, experimental cases were completed where pilots were asked to increase their aggression, in order to observe differences in RPC potential. The difference in RPC potential through a reduction in hover board size was observed, and offered an interesting outcome. Forcing the pilots into tighter control caused them to expose more deficiencies in the vehicle, and increases their incipience to RPC. Moreover, the results from simulation were found to better reflect predictions.

The manoeuvre task performance was engineered by making changes to the reference pole location. Pilots were required to maintain a stabilized hover whilst keeping the pole reference position within the hover board from their point of view. It is usual for the pole to be placed midway between the hover board and the reference hover location. ADS-33 recommends a distance of 150ft between the aircraft and hover board, with the pole located 75ft from the aircraft. If the reference pole is moved closer to the aircraft, it decreases the tolerances for completion of the task. In the investigation, 3 pole locations were used; 75ft, 40ft, and 20ft from the aircraft. The distance between the aircraft and the hover board was kept constant at 150ft. This causes changes to the lateral, longitudinal, and height tolerances, given directly by the cueing environment. For example, with the reference pole at 20ft, tolerances are reduced by a factor of 5. However, heading tolerances directly given by the cueing environment, along with longitudinal track position, remain unchanged. Figure 16 and Figure 17 show the pole at the central location (75ft) and at the closest (20ft) location. Excluding changes in the reference pole location, the course was set-up to replicate performance standards for Scout/Attack and Cargo/Utility rotorcraft (as outlined in ADS-33).

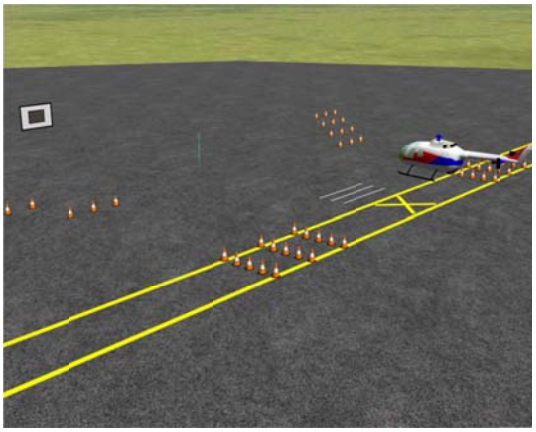

Figure 16: External view of standard ADS-33 Precision Hover course set-up

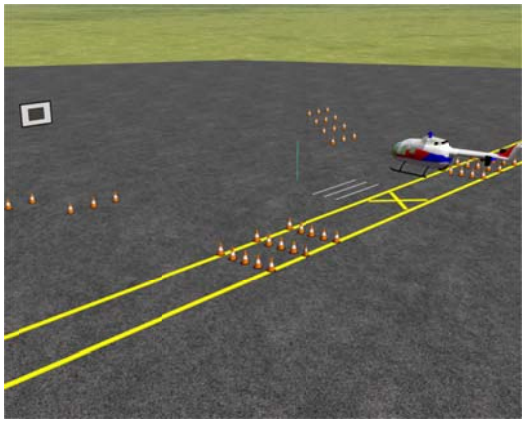

Figure 17: External view of modified Precision Hover course set-up

Roll Step Modifications

The Roll Step manoeuvre, originally presented by Cameron and Padfield [ref. 20], is a lateral reposition task derived from the Slalom manoeuvre contained in ADS-33. The slalom manoeuvre requires the vehicle to traverse a lateral distance similar to the width of a runway. These translations should be completed at certain, pre-defined positions along the runway. The problem with the slalom in this way is that if the vehicle exhibits good handling qualities, there is no 'high gain' element of the task. The actual task bandwidth of the manoeuvre is considered low, with the minimum control inputs to complete the manoeuvre very low (< 20 inputs). Therefore, Cameron and Padfield [ref. 20] proposed combining the manoeuvre with a 'tracking' element, choosing to track the edge of the runway following each translation. Therefore, instead of translating back, the pilot was required to stabilize the vehicle. This portion of the manoeuvre forces tighter control of the vehicle, and causes a significant increases task bandwidth.

Modifications to the Roll Step course were completed in an attempt to improve its usefulness in RPC research campaigns. The manoeuvre was used in the 1st RBTC, in preference to the Slalom manoeuvre used in previous research efforts. However in the 1st RBTC, different Roll Step courses were flown in SRS and HFR, and therefore results were not directly comparable. Therefore, in the 2nd RBTC, the same course set-up was used in both simulators. The course set-up is shown in Figure 18. Black numbered 'posts' denote adequate lateral track. Desired track is half of this width. Striped poles can be used for additional height cueing. The manoeuvre requires the pilot to translate across the runway at two points, stabilizing and maintaining track after each translation.

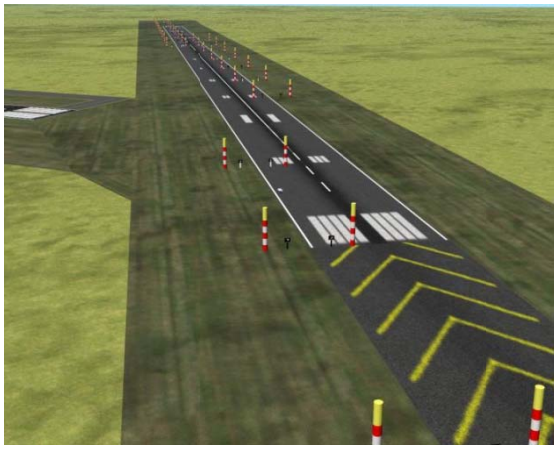

Figure 18: Roll Step Course Layout

In the 1st RBTC, aggression was engineered solely through changes to vehicle flight speed. Increase in forward flight speed forces the pilot to apply more aggressive control inputs, completing more rapid translations.

In the 2nd RBTC, aggression was also engineered through changes to the course layout. Four different Roll Step configurations were flown, in both HFR and SRS. The 'standard' Roll Step manoeuvre tolerances, employed in the 1st RBTC, are shown in Figure 19. Tolerances are set for a runway with a width of 200ft. Transitions are to be achieved within 1500ft, and the vehicle must pass through 'gates' with a minimal roll attitude. This was referred to as Roll Step Configuration 1. Three additional configurations were derived. Configuration 2 used the poles with the same longitudinal runway position, but 'gate' lateral tolerances were tightened. Desired and adequate track positions through the gates were reduced from 60ft and 30ft to 30ft and 15ft respectively. This was in order to increase the pilot gain during the stabilisation phase of the manoeuvre. Pilots were required to apply tighter control, to track the edge of the runway. Configuration 3 used the same 'gate' tolerances as Configuration 1, but applied changes to the longitudinal position of the gates. The longitudinal distance between gates was reduced by 1/3. Therefore, distance for runway transition reduced from 1500ft to 1000ft. Configuration 4 was a combination of the gate positions used in Configuration 3, and the gate lateral tolerances used in Configuration 2.

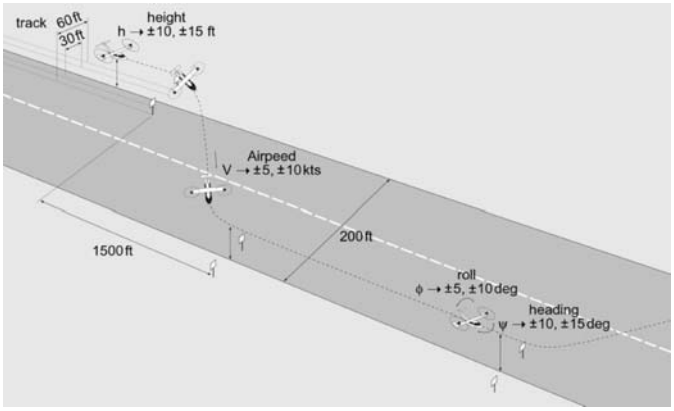

Figure 19: `Standard' Roll Step manoeuvre tolerances

Vehicle Configurations Tested

All vehicle configurations flown during the investigation, for both the Precision Hover and Roll Step tasks, are shown in *Table 4*. These configurations were selected to represent different levels of PIO susceptibility. Only vehicle Configuration 1 was considered to exhibit no susceptibility for PIO. Configurations 1-4 were used during completion of the Precision Hover manoeuvre, whilst Configurations 1, 5-6 were used during completion of the Roll Step manoeuvre.

Table 4: Vehicle Configurations used during task investigation

CONF.	Long. Delay Lim	Long. Rate Lim.	Lat. Delay	Lat. Rate Lim.	PIO Susceptibility
1	0	∞	0	∞	NO
2	0	∞	250	∞	CAT. I
3	0	5	0	2.5	CAT. II
4	180	5	250	2.5	CAT. I & II
5	0	∞	220	∞	CAT. I
6	0	∞	220	2.5	CAT. I & II

Results – Precision Hover

Here, only the key results relating to the task suitability to expose RPC are shown. In Deliverable 4.8, further results relating to the Handling Qualities Ratings and Novel PIO ratings are discussed. Figure 20 to Figure 25 display the PIO ratings obtained for all configurations flown for the Precision Hover manoeuvre, by all pilots, and in both motion-based flight simulators. Results are separated by the hover task flown.

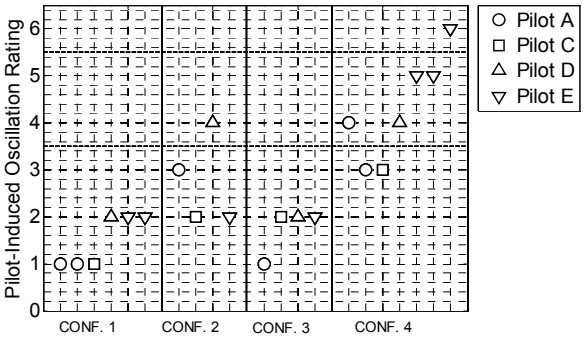

Figure 20: Precision Hover Results – Pole Location = 75ft, HFR

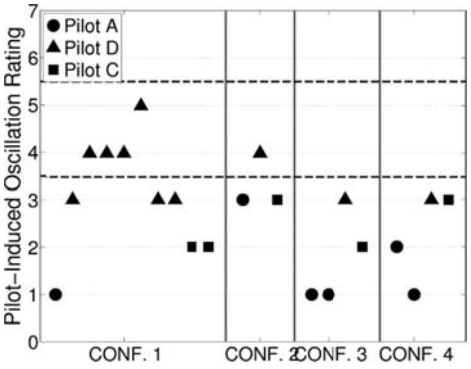

Figure 21: Precision Hover Results – Pole Location = 75ft, SRS

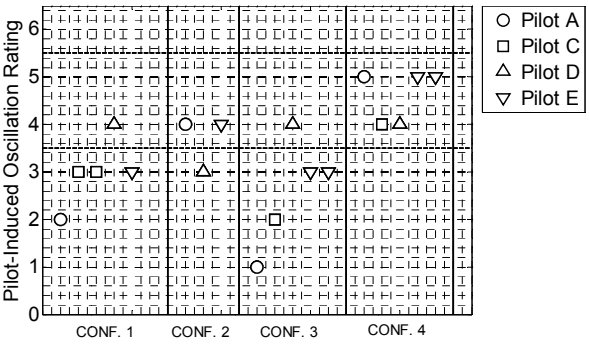

Figure 22: Precision Hover Results – Pole Location = 40ft, HFR

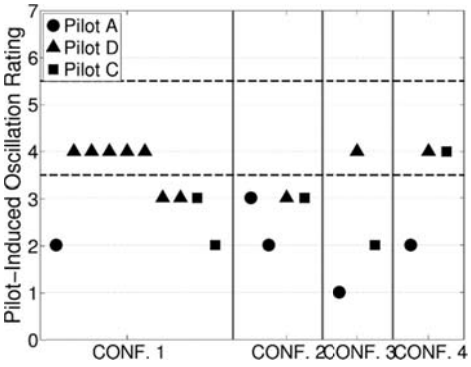

Figure 23: Precision Hover Results – Pole Location = 40ft, SRS

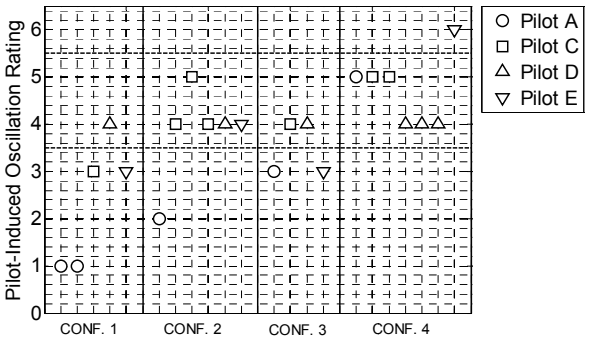

Figure 24: Precision Hover Results – Pole Location = 20ft, HFR

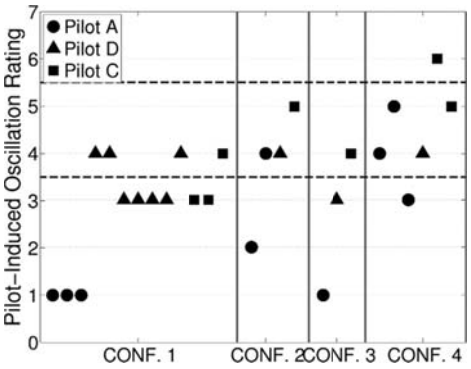

Figure 25: Precision Hover Results – Pole Location = 20ft, SRS

There are a number of observations that can be made through the appraisal of these ratings. Firstly, it is observed that differences between simulators has caused differences in the ratings obtained, for the same conditions. For the ADS-33 specification Precision Hover manoeuvre, a large difference is observed between the results for Configuration 1 and Configuration 4. In HFR, the ratings given for CONF. 4 showed a strong tendency for PIO. This correlates well with the predictions made prior to the campaign. However, in SRS, no strong tendency for PIO is shown. This is likely to be due to the visual environment, restricting piloting performance, and masking PIO tendencies. Performance in the Precision Hover task is very dependent on the pilot sensing visual cues through the simulation environment. Due to SRS' restricted visual environment, it is likely that pilots were not able to maintain task performance, and did not exert the same levels of tight control as in HFR. This is the hypothesized reason for the differences.

However, it is noted that, as task performance tolerances are reduced, and task bandwidth is increased, consistency between results obtained using the different simulators improves. For the case where the pole

location is placed at 20ft, both simulators show strong PIO tendencies for CONF.4. This matches the predictions made prior to the investigation. One advantage that was found through moving the location of the hover pole was the increase in importance given to the forward cueing elements. Particularly in SRS, the strongest visual cueing is offered forward of the pilot seat. Poor peripheral cueing leads to difficulty in judging lateral and longitudinal drift. This shift of task performance to the region where cueing is most similar between the simulators leads to consistency in task performance, and consistency in the ratings awarded.

The observation made when the pole location is brought closest to the pilot is that all of the pilots are now shown to experience oscillations. For the other cases, all pilots were not found to experience PIO events, and the incipience to PIO was found to be a function of pilot control strategy. The difference between Pilot A and Pilot D is a good example of this difference. Pilot A was found to be very high gain during task completion. The pilot always fought to find the best performance possible. Furthermore, he was very resistant to abandoning the task, or to apply a reduction in control amplitude/frequency to improve vehicle handling characteristics. Conversely, Pilot D was found to be very low gain throughout. The pilot was keen to 'break out' of the loop whenever there was an opportunity. Furthermore, he was much more reluctant to apply tight control and was only interested in achieving the task performance standards set. By this, it is meant that the pilot would make no effort to achieve performance better than given by required standards. This led to the suggestion that the task performance standards were not tight enough for the evaluation of PIO tendencies. A difference in their strategies may be a result of their experience. Pilot A has been a consultant test pilot for the University of Liverpool for over 10 years and no longer flies helicopters regularly. Pilot D however is a current military test pilot for the Royal Netherlands Air Force, but with much less experience than Pilot A. Evaluations in SRS and HFR were his first experience of testing in an academic environment. Their flying was much more in-line with that expected during normal operations; he was wary of over-controlling the vehicle, and treated situations where he entered oscillations in a much more safety-conscious manner. Pilots were not specifically instructed to fly a particular way during the briefing process, as it was more important that pilots approached tasks as they saw fit. Instructing pilots to fly in a certain way may cause results obtained to lack any relation to realistic piloting strategy. However, what is shown by the ratings awarded is that both Pilots had similar experiences for the modified Precision Hover. This suggests that the changes to the manoeuvre have achieved, to some extent, the goal of increasing consistency between pilots.

Figure 26 and Figure 27 show typical results from completed Precision Hover manoeuvres in HFR, with the most PIO prone configuration, CONF4. The cases show pilot control activity with respect to time for all control channels. As shown, both Pilot A and D approach the task in similar ways; they both disturb the aircraft from trim and begin a translation using small, non-oscillatory control inputs. Between 10 and 20 seconds, both pilots reach maximum ground speed, at a value of only 1 knot difference (shown in Figure 28). Both pilots arrest the vehicle translational rate through a commanded oscillatory control input. However, following this input, Pilot D almost opens the control loop, and applies only very small control inputs. Furthermore, the pilot keeps translations slow (i.e. a ground speed lower than 1 knot). Pilot A however maintains closed-loop control, to achieve performance parameters to the best of his ability. However, this results in a faster translational rate, requiring sustained control inputs for a longer period of the manoeuvre. Furthermore, throughout the manoeuvre, Pilot D is almost inactive on the longitudinal, collective and pedals. Only small corrections are made during the transition from translation to hover. Pilot A makes effort to use all controls, and possibly becomes susceptible to vehicle cross-couplings in the process.

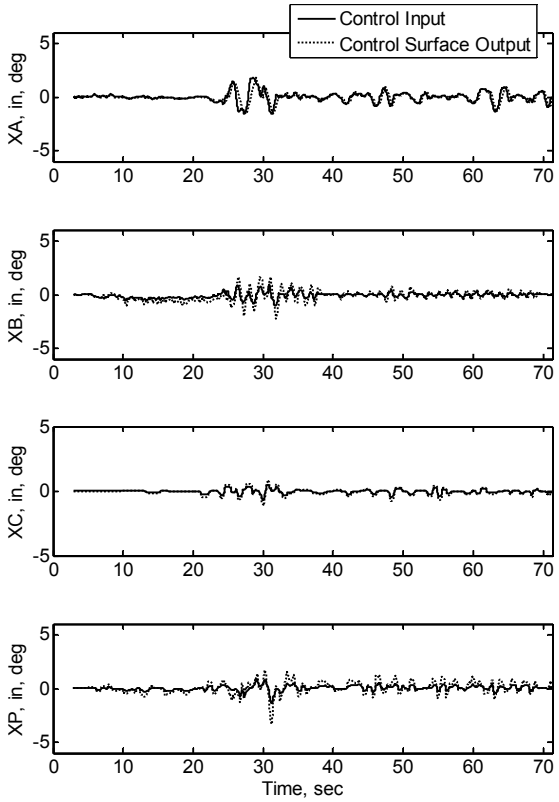

Figure 26: Pilot A, CONF.4, Pole Location = 75ft

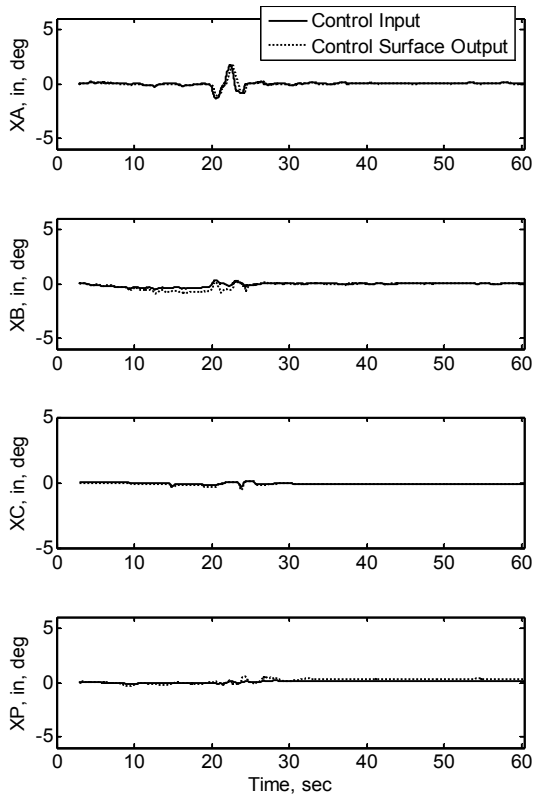

Figure 27: Pilot D, CONF.4, Pole Location =75ft

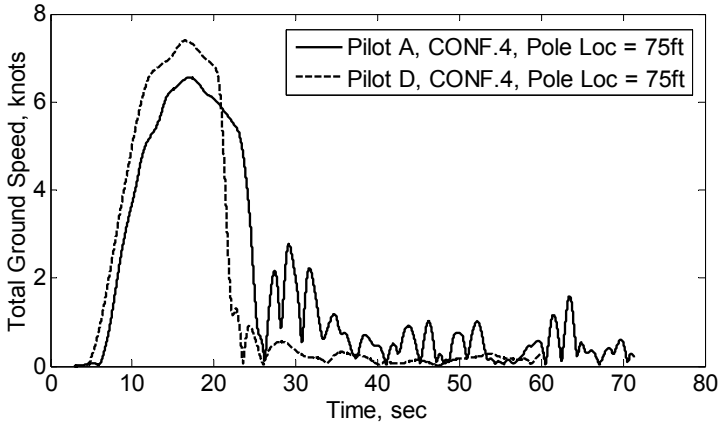

Figure 28: Ground Speed from Precision Hover manoeuvres completed by Pilot A and D.

HQRs were used to judge both the vehicle handling qualities (linked to RPC) and the task performance. With changes in HQR, one can observe the relative changes in task difficulty caused by changes in the MTE tolerances. Table 5 shows Handling Qualities Ratings (HQRs) for the baseline vehicle model (PIO robust). Results are shown for both tests completed in HFR and SRS. Next to each numerical rating, subscripts denote the number of times the rating was awarded. For HFR results, predominantly Level 1 HQRs were awarded for the 75ft pole location, the task as defined in ADS-33. However, in SRS, due to the poorer cueing environment and lack of ground references, the task was found to have predominantly Level 2 HQRs. HQRs were not shown to be sensitive to pole location within SRS. This is due to the initial difficulty in task performance. However, in HFR, the position of the pole location changed ratings from predominantly Level 1 to Level 2 HQRs.

Table 5: Handling Qualities Ratings awarded using Configuration 1

	Pole Location (ft), HFR			Pole Location (ft), SRS		
Pilot	20	40	75	20	40	75
A	4,5	4	3,2	5	6	6
C	5	5	3	5,7	4,5	4
D	7	5	3	5,6,7	6,7	5,6,7
E	4	5	4	-	-	-

In HFR, CONF.4 led to 'high profile' PIOs for all hover pole locations. However, the majority of the most explosive cases where experienced by Pilot E, who did not complete tests in SRS.

The increase in PIO tendencies for CONF.2 and CONF.3 was shown when the reference pole location was moved closer to the pilot. Furthermore, this increase was observed in both simulators. An example is shown by observation of time history traces of pilot control during two evaluations of CONF.2. The examples, given in Figure 29 and Figure 30, show pilot lateral control input with respect to time. In these examples, the transition to hover occurs at approximately 20 seconds. This can be observed in Figure 31, which shows the ground speed for both cases. As illustrated, in the case where the Pole Location = 75ft, an oscillatory vehicle response occurs between 20 and 40 seconds. This is during the stabilisation period. However, one can see that at approximately 40 seconds, the pilot 'freezes' the control stick, as he has reached the desired hover position. From this point, there are no significant oscillatory inputs, and the pilot is almost open-loop.

For the case where the Pole Location = 20ft, the same oscillations on stabilisation are observed (i.e. between 20 and 30 seconds). However, in this case, the pilot is unable to 'freeze the stick', as they must continue to correct position. However, rather than the oscillations subsiding during the stabilised period, oscillations are driven by the task performance. At approximately 60 seconds, oscillatory control amplitude increases, remaining at this increased level until the attempt is stopped at approximately 100 seconds.

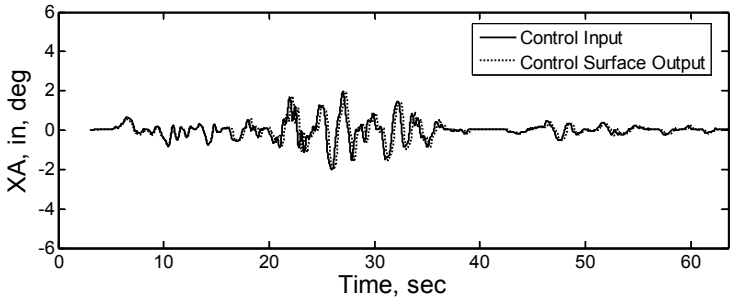

Figure 29: Pilot E, CONF.2, Pole Location = 75ft

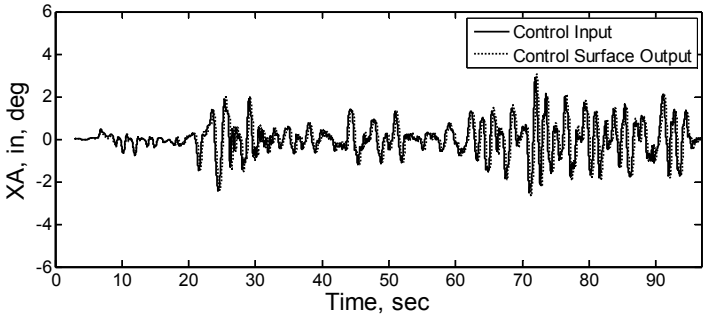

Figure 30: Pilot E, CONF.2, Pole Location = 20ft

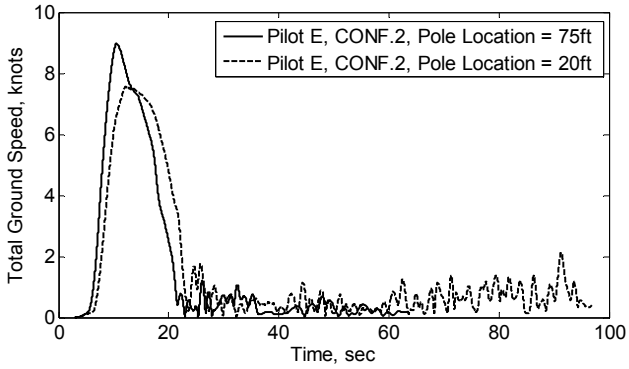

Figure 31: Ground speed for CONF.2 cases

The difference displayed in *Figure 29* and *Figure 30* perhaps shows why many RPCs currently go undetected in current evaluations. Testing only the 'normal' operations of the rotorcraft will not necessarily expose dynamics that will be experienced at one stage in the rotorcraft life cycle.

Although changes in task performance increased the susceptibility to PIO, a difference in susceptibility of each pilot, based on their strategy was observed. Pilot D consistently exhibited the lowest change in performance. HQR and PIOR showed little sensitivity, with his robustness to PIO suggesting that further changes to the task performance are still required.

Therefore, there are a number of recommendations for use of the manoeuvre when trying to expose RPCs. Firstly, there must be greater control on the way the pilot attempts the stabilisation period of the manoeuvre. This can further decrease the variability in results obtained. One way this could be attempted is to form a target, rather than the current region that is contained on the hover board. This would further force the pilots to apply tight control, rather than opening the loop at the earliest opportunity.

The effect of changing PH tolerances is further shown in Figure 32 to Figure 35. Here, the Root Mean Square (RMS) outputs for pilot control and vehicle output are shown for all configurations flown in HFR. As shown, for all PH completed in the baseline vehicle, all pilots were found to exhibit similar RMS control inputs, producing similar vehicle output response. However, for the PIO prone configurations, RMS input for both longitudinal and lateral control are much more widely distributed. As shown, Pilot E applied the largest control inputs, and was generally the most aggressive when encountering RPCs. The distribution of points shows that, although not a guarantee, the tighter task performance had more chance of causing both higher pilot control input and vehicle rate output for the PIO prone configurations. As this trend is not shown for the PIO robust case, the increased control activity and vehicle rate outputs is not due simply to the task performance requirements, and indicates the triggering of oscillations.

Here, a recommendation may be made that one should determine the relative `pilot susceptibility' to triggering PIO, and use them for further investigations. This may involve some preliminary tests to qualify the levels of pilot `gain', or the aggression of their command. The danger here is that there may not be a way to qualify the overall PIO susceptibility 'envelope' of each pilot, as their response to different situations may vary. This recommendation can be considered for future test and evaluation.

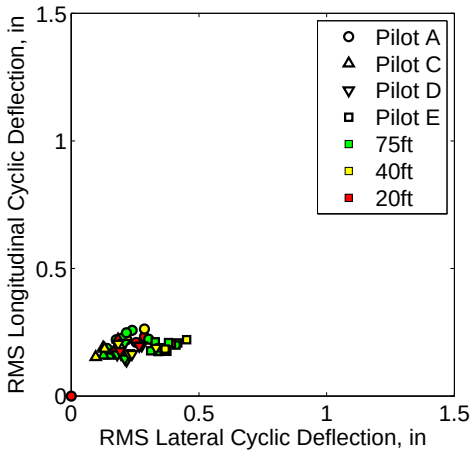

Figure 32: RMS Long. Cyclic w.r.t. Lat. Cyclic for baseline conf., PH

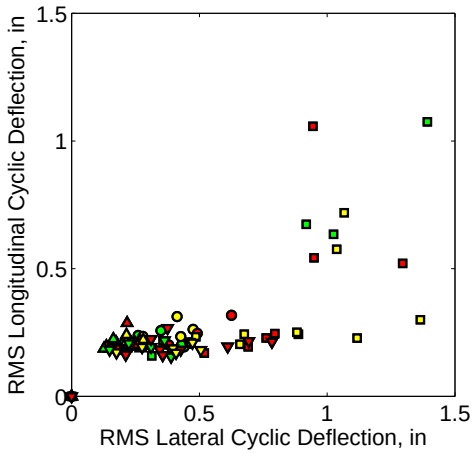

Figure 33: RMS Long. Cyclic w.r.t. Lat. Cyclic for PIO Prone Conf., PH

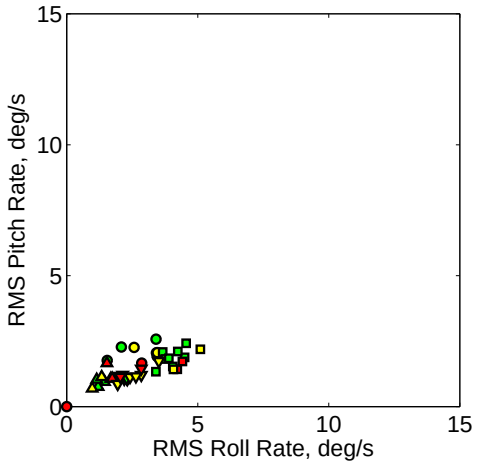

Figure 34: RMS Pitch Rate w.r.t. Lat. Cyclic for baseline conf., PH

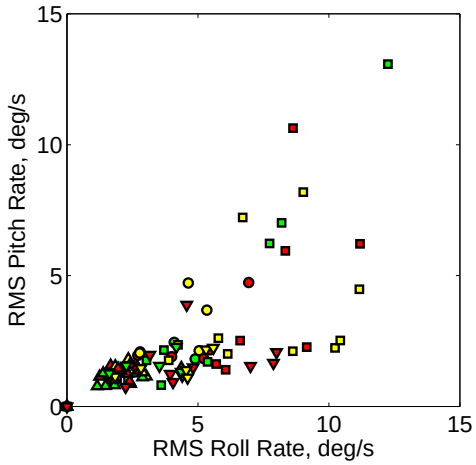

Figure 35: RMS Pitch Rate w.r.t. Lat. Cyclic for PIO Prone Conf., PH

Overall, a finding of the investigation was that with the pole location closest to the vehicle, the consistency of triggering PIOs was much higher. HQRs predominantly within Level 2 for Configuration 1 suggest that this task is not entirely removed from the requirements of the rotorcraft. Although the task performance standards may be higher than is usually required for regular flying tasks, setting the difficult performance standards helps to detect the underlying RPC tendencies that could be exposed during extreme flight conditions. For example, in difficult conditions, the pilot may be forced into tight loop control and it is important that the PIO tendencies are known. As stated by McRuer in Ref. 21, "*Pilot evaluations for (APC) tendencies should increase the pilot gain or workload and so increase the possibility of finding hidden (APC) tendencies*". Although these experiments show an increase in detection of PIOs when task performance standards for the PH manoeuvre are changed, the changes are not necessarily appropriate for different rotorcraft. For the original PH manoeuvre, in HFR and with the baseline vehicle configuration, Level 1 HQRs were awarded. Furthermore, during the stabilisation element of the task, pilots were able to go `open-loop', due to the stable nature of the model. Therefore, tolerances were reduced in order to force pilot gain, and force closed-loop control during stabilisation. However, for vehicles with poorer handling, it may not be necessary to modify the tolerances. The suggestion is that one should complete a number of tests and observe awarded HQRs to judge whether tolerances must be adjusted to look specifically at PIO tendencies. Defining the process for this judgement is a recommendation for further research effort.

Results – Roll Step

As with the Precision Hover, modifications to the Roll Step course led to differences in subjective ratings awarded. Only a limited amount of test cases were completed in both simulators. These were for Task 1, at 60 knots and 80 knots, and Task 3 at 60 knots. However, results from the Roll Step manoeuvre were less conclusive than those from the Precision Hover. Fewer PIOs were encountered during the manoeuvre than for the Precision Hover. In HFR, there was an increase in PIO tendencies for Task 1 when the speed was increased from 60 knots to 80 knots. However, with only limited cases of Task 3, no real difference was found from Task 1.

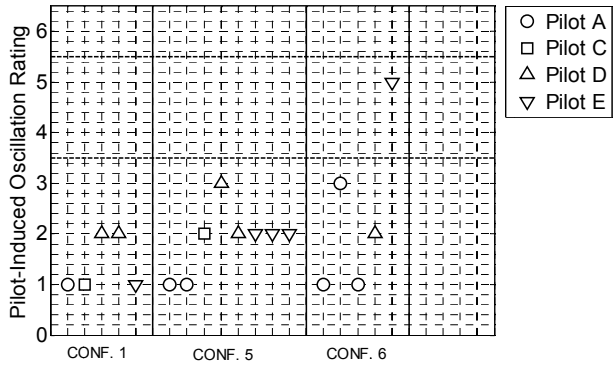

Figure 36: Roll Step Results – Task 1, 60 knots

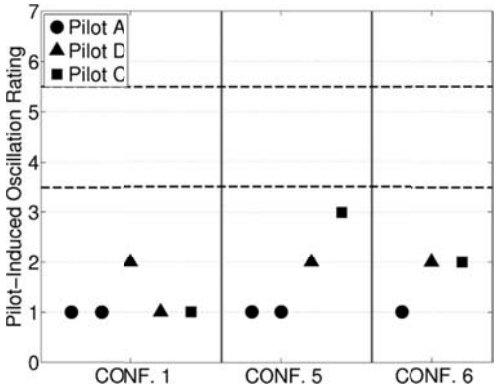

Figure 37: Roll Step Results –Task 1, 60 knots

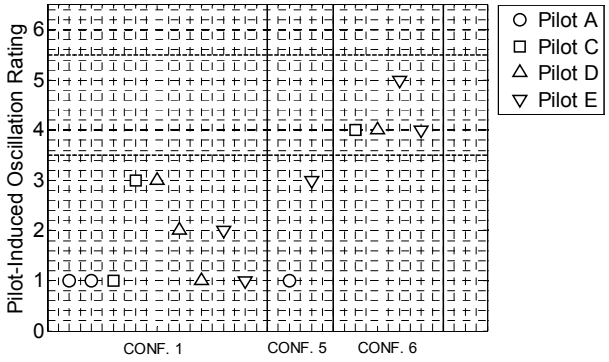

Figure 38: Roll Step Results – Task 1, 80 knots

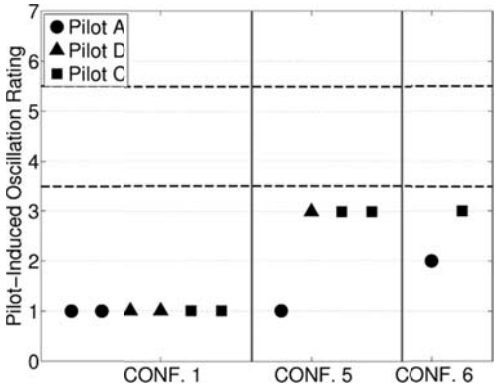

Figure 39: Roll Step Results - Task 1, 80 knots

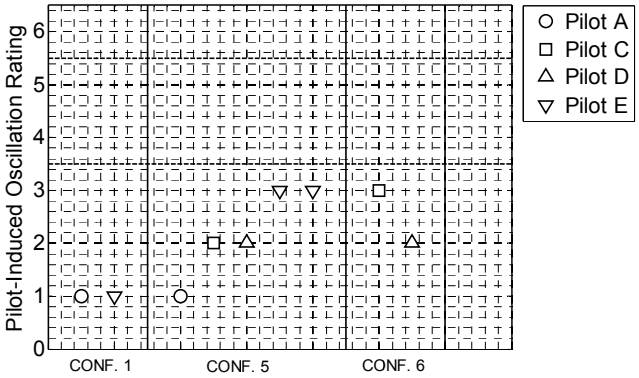

Figure 40: Roll Step Results – Task 3, 60 knots

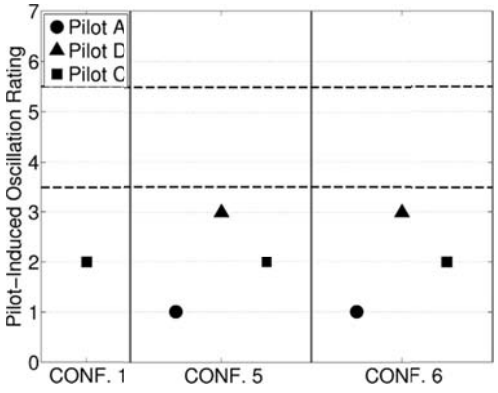

Figure 41: Roll Step Results – Task 3, 60 knots

Pilot strategy significantly affected the results obtained during the Roll Step investigation. Some examples of the strategy employed by pilots are shown in Figure 42 to Figure 45. These results are for the configurations for the Roll Step configuration 1, flow with vehicle CONF. 1. This model was not susceptible to PIO. As in the Precision Hover investigation, Pilot D was the least prone to PIO during the Roll Step investigation. Observation of this pilot's strategy shows a very aggressive input to translate, and then only small, corrective inputs thereafter. Using this method, the pilot avoided triggering PIOs on a number of occasions. Furthermore, Pilot D was less active on off-axis control.

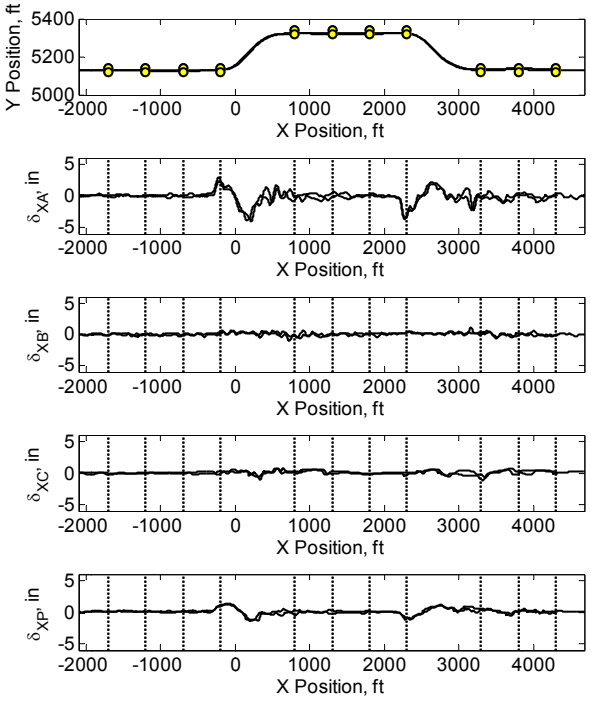

Figure 42: Baseline Task Strategy – Pilot A

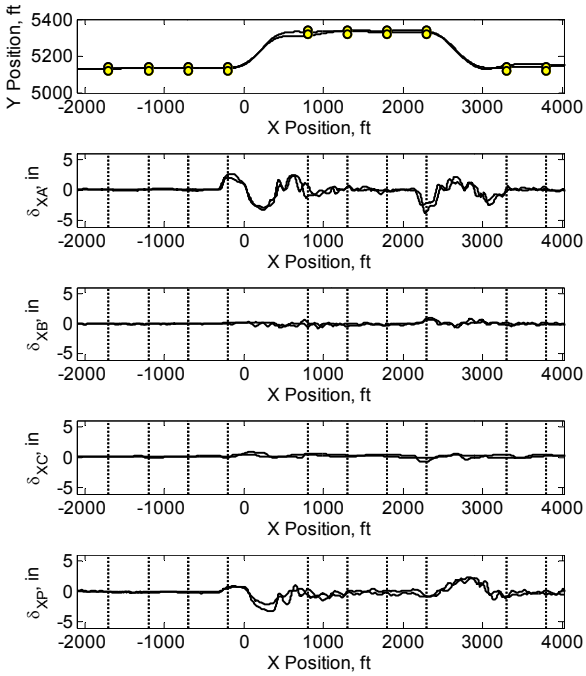

Figure 43: Baseline Task Strategy – Pilot C

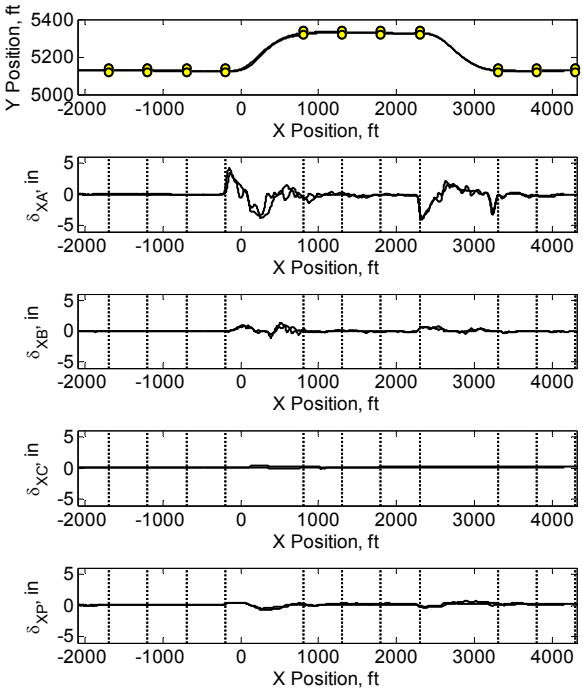

Figure 44: Baseline Task Strategy – Pilot D

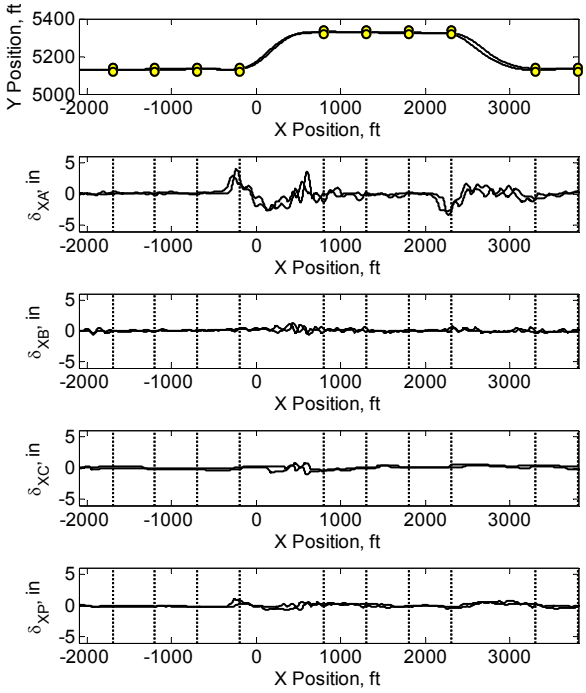

Figure 45: Baseline Task Strategy – Pilot E

One factor that was apparent during completion of the Roll Step was pilot learning. Pilots were quickly able to adapt during completion of the manoeuvre, and apply knowledge to the next run to successfully avoid PIO. This level of pilot learning and adaptation is perhaps a concern when using the manoeuvre to observe PIO tendencies. One must ensure that pilots do not mask PIO tendencies, and perhaps the task performance requirements must be further constrained.

An example of pilot learning is shown though a comparison of Figure 46 and Figure 47. The former example is the first attempt of the manoeuvre completed by Pilot A, with a PIO prone vehicle configuration. As shown, following the first translation, the pilot applies some large, oscillatory control inputs to stabilise the aircraft roll motion. Furthermore, some high frequency small longitudinal control inputs are shown. The second attempt at the manoeuvre is shown in Figure 47. In this attempt, the pilot applies more calculated control input, and during the section of the manoeuvre where he encountered problems in the first run, the pilot does not apply any control inputs. The pilot uses the pedals to make small corrections to the heading during the test. Interestingly, at the end of the manoeuvre, the pilot wanted to explore the limits of the vehicle, and quickly triggered a divergent PIO. This was achieved through the high gain tracking when going through the last three gates. In this case, the simulation was stopped to prevent loss of control. These examples show how the pilot can avoid triggering PIOs, in vehicles where clear PIO tendencies exist.

A recommendation here is that the task (or tolerances) should be redesigned to prevent pilots from completing the manoeuvre using a strategy that has resulted from learning in previous manoeuvre attempts. If the pilot is able to both complete the manoeuvre and avoid PIO tendencies (if they exist within the vehicle), the task performance requirements are not stringent enough. The risk here is that the task may become so difficult that is impossible to achieve. Therefore, another method to disturb pilot control, such as turbulence, could be used to force closed-loop control. The requirement for all tasks is that they are repeatable, which is something that needs to be investigated with future versions of the Roll Step manoeuvre. In any case, attention must be given to PIO susceptibility for all completed test runs. When assessing handling qualities, it is often only the cases where the pilots provide ratings that are considered, after they have become comfortable with their levels of task performance.

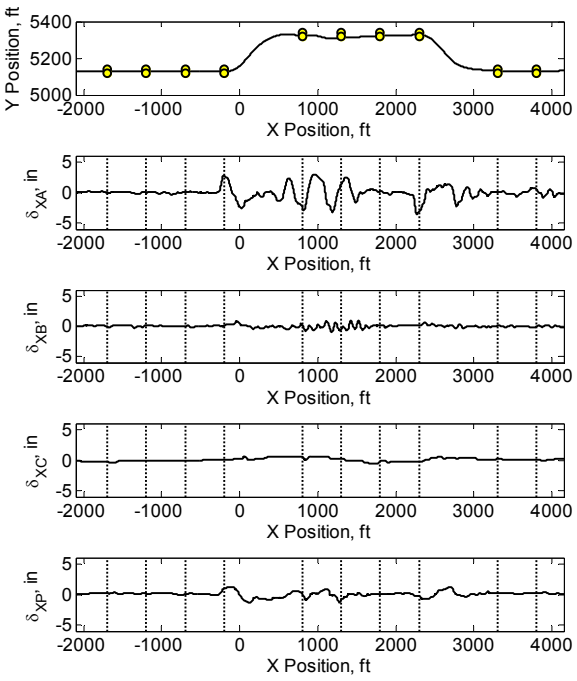

Figure 46: Pilot A, 1st completion of Roll Step manoeuvre, PIO prone configuration

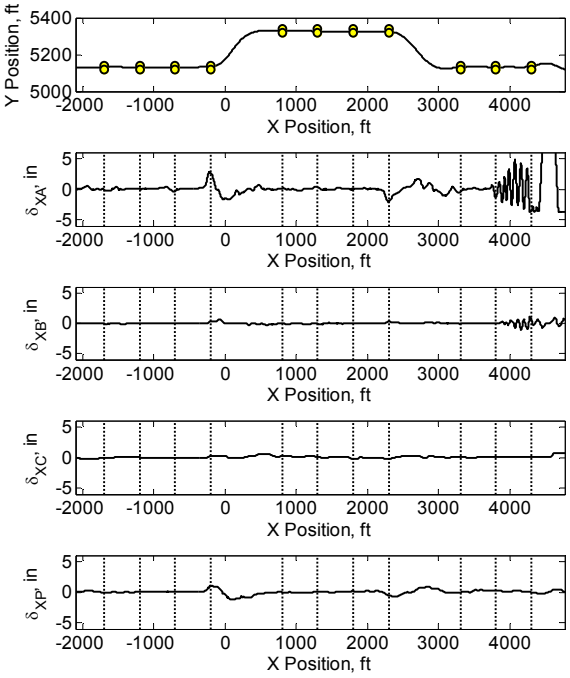

Figure 47: Pilot A, 2nd completion of Roll Step manoeuvre, PIO prone configuration

2.3.2 Task Design Guidelines for exposing to RPCs

This part presents the key factors that need to be taken into account when developing an effective task to expose RPCs. These factors are generalised from the results of two test campaigns conducted on the HELIFLIGHT-R Simulator (HFR) in the University of Liverpool and SIMONA Research Simulator (SRS) in TU Delft to compare effects of different simulator platforms on rotorcraft pilot coupling (RPC) prediction with four ADS-33E-PRF manoeuvres: Acceleration-Deceleration, Vertical Manoeuvre, Precision Hover, and Roll Step. Therefore, the results are presented first and then the key factors are summarised.

The HQR and PIOR values of the four MTEs from both simulators are shown from Figure 48 to Figure 51.

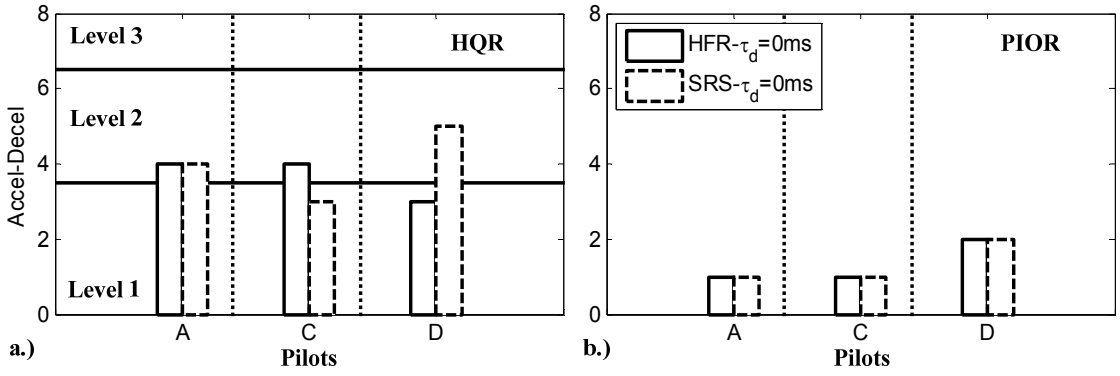

Figure 48 **Subjective HQR and PIOR comparison between HFR and SRS from AD manoeuvre**

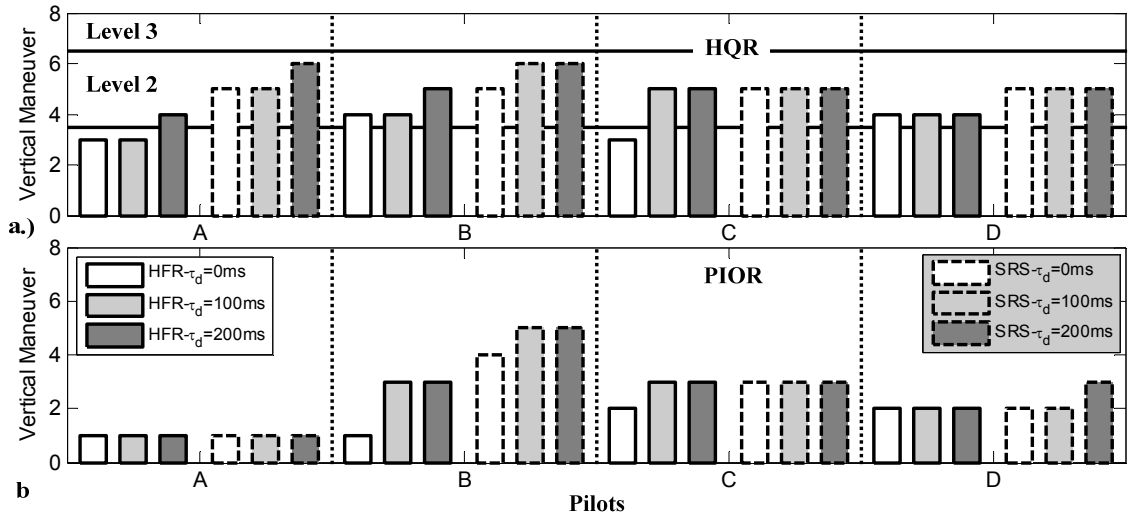

Figure 49 **Subjective HQR and PIOR comparison between HFR and SRS from Vertical manoeuvre**

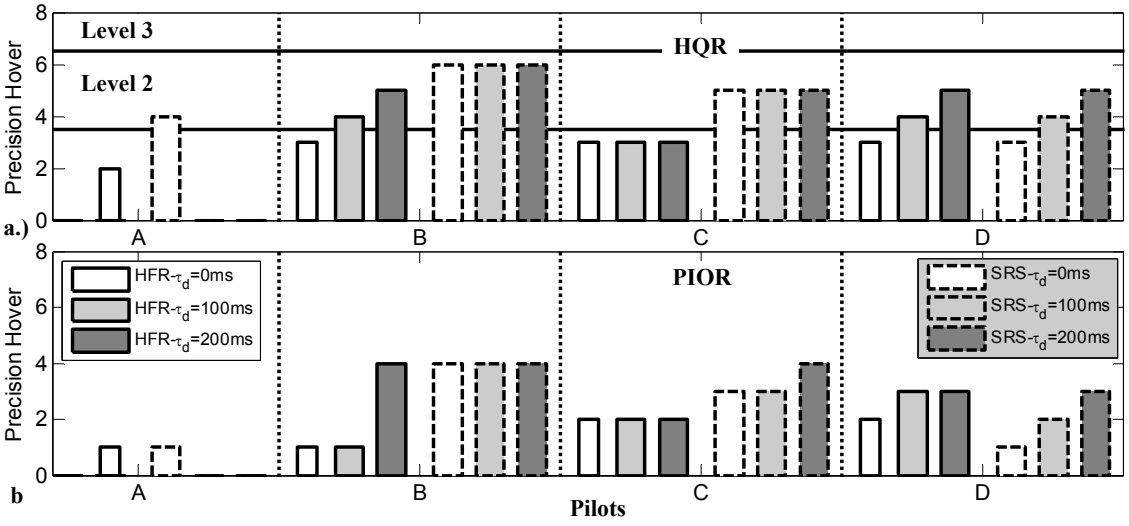

Figure 50 **Subjective HQR and PIOR comparison between HFR and SRS from Precision Hover**

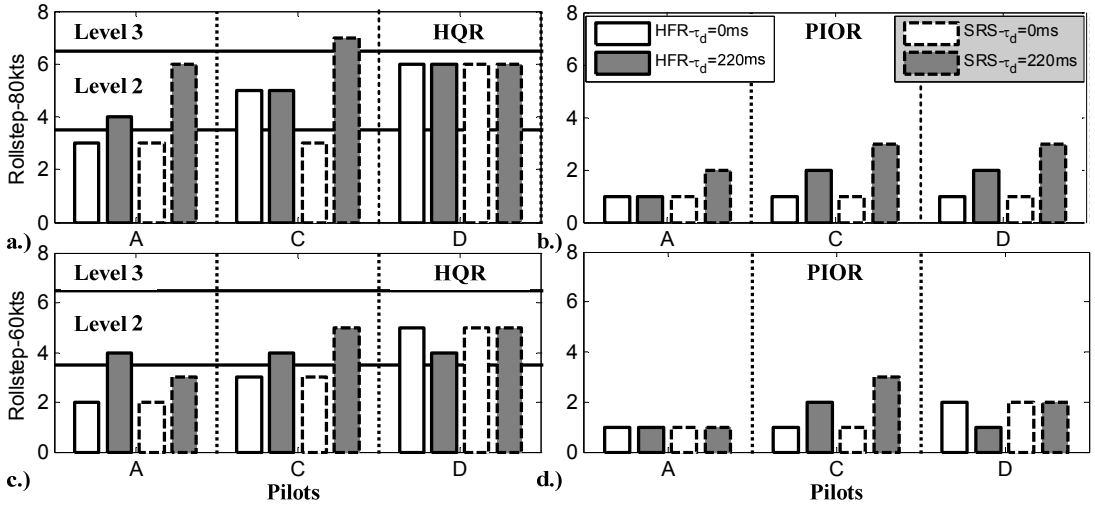

Figure 51 **Subjective HQR and PIOR comparison between HFR and SRS from Roll step (60 kts)**

The cut-off ω_c values from the investigated cases are shown from Figure 52 to Figure 54.

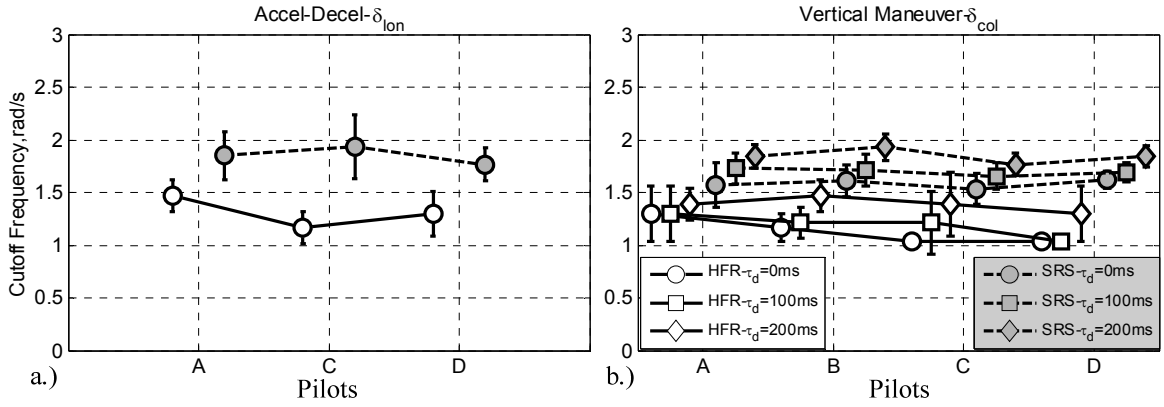

Figure 52 **Cut-off frequency values of two simulators from Accel-Decel and Vertical Manoeuvre**

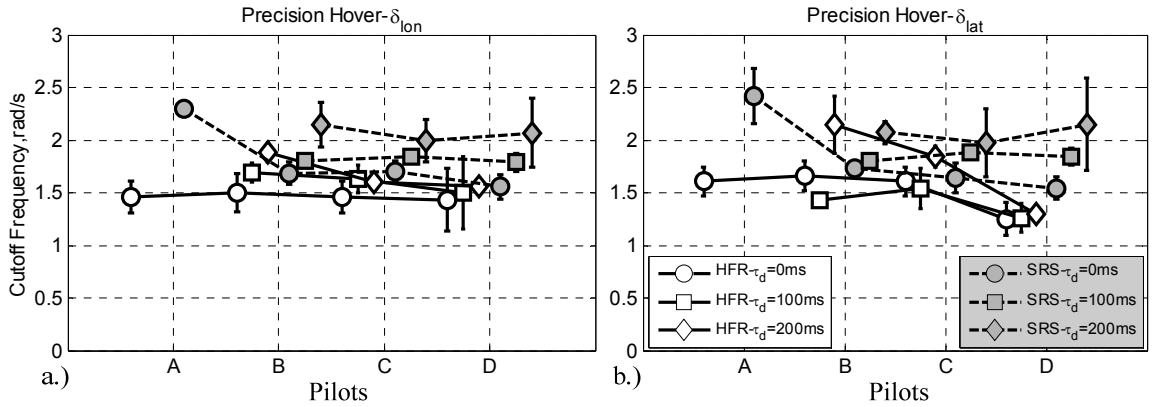

Figure 53 **Cut-off frequency values of two simulators from Precision Hover**

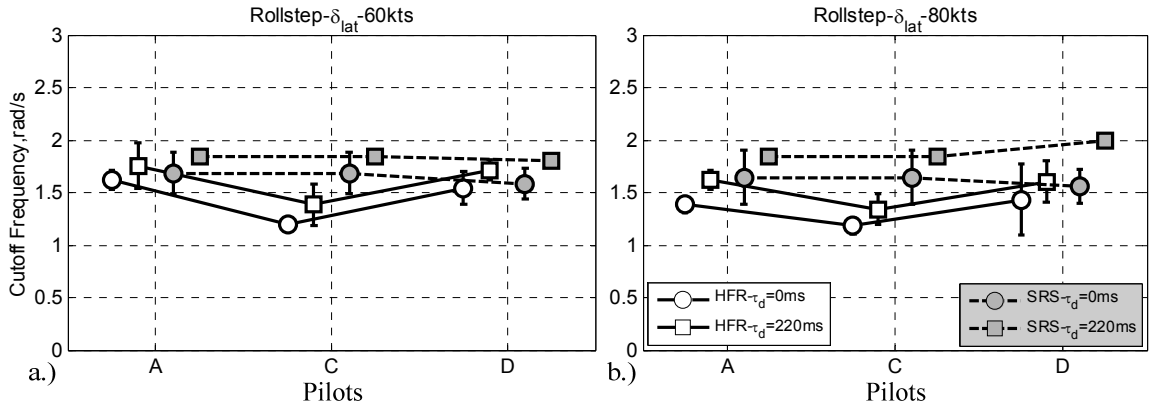

Figure 54 **Cut-off frequency values of two simulators from Roll Step**

The time-varying cut-off frequency ω_G values based on the Wavelet scalogram and their related control inputs of the cases with the same subjective HQR and PIOR selected from two test campaigns are shown from Figure 55 to Figure 57.

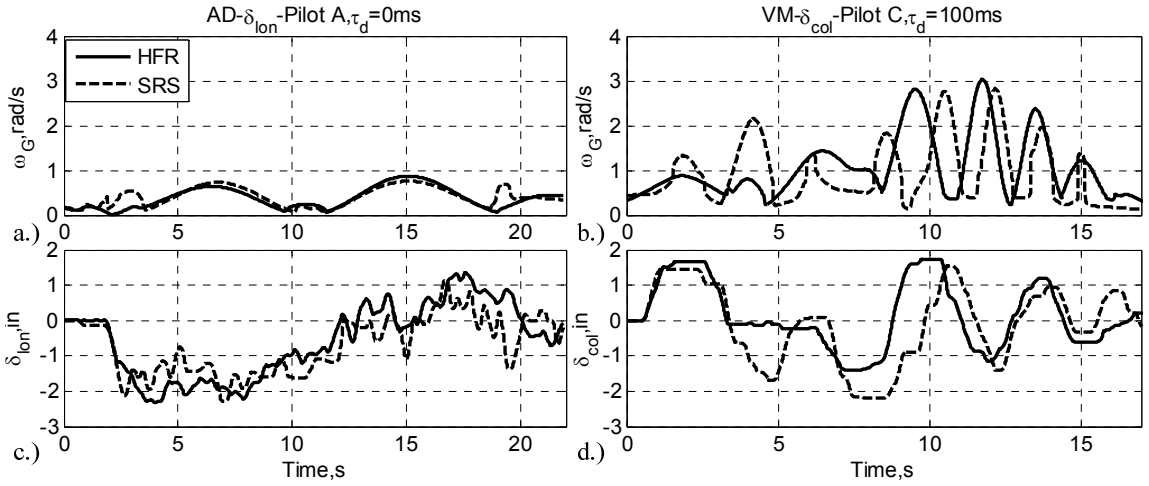

Figure 55 **Comparisons of pilot control behaviours on HFR and SRS with the same HQR and PIOR**

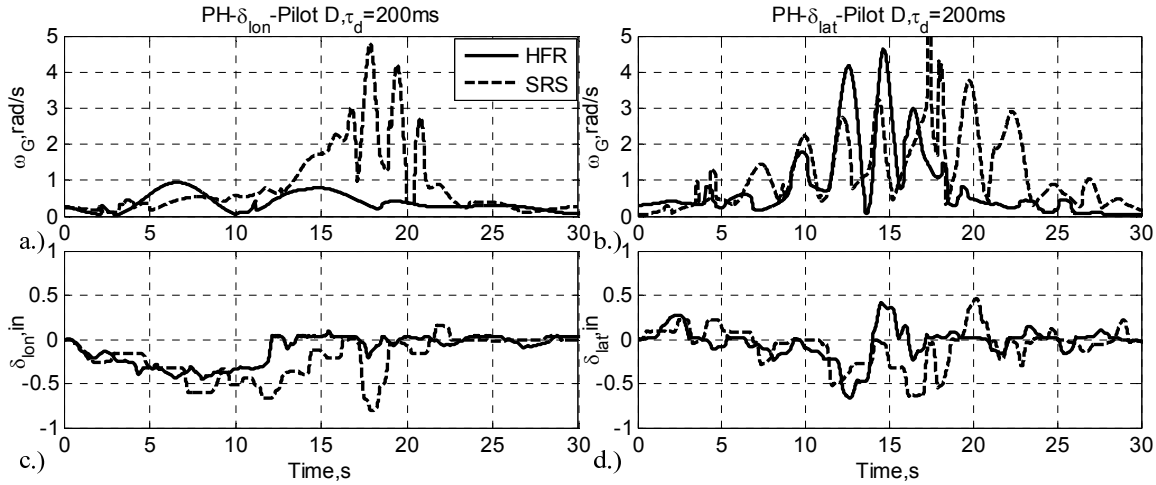

Figure 56 **Comparisons of pilot control behaviours on HFR and SRS with the same HQR and PIOR**

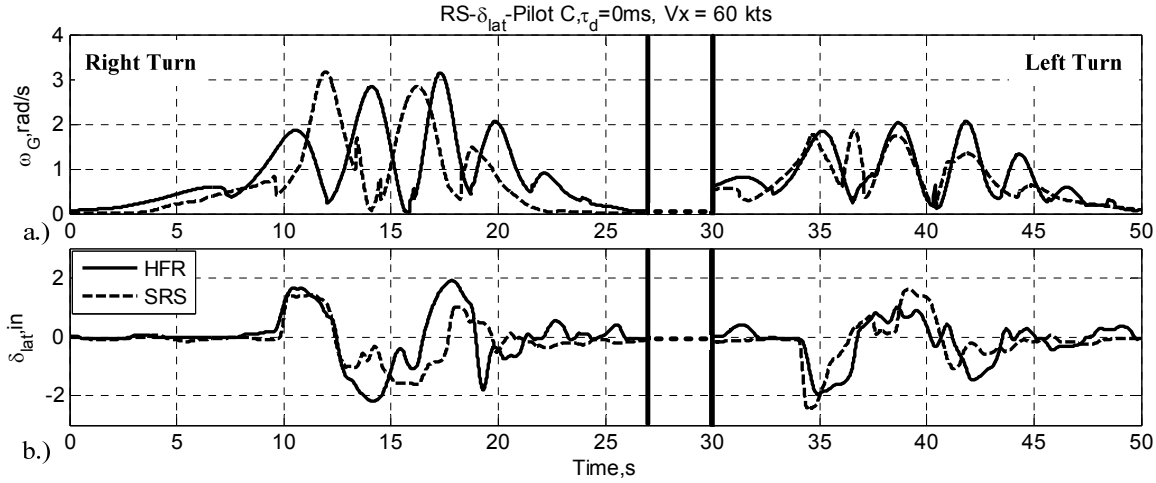

Figure 57 **Comparisons of pilot control behaviours on HFR and SRS with the same HQR and PIOR**

The four manoeuvres being investigated here can be generally considered as high-gain tasks. However, among them, the PH manoeuvre shows the highest pilot control activities (Figure 53 and Figure 56) and is awarded with

the highest PIORs (averaged across the pilots). For example, the time-varying cut-off frequency of the PH task shows the highest frequency 5 rad/s in Figure 56. There are two possible factors contributing to this phenomenon. Firstly, the PH task involve strong multi-axis coupling due to the vehicle being operated near the hover. Both the approach to the hover position and the subsequent stabilization phases result in strong coupling between the longitudinal and lateral axes. These inter-axis couplings thereby increase the pilot gain and workload. On the contrary, the other three manoeuvres are one-axis dominant tasks. Although the RS involves both the lateral and longitudinal flying phases, these two phases work at different time scales. Second and probably most importantly, there is a task-mode change occurring from the low-speed transition to the long stabilization process in the PH manoeuvre. This task model change results in pilot control strategy adaption which to some extent, can be considered as a PIO triggering factor. Therefore, the two factors (multi-axis coupling and pilot control strategy adaptation) lead to the most effective manoeuvre to expose RPCs here.

The results here are consistent with the traditional findings that high-gain missions are normal and ordinary in the practical flying duties, whereas severe PRCs are extraordinary events. The RPCs are usually related to abnormal transitions in the pilot or the effective vehicle dynamics. The lessons in the paper thereby are useful for the development of flying tasks to expose the potential RPCs.

2.3.3 Simulator Settings Guidelines to expose RPCs

Motion Base Guidelines

Experience during both rigid body test campaigns in HFR and SRS suggest the following considerations for the motion base settings of simulators to be used in an RPC exposure test campaign:

- The classical compromise while adjusting a motion base washout filter for any flying task should be taken into account for the first step, and then further comprise should be carried out for the RPC candidate task. These two steps are described below:
    - **First step:**

      Table 6 briefly summarizes the primary effects of motion base settings on the motion response.

Table 6. Brief summary of effects motion base settings

		Low	High	Notes
High pass filter	Filter order	High drift Low phase distortion	Low drift High phase distortion	Due to gravity, the heave axis generally uses high order filters.
	Filter gain	Less Responsive Too low: lack of noticeable motion cue	More Responsive Too high: too aggressive cue commands	When combined with high break frequencies, unpleasant washout effects could appear with high gain.
	Filter break frequency	More mid-frequency content in response Less Phase distortion	Less mid-frequency content in response More Phase distortion	Depending on the desired frequency range, keeping the break frequency low is preferable
	Tilt Coordination	Higher filter order required for surge and sway	Lower filter order required for surge and sway	Surge and sway channels achieve one more order due to tilt coordination
	On-axis harmonization	Higher risk of on-axis abrupt response	Lower risk of on-axis abrupt response	Matching pitch & surge and roll & sway could

				provide more smooth on-axis response
	Stroke actuator position and rate limits	Larger motion space Higher risk of damage	Lower motion space Lower risk of damage	

Simulator motion bases should be adjusted according to the task to be flown while performing compromises similar to ones that are listed in Table 6. During the first step, the task could be introduced with its nominal configuration (e.g. no RPC trigger, least aggression demand). Motion space and filter settings should be considered as task-dependent, and the user should adjust the proper channel parameters to benefit from the simulator capabilities for the selected task.

- **Second step:**

Adjust filter parameters depending on the task to be flown, with the most RPC candidate task configuration flown by a pilot with high gain and aggressive control strategy. Nominal task progression may not stress the motion base enough when compared to a developed severe RPC case. In order to avoid psychologically blocking pilots to enter a possible RPC cycle, the motion base should be able to provide sufficient and 'safe' motion cueing during the worst case scenario (e.g. highest aggression task setup and triggering effect).

Control Loading Guidelines

Control loading settings should represent the actual vehicle characteristics as closely as possible. Varying the fundamental parameters may increase or decrease the tendency to expose RPC occurrences, depending on the task and the participating pilots control strategy. Considering the recommendation for including a wide range of pilots with various control strategies in a RPC-focused test campaign, the best practice could be setting the control loading system into the baseline, which is the feel characteristics of the vehicle to be modelled.

Most likely the control loading system of the simulator includes tuning software, and having an easily accessible and configurable software is highly recommended. Furthermore, using as many pilots as possible with considerable experience on a 'reference' vehicle with close dynamics and operational capabilities could improve the matching of control loading system in the simulator with the real rotorcraft to be designed. However, using control loading parameter values of the 'reference' vehicle could not be proper. Because, artificial feel systems include representative subsystems, which may not provide the same feeling if the actual vehicle control system values are plugged in. Thus, the control loading tuning software should provide sufficient freedom to change parameters of the feel systems.

Visual System Guidelines

A larger field of view is suggested for any rotorcraft test campaign using simulators, particularly for tasks close to ground, during which pilots use all possible reference visual cues. The brightness, resolution, refresh rate, edge blending, and other technical aspects of projection system should provide a visual environment that is sufficient for pilots to complete task especially during a RPC prone flying task.

2.4 Aeroelastic Testing Guidelines to Expose RPCs

The success or not for a rotary-wing aero-elastic test is mainly determined by the following three elements: a reasonable vibration environment, an appropriate elastic aircraft model, and a triggering factor. The guidelines used to design an effective rotary-wing aero-elastic test are given based on each of these factors.

How to select a vibration signal

It is known and accepted that APC and RPC usually need a trigger that initiates the phenomenon by perturbing the control of the pilot and inducing a change in the status of the pilot (a change in the actual or mental model of the vehicle, a shift of the focus of the pilot from the primary task).

During the aeroelastic RPC experiments, it has been observed that a certain amount of disturbance was useful as the trigger for adverse interaction events. This was especially true for investigations related to the vertical axis using simple two-degree of freedom models (2DOF). Apparently, the frequency of the disturbance (a white noise filtered to mainly act in the 0.25-1 Hz band) increases the workload of the pilot while trying to perform tracking tasks involving the collective control, and may alter (increase) the muscular activation required to perform the task, changing the impedance of the pilot's limbs.

Tests involving the roll axis also benefited from the presence of a disturbance, although the effect was less pronounced. In such case, the task showed a tendency towards initiation of adverse RPC events after the double turn, during the subsequent capture phase in which a higher precision was required of the pilot in tracking the roll angle. The presence of a disturbance makes the task more difficult and, as such, it may trigger an adverse event. Such manoeuvre triggered a few PIO events and a clear, repeatable PAO event.

How to select an aircraft model

The experimental verification of aeroelastic APC and RPC requires specifically tailored vehicle models. Intuitively, the model must have the capability to perform the required task. Thus needs the required rigid-body degrees of freedom. In addition, as many aeroservoelastic degrees of freedom (including those required to model the dynamics of the actuators and of the control system dynamics, if any) as required to correctly model the vehicle dynamics relevant for the phenomenon must be present. Indeed, understanding the model fidelity required to unveil any foreseen A/RPC proneness while meeting the real-time requirement of pilot-in-the-loop simulation is a critical task. Understanding what is required to anticipate unforeseen A/RPC proneness could be even harder.

A characteristic of adverse A/RPC is that there is indeed a relationship with the biomechanical characteristics of the pilot. The tests confirmed that A/RPC prone vehicle configurations only develop a clear adverse A/RPC event only with some pilots, whereas they appear to be immune when interacting with other pilots. A clear example is provided by the roll step manoeuvre performed using a vehicle model with lightly damped regressive lead-lag mode strongly interacting with the airframe roll mode.

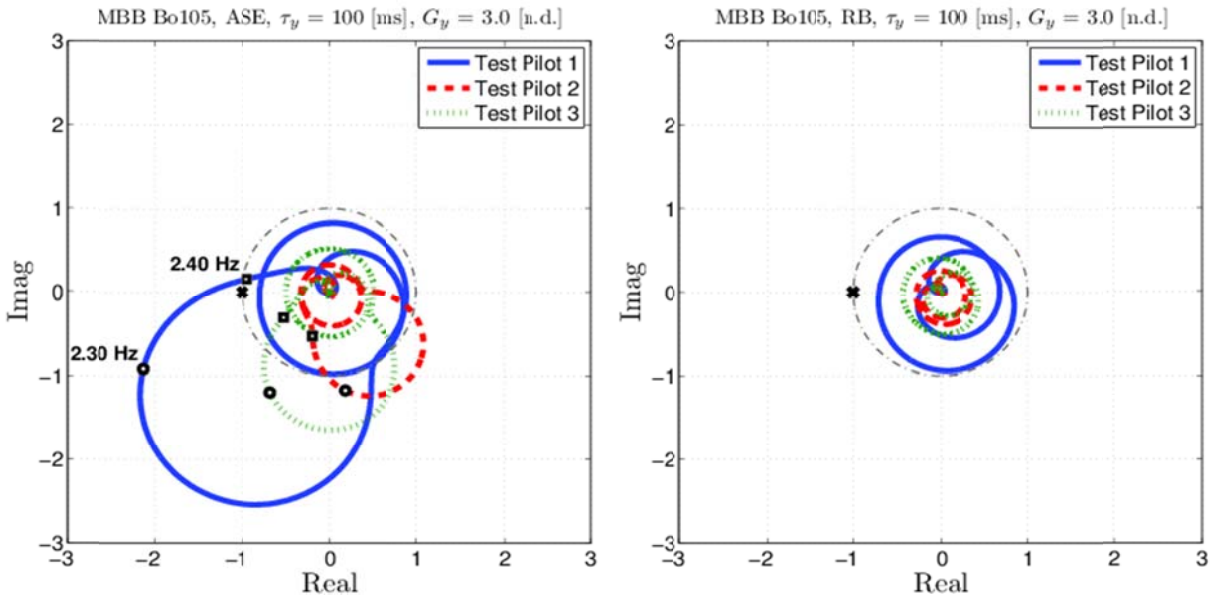

Figure 58 Loop transfer functions of the aeroservoelastic (left) and rigid-body (right) models of the helicopter (a BO105-like vehicle) in closed loop with the biomechanical transfer functions of the test pilots.

Figure 58 illustrates the Nyquist plot of the loop transfer functions of the aeroservoelastic (left) and rigid-body (right) models of the helicopter (a BO105-like vehicle) in closed loop with the biomechanical transfer functions of the test pilots that flew it in the flight simulator, identified from specific biodynamic tests about the lateral axis (Figure 59). In this specific configuration, the gearing ratio between the lateral displacement of the cyclic

stick and the lateral cyclic applied to the main rotor of the helicopter is three times the nominal value, and a time delay of 100 ms is applied.

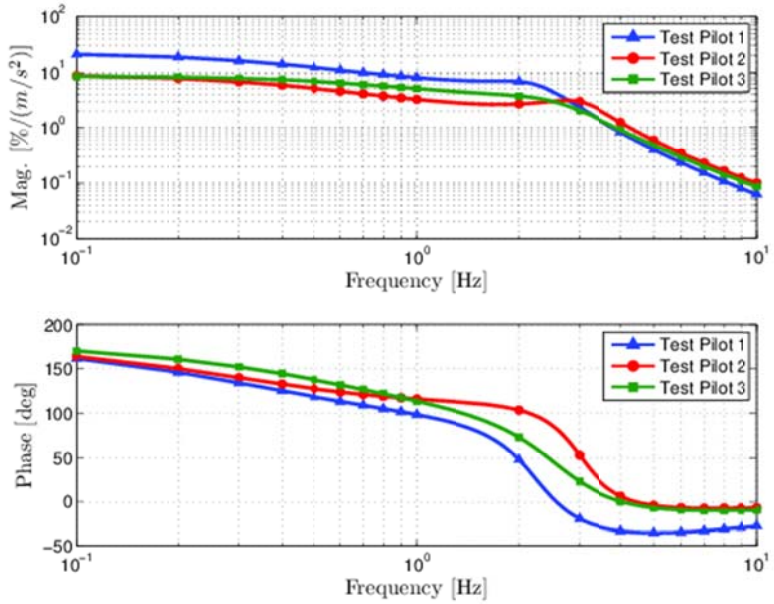

Figure 59 Biomechanical transfer functions of the test pilots; lateral motion of the cyclic control inceptor as a function of the lateral acceleration of the cockpit.

Figure 58 clearly shows that the loop transfer function is significantly affected by the biomechanical properties of the pilot. Figure 58 (left) also shows that for test pilot 1, such a configuration is predicted to be slightly beyond the stability limit, and thus unstable. Indeed, a PAO event resulted for such a pilot at a gearing ratio slightly lower than that in the figure: 2.5 instead of 3.

Determining what pilot model yields the smallest stability margin for a given vehicle, or determining whether available pilot models include the "worst case scenario" is an open issue. Recall that what is considered here as biomechanical pilot model includes the layout, geometry and often dynamics also of the cockpit and of the control device; thus, further separating it in components in order to determine the impact of specific parameters is even more difficult. At the present stage of maturity, the preliminary identification of test pilots' biodynamic feed through in the flight simulator before actually simulating flights aimed at unveiling A/RPC proneness seems to be a viable trade-off. In fact, it only requires a limited amount of time and operations that in principle could be automated and even performed on-line or at least right after the biomechanical data acquisition with minimal computational effort.

How to trigger a PAO (control gear gain and disturbance level), and necessary measures taken to assure the success of the experiment.

Triggering an adverse A/RPC event in the flight simulator may require the conception of specific Mission Task Elements (MTE) capable of unveiling the phenomenon. Among the manoeuvres tested in the flight simulator at the University of Liverpool, the vertical manoeuvre was partially successful with specially tailored, yet simple helicopter models. The roll step manoeuvre was successful with a single test pilot flying a realistic helicopter only modified in the gearing ratio between the control inceptors and the blade pitch and with the addition of time delay.

A specific aspect of the vertical manoeuvre that should be able to induce an adverse PAO is the transition from climb/descent to hover through a capture phase; the latter requires the pilot to move the collective control inceptor and start a tight tracking task to reach and maintain the desired performance, which represents a change in piloting attitude and thus may act as the trigger of the PAO.

Similarly, the roll step manoeuvre requires the pilot to change from straight and level flight along one side of the track to straight and level flight along the other side of the track, going through a turn to the right immediately followed by a second turn to the left. The last turn is followed by a capture manoeuvre in which the pilot tries to

put the aircraft into level flight. Such changes from a sharp turn to level flight, which require higher precision in positioning than the turn itself, also represent a change in piloting attitude and thus may act as the trigger for a PAO. Indeed, in the tests it was at such stage that the only pilot repeatedly undergoing PAO for a specific helicopter configuration had to abandon the task because of the uncontrollable oscillations associated with aeroelastic modes (the lightly damped regressive lead lag mode interacting with regressive flap and roll).

In conclusion, manoeuvres requiring the pilot to transition from one flight condition to another requiring higher precision through a capture phase seem to have the potential to act as triggers for adverse A/RPC events.

3 Simulator Guidelines for Fixed-wing

For the ARISTOTEL project, both the TsAGI PSPK-102 and NLR GRACE research simulator facilities were complementary to each other (each having their particular cockpit control capabilities) and are comparable to modern high fidelity fixed-wing flight simulators. Both facilities represent at least the industry standard applied by aircraft manufacturers for the design and implementation of new aircraft flight control systems and evaluation of large transport aircraft APC proneness. The results in this chapter are based on the practical experiences during the piloted testing of aeroelastic fixed-wing APC in both the TsAGI PSPK-102 and NLR GRACE facilities. The simulator settings and selected flight tasks can be applied as best practice for aircraft manufactures having facilities with similar specifications and/or hardware capabilities to test APC proneness during the flight control development process. These guidelines provide recommendations to experimentally verify the fixed-wing aeroelastic APC development criteria as reported in ARISTOTEL document D-5.1 “Design Guidelines for A/RPC Prevention” (ref. 18).
Based on the experimental data obtained during the simulator experiments, the Chapter determines guidelines to help recognize APCs on a simulator and contains requirements for all components of the flight simulation procedure, i.e.: simulated flight tasks, simulator characteristics and motion system drive algorithms, the aircraft models, and inceptor loading characteristics.

3.1 Simulator Settings for Aeroelastic APC

Aeroelastic APC is a result of a biodynamic interaction in the pilot-aircraft system. It means that APC phenomenon can be detected if only the disturbing accelerations are reproduced. This means that the equipment for piloted testing of aeroelastic APC should meet certain requirements and settings to adequately expose this particular APC phenomenon.

NLR GRACE facility

The Generic Research Aircraft Cockpit Environment (GRACE) is the NLR transport cockpit research simulator facility. The GRACE simulator features a two-seat flight deck typical of a transport aircraft. The instrumentation panel installed in the cockpit is equipped with large liquid-crystal displays that were configured to display the selected ARISTOTEL tracking tasks (

Figure 60). The main GRACE hardware settings as applied in the experiments are summarised in the following subsections.

Figure 60 NLR Generic Research Aircraft Cockpit Environment GRACE (left) and modular transport aircraft cockpit configuration (right).

TsAGI PSPK-102 facility

The general view of the TsAGI hexapod ground-based flight simulator PSPK-102 is presented in Figure 61. The instrument panel (see Figure 62) is equipped with 5 liquid-crystal displays: 2 duplicated displays (primary flight display and course-direction display) for both pilots (left and right) + 1 display located in the centre of the instrumental panel. The latter is used for research (or training) purposes, for example, for operational (during the experiments) displaying of flight parameter time histories. All of the displays are programmed with the help of a special program, DeskSim, developed by TsAGI. The program allows us to draw displays of any types for various aircraft. The screen resolution is 800x600 and the screen size is 10.4". Further PSPK-102 hardware settings are described in the following subsections.

Figure 61 TsAGI PSPK-102 flight simulator

Figure 62 PSPK-102 cockpit interior.

3.1.1 Motion filters

NLR GRACE facility

The NLR GRACE simulator has an electrically driven hexapod motion platform delivered by Bosch-Rexroth. Its performance capabilities are representative for today's commercially used motion platforms (Table 7). However, as can be seen from Table 7, its motion space is smaller compared to such commercial used platforms and the one that has been used by TsAGI for the ARISTOTEL experiments.

Table 7. NLR's GRACE Motion Platform Characteristics

Degree of Freedom	Excursions (pos, min)	Acceleration	Velocity
Surge	660 [mm], -557 [mm]	± 6.0 [m / s^2]	± 0.855 [m / s]
Sway	553 [mm], -553 [mm]	± 6.0 [m / s^2]	± 0.855 [m / s]
Heave	446 [mm], -414 [mm]	± 8.0 [m / s^2]	± 0.611 [m / s]
Roll	17.75 [°], -17.75 [°]	± 130.0 [° / s^2]	± 30.0 [° / s]
Pitch	16.60 [°], -17.25 [°]	± 130.0 [° / s^2]	± 30.0 [° / s]
aw	22.05 [°], -22.05 [°]	± 200.0 [° / s^2]	± 40.0 [° / s]

The motion drive algorithms used for the ARISTOTEL experiments are Bosch-Rexroth's implementation of the classical motion filter as developed by Reid and Nahon (Ref. 19). Configured with a conventionally tuned parameter set, these Bosch-Rexroth motion drive algorithms are assumed to be representative for a conventional hexapod motion cueing as nowadays is deployed by airline training facilities and manufacturer developmental testing. This base-line motion drive algorithm implementation is referred as the "classic" motion filter and, in contrary to the TsAGI motion drive algorithm, has not been modified during the test campaigns.

TsAGI PSPK-102 facility

TsAGI's PSPK-102 research simulator has a 6-DoF hydraulic motion system of a synergistic type. The motion system consists of six actuators with hydrostatic bearings. The actuator's stroke is 1.8 m. The maximum values of displacement, velocity and acceleration in this motion system for each degree of freedom respectively are shown in Table 8.

Table 8. TsAGI's PSPK-102 motion platform physical characteristics

	Travel, *m , deg*	Velocity, *m/sec, deg/sec*	Acceleration, *m/sec^2, deg/sec^2*
Surge	±1.75	1.5	7
Sway	±1.475	1.3	7
Heave	±1.23	1.1	8
Roll	±35.1	30	230
Pitch	±37.8	30	230
Yaw	±60	50	260

To measure and register the accelerations reproduced, six acceleration transducers are placed in the simulator platform which allows the measurement of linear and angular accelerations along all degrees of freedom.

The simulator frequency responses for all the six DoF are shown in

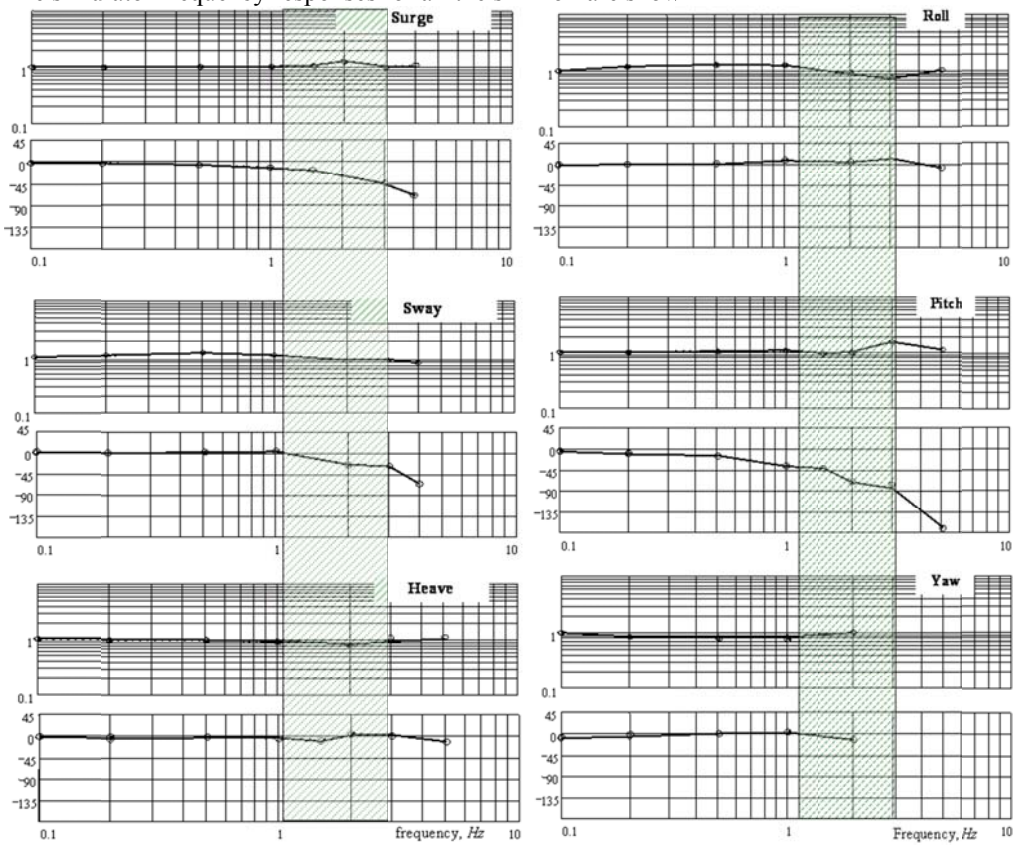

Figure 63.

It is seen that the motion system dynamics is sufficient for the purposes of our experiments: the amplitude and phase at the frequencies of structural elasticity (shown in green) do not have visible distortions, which can affect simulation results.

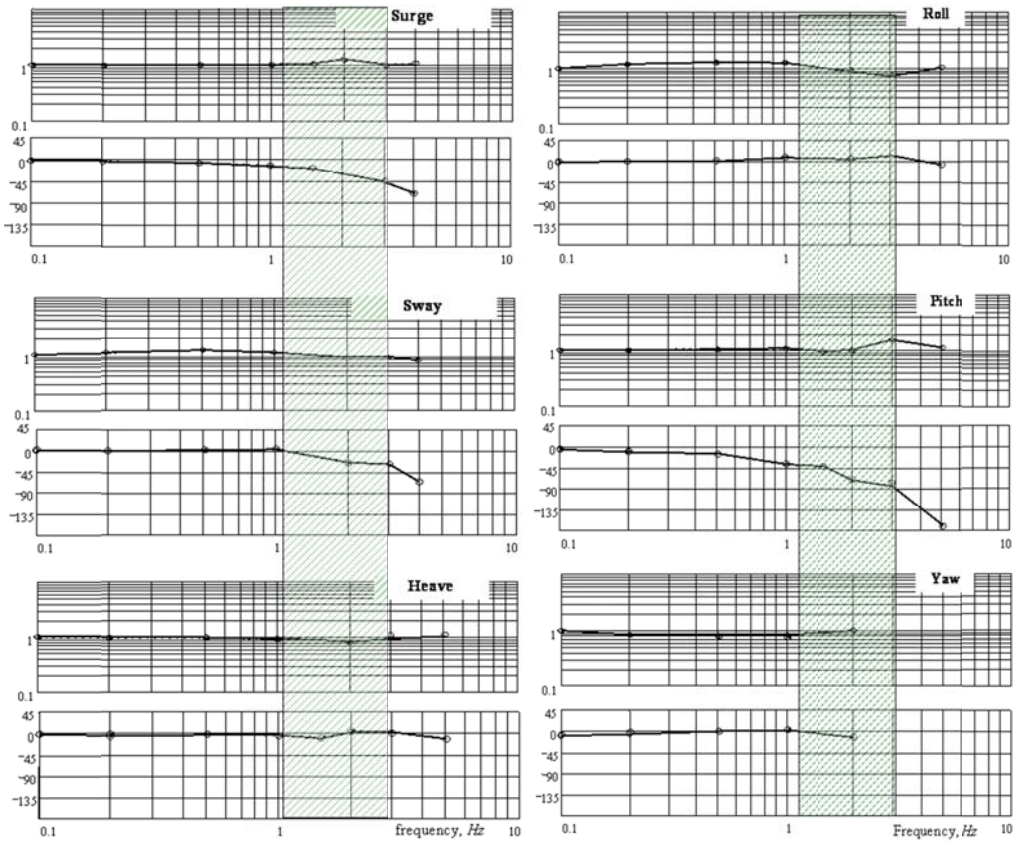

Figure 63 PSPK-102 frequency responses for all the 6DoF

Roughness of acceleration modelling for all degrees of freedom is determined according to AGARD's methods [12] and is shown in Figure 64. The data were obtained for a sinusoidal input signal with various amplitudes and at a frequency of 0.5 Hz. These characteristics are the root-mean-squares of the following parameters related to the amplitude of the first (basic) harmonic: all but the first harmonics, rtn (total noise); the second and the third harmonics, rln (low frequency noise); all but the first three harmonics, rhn (high frequency noise).

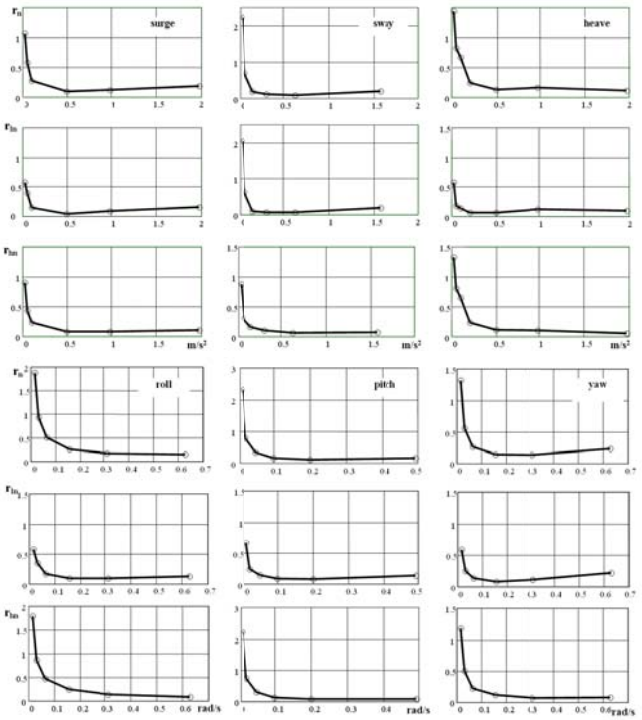

Figure 64 Roughness of acceleration reproduction.

3.1.2 Visual system

NLR GRACE facility

The GRACE visual system comprises a four-window collimated CGI system. The system offers each pilot a field of view of 89^0 (horizontal) and 27^0 (vertical).

TsAGI PSPK-102 facility

The PSPK-102 visual system is a four-window three-channel collimated system consisted of four optical collimators (2 for each pilot). The system provides 80deg(horizontal)x30deg(vertical) field of view for each pilot. The screen resolution is 1024x768 and the frame rate is 70 Hz. Out-window software was produced by the Russian Company “Transas”. The example of a visualization of a landing approach mode is shown in Figure 65.

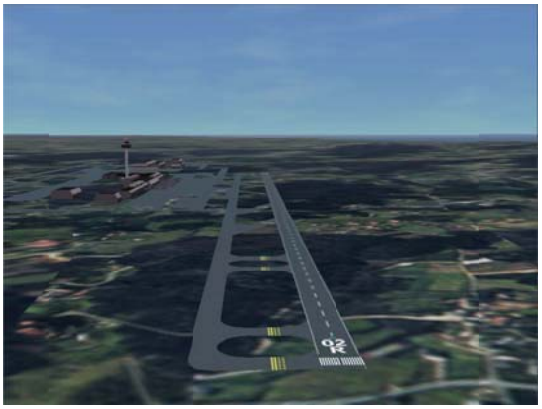

Figure 65 Landing approach visual scene.

The structural elasticity oscillations for frequencies above 1.5 Hz are not visually perceived by a pilot. Thus, no specific requirements were formulated and analyzed here for the visual system. Transport time delay and the time discrepancy between the visual and motion cues are small and correspond to the requirement, common for all simulators [ref. 22].

3.1.3 Flight control system

NLR GRACE facility

The GRACE electronic control loading and inceptor system for the ARISTOTEL trials included a right-hand centre stick configuration (e.g. applied in Boeing C-17, Figure 66 left) and right-hand sidestick (Airbus type configuration, Figure 66 right). Both inceptor control loading systems are programmable via software scripts that included the TsAGI/NLR specified and variable manipulator design characteristics.

Figure 66 NLR GRACE centre stick configuration (left) and side stick configuration (right).

3.1.3.2. TsAGI PSPK-102 facility

The two pilots' stations (left and right) are equipped with traditional column/wheels, pedals and side sticks. The latter are located at the left for the left seat pilot and at the right for the right seat pilot. The photo of the left pilot station with control inceptors is presented in Figure 61 (right).

All of the control inceptors are loaded by universal electrical loading systems from MOOG [ref. 13]. The systems of such a type are capable of reproducing any control forces, including that from aircraft hinge moments.

The standard control loading model reproduces static and dynamic feel system characteristics (in each control axis) in accordance with the following equation:

$$m\ddot{\delta} + F_{\dot{\delta}}\dot{\delta} + F_{\delta}\delta + F_{br}\,sign\delta + F_{fr}\,sign\dot{\delta} = F_{pilot}$$

where: m is inertia, $F_{\dot{\delta}}$ is damping, F_{δ} is force gradient, F_{br} is breakout force, F_{fr} is friction, F_{pilot} is forces applied by a pilot.

In of the experiments that were conducted during the project, all the feel system characteristics varied in a wide range.

3.2 Simulator Guidelines for Fixed wing aeroelastic APC

3.2.1 Selection of Flight Tasks

The tasks should be selected to demonstrate, first of all, the effect of structural elasticity and the role of inceptor characteristics in contributing to this effect. The effect of high-frequency lateral accelerations is most noticeable while performing two main piloting elements: step-wise inceptor deflections, when the pilot is in the open loop, and/or short and abrupt inceptor deflections while tracking. Taking this fact into account, the following piloting tasks were selected: Gust landing, Tracking the "jumping" runway, Roll tracking. All these piloting tasks assume abrupt inceptor activity, which results in intense lateral accelerations.

Gust landing

Initial conditions: altitude 262 *ft*, heading 0, distance from the runway 0.81 miles.

At 115 *ft* altitude a side step-wise left or right (random) wind gust is introduced:

$W_y = 8 \cdot t$ *knots* at $0 < t < 3$ *sec*,
$W_y = 24$ *knots* if $t > 3$ *sec*.

The task diagram is shown in Figure 67.

The wind gust introduced leads to aircraft rolling and lateral drifting. To compensate for the aircraft motion, a pilot should respond quickly to align the aircraft along the runway whilst avoiding large bank angles.

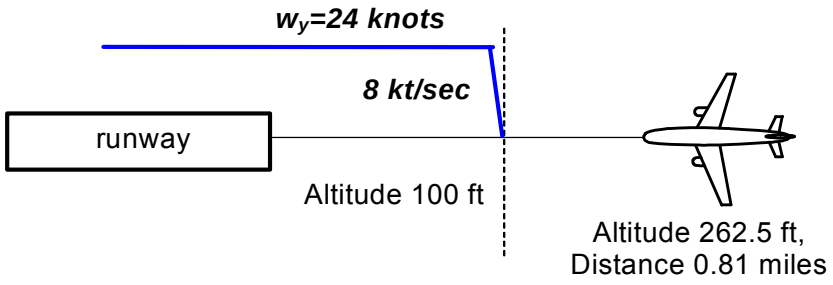

Figure 67 The diagram of the "Gust landing" task.

Tracking the "jumping" runway

The task is performed at altitude 50 *ft*, heading and bank angle are zero. In the course of experiment the runway right- and left-side shifting is simulated in turns every 20 seconds. The size of shifting is equal to the half-size of runway 98 *ft*.

The task diagram is shown in Figure 68.

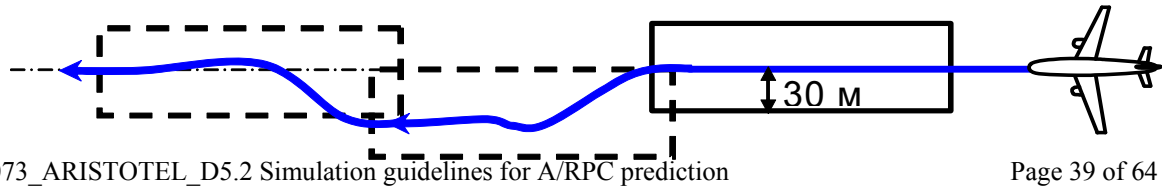

Figure 68 Block-diagram of the "jumping" runway task.

Roll tracking task

In the task, the block-diagram of the pilot-aircraft system corresponds to that shown in Figure 69. The pilot is to closely compensate for the tracking error, indicated on the HDD as a moving bar. The indicator is illustrated in Figure 69.

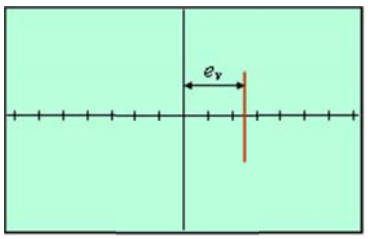

Figure 69 Indication of the visual signal for the "Roll tracking" task.

The visual input $\phi_{vis}(t)$ is a sum of sines:

$$\phi_{vis}(t) = \sum_i A_i \sin(\omega_i t + \phi_i) \text{ , where } i = 1...16$$

Parameters for the input signal are shown in Table 9.

Table 9. *Numbers (n_i) and frequencies (ω_i) of each of 16 harmonics, their amplitudes (A_i) and phases (φ_i).*

n_i	$\omega_i\ [rad/s]$	A_i	$\varphi_i\ [rad]$
3	0.2301	1.0	5.9698
7	0.5369	0.95	1.4523
11	0.8437	0.8	3.8129
17	1.3039	0.55	3.0535
31	2.3777	0.26	5.6002
47	3.6049	0.14	4.7884
59	4.5252	0.095	2.8681
83	6.3660	0.065	0.1163
109	8.3602	0.041	5.1611
137	10.5078	0.032	2.7942
157	12.0417	0.025	3.8669
191	14.6495	0.019	4.9759
211	16.1835	0.017	5.7919
239	18.3311	0.014	4.6383
281	21.5524	0.011	1.1075
331	25.3874	0.0085	2.5491

Figure 70 to Figure 72 presents recordings made in the course of simulation of the three tasks for the aircraft landing configuration. The configuration of the aircraft was as follows:

- inceptor type: a side stick;
- feel system characteristics: force gradient 6 N/cm, damping 0.27 N/cm/s, breakout force 4 N, friction 0. The listed values of the characteristics correspond to their optimum combination.
- structural elasticity: baseline

- roll control sensitivity: optimum

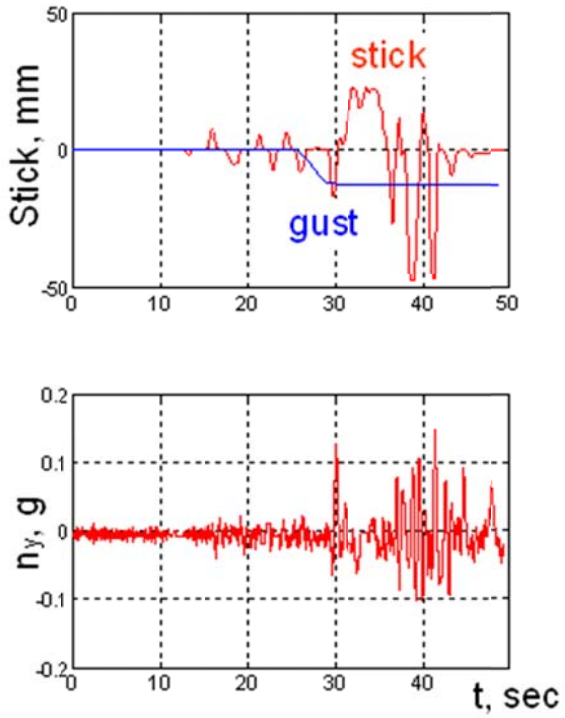

Figure 70 Time traces for Gust Landing task.

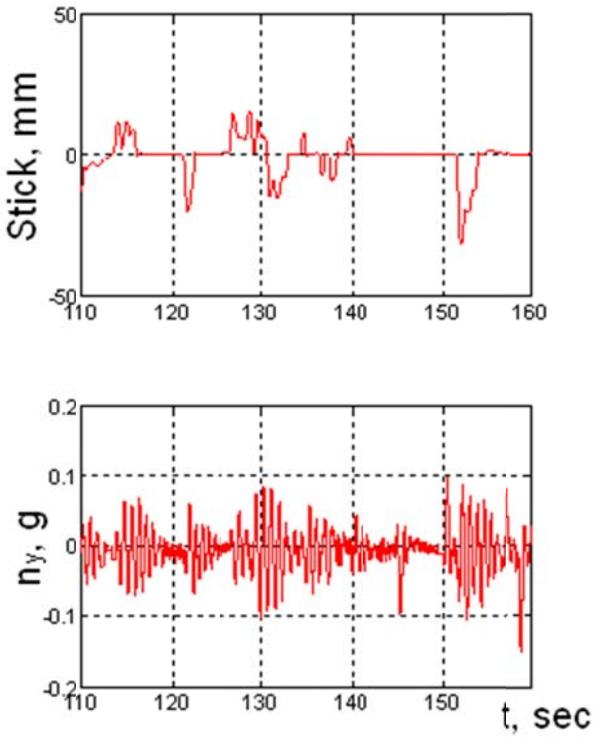

Figure 71 Time traces for Jumping Runway task.

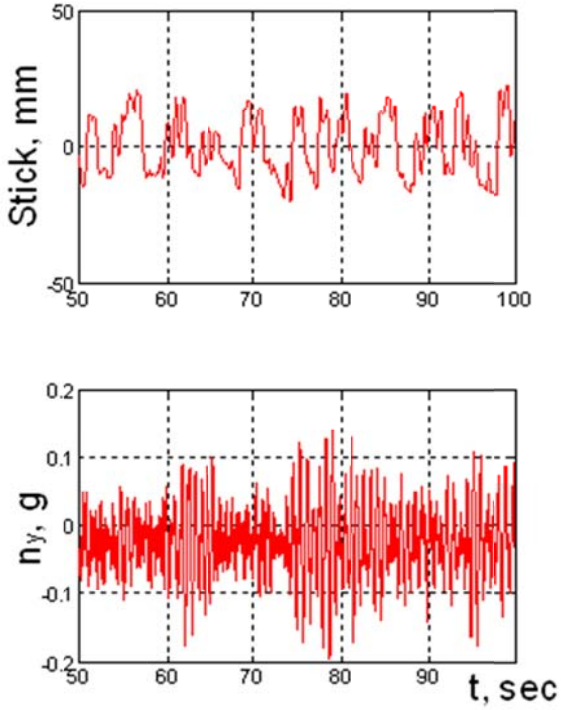

Figure 72 Time traces for Roll Tracking task.

It is seen that the selected flight tasks provoke high-frequency accelerations due to structural elasticity and, thus, can be recommended for purposes of demonstration and selection of aircraft characteristics and control inceptor feel system characteristics.

The more intense accelerations arise while performing the roll tracking task. Though the task is far from those typical of practice, its use can lead to more quick results in terms of APC detection, since, as it was shown in Ref. 4, one of the triggers for APC to arise is the level of the high-frequency accelerations.

3.2.2 Requirements for Aircraft Model

To develop a HQ criterion to assess the effect of structural elasticity and possible APC phenomenon caused by unfavorable configurations of control inceptor and structural elasticity characteristics, the general aircraft model was developed. The model allows a wide-range of variation for all of the pertinent factors, which can affect pilot-aircraft interaction and structural elasticity oscillations intensity: structural mode characteristics (frequencies, amplitudes), roll control sensitivity, inceptor feel system characteristics. The detailed description of the model is given in deliverable Ref. 14.

The simulator experiments conducted with the general model in Ref. 4 led us to the following recommendations helpful while deriving aircraft model for the particular aircraft.

Structural elasticity characteristics.

The Biodynamic effect of structural elasticity depends on the level of the high-frequency lateral accelerations, which, in turn, is a function of the structural mode amplitude, frequency and damping. Figure 73 and Figure 74 show time traces recorded in TsAGI simulator experiments for different structural mode amplitudes and different structural mode frequencies corresponding to the 1st (Figure 73) and the 2nd (Figure 74) single modes. It can be seen from the Figures that the level of lateral accelerations increases approximately in proportion to the elastic mode amplitude.

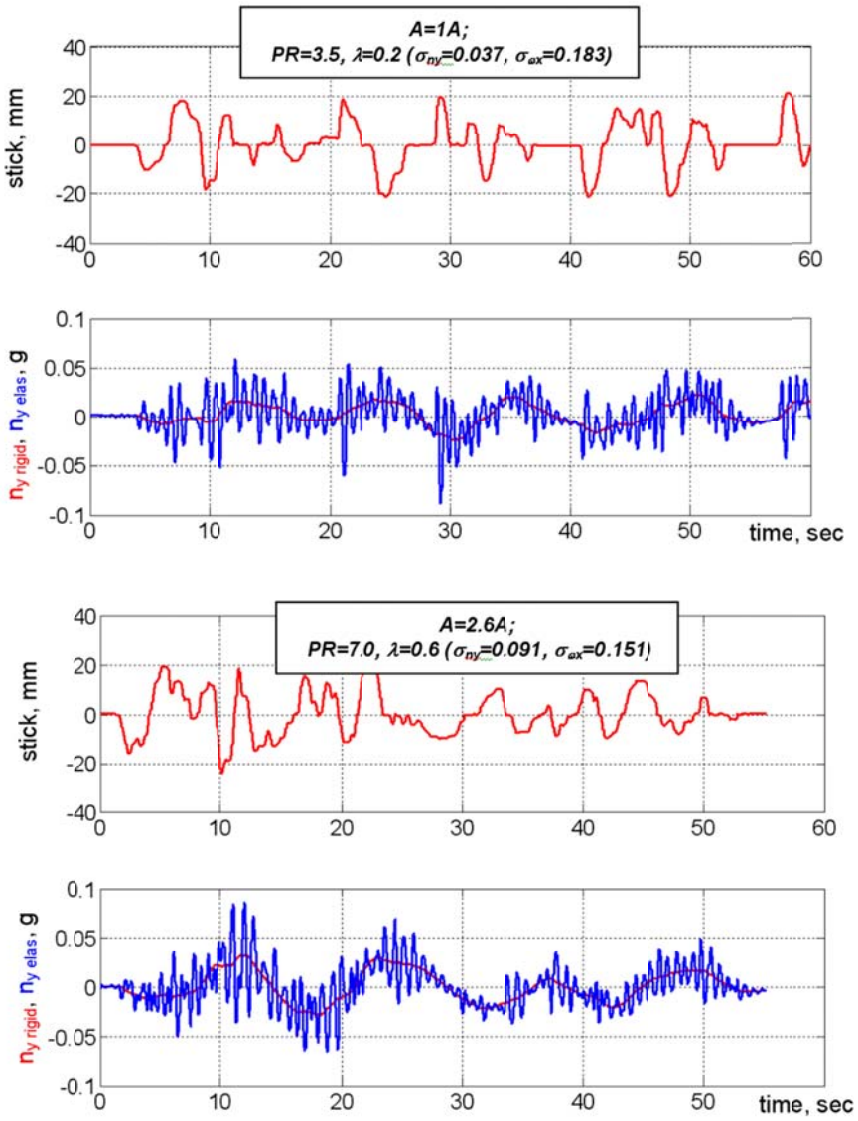

Figure 73 Effect of structural mode amplitude. Single 1st mode (f=1.57 Hz). Side stick. "Jumping runway".

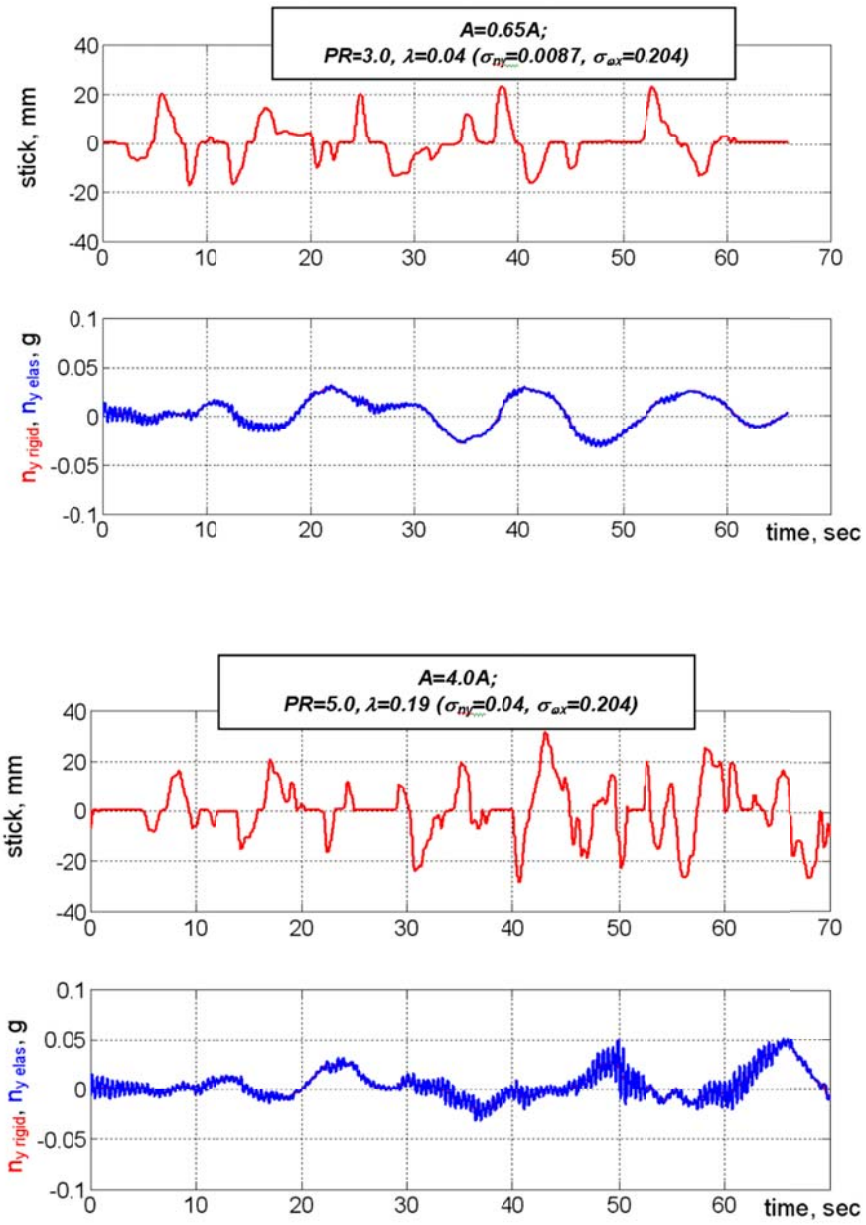

Figure 74 Effect of structural mode amplitude. Single 2nd mode (f=2.2 Hz). Side stick. "Jumping runway"

A criterion developed in the project shows, the pilot rating of an elastic aircraft is a function of the acceleration intensity, i.e. the level of the lateral accelerations. Thus, the structural elasticity characteristics should be accurately modeled to ensure adequate pilot opinion of the aircraft HQ, or to give a student pilot an adequate idea of the aircraft performance.

Even if structural elasticity itself is not noticeable and does not cause any negative reaction in a pilot, its reproduction can affect pilot performance and selection of aircraft characteristics. It can be seen from Figure 75 that, being added, the structural elasticity affects pilot control activity (wheel deflections become much smaller).

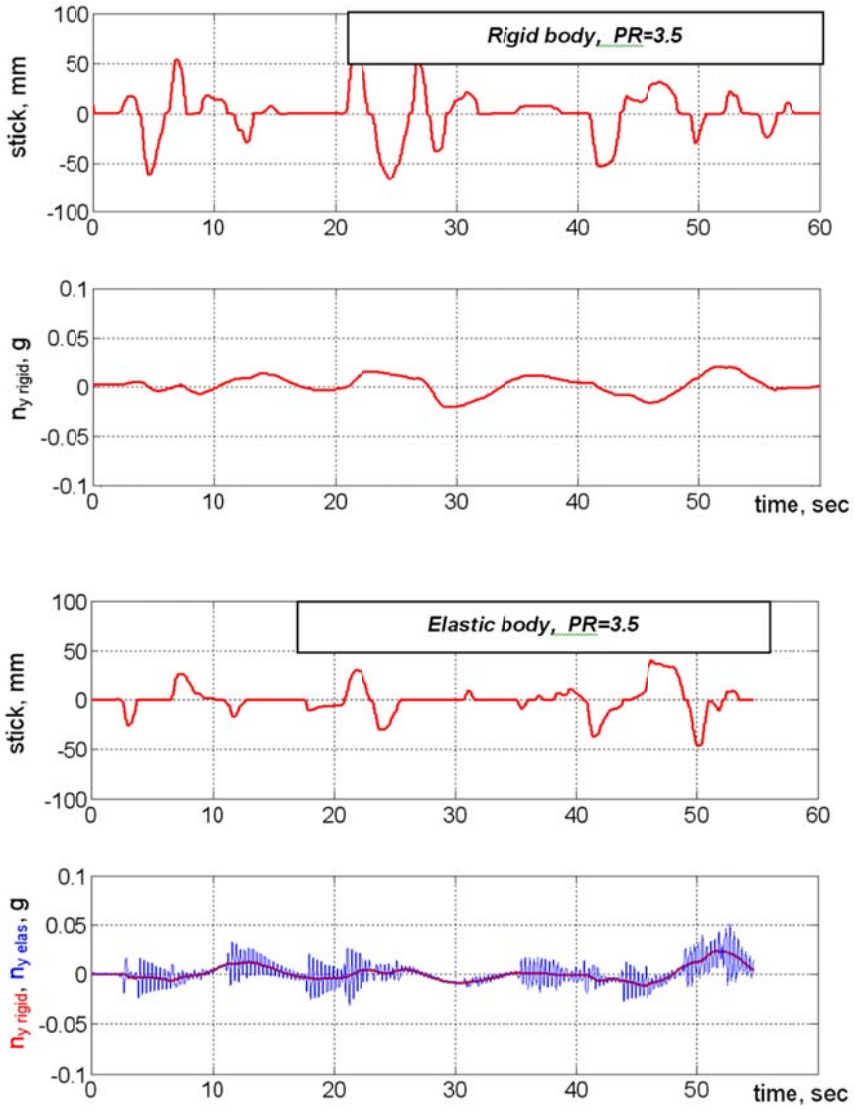

Figure 75 Effect of structural elasticity on pilot activity. Single 3rd mode (f=3.0 Hz). Wheel. "Jumping runway".

Rigid-body characteristics

Aircraft dynamic characteristics affect, first of all, the HQ of the rigid-body aircraft. Roll control sensitivity is the characteristic, which affects both rigid-body and elastic-body aircraft HQ. In order to isolate the effect of structural elasticity, the experiments, in which roll control sensitivity was varied, were conducted for both rigid-body and elastic-body configurations.

Aircraft gain (control sensitivity) affects high-frequency lateral accelerations caused by structural elasticity to a considerable extent, which can be seen from the time histories in Figure 76. This and other data show that as roll control sensitivity increases, the intensity of accelerations due to structural elasticity increases and pilot ratings worsen and, vice versa i.e. as control sensitivity is below the optimum value, the tendency to biodynamic interaction reduces.

That is why the pilot can select an optimum control sensitivity for an elastic aircraft, which is lower than that selected for the rigid-body configuration. It means that the selection of the control sensitivity for the elastic aircraft must be conducted for the aircraft model with structural elasticity. This fact should be borne in mind when selecting a control sensitivity value.

The peculiarity of the effect of control sensitivity is in agreement with the data obtained earlier by Johnston and McRuer (see ref. 15) for the ratchet phenomenon caused by low roll mode time constant.

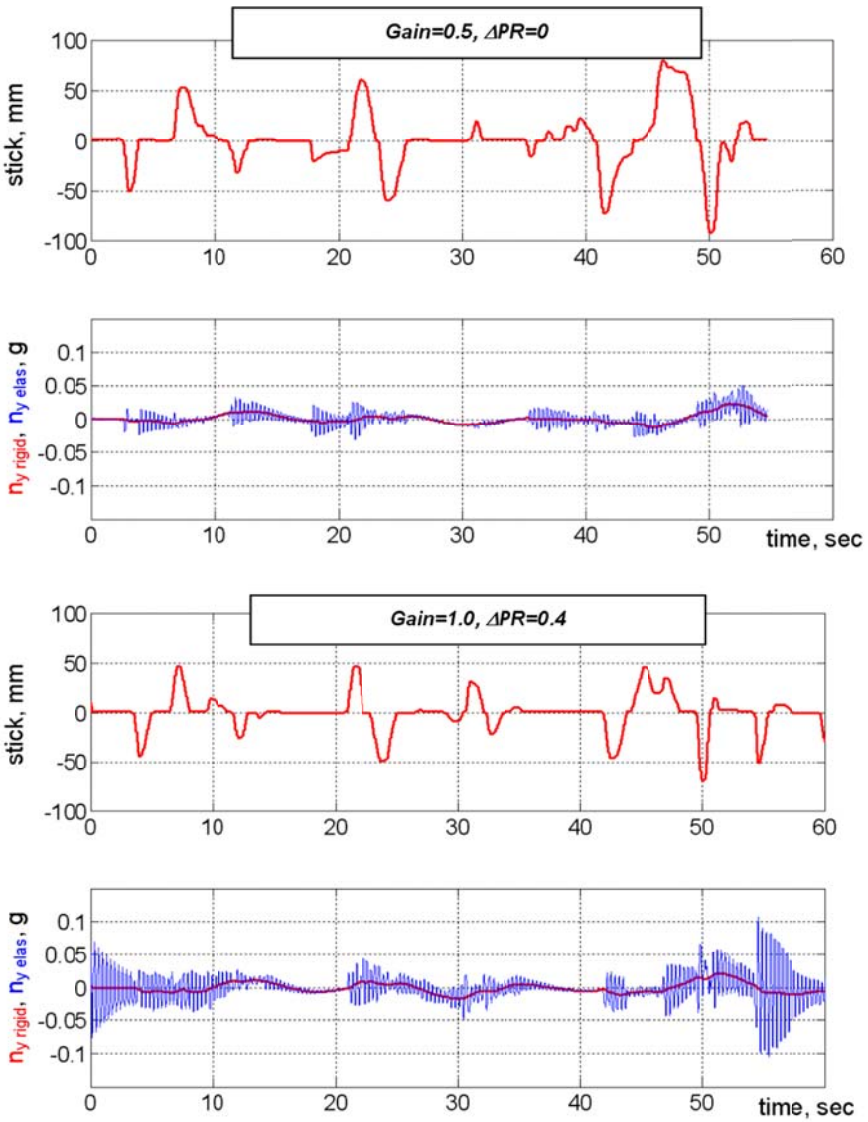

Figure 76 Effect of control sensitivity. Single 3rd mode. Wheel.

It has been mentioned in some publications (see Ref. 14, for example), that the ratchet phenomenon caused by low roll mode time constant (rigid-body dynamic performance) is difficult to detect in on-ground simulators. As opposed to that, high-frequency accelerations due to structural elasticity are easily reproduced and, thus, their effect can be studied experimentally in simulator tests.

3.2.3 Requirements for Motion System Dynamics

The results of APC simulation may be different depending on the motion system performance of the particular simulator. Usually, the modern flight simulators have good dynamic performance with the wide bandwidth and small phase at the high frequencies. Nevertheless, we need to know the flight simulator frequency characteristics in order to prevent possible simulation distortions caused by amplitude or phase imperfection. Thus, experiments for the 2nd fixed-wing test campaign (see Ref. 4) were dedicated to estimate the effect of the motion system distortions on the simulation results.

Speaking about the high-frequency oscillations due to structural elasticity, the differences are determined mainly by motion system frequency response, i.e. amplitude and phase distortions. The effects of amplitude and phase distortions are different in terms of pilot's perception and interpretation, and, thus, treated differently. Let's consider first amplitude distortions.

Amplitude distortions

The amplitude distortion means local amplitude increases or decreases, as it is shown in Figure 77. In terms of elastic oscillation reproduction, it means that some of the elastic modes would be intensified, and the other would be diminished. The pilot cannot isolate the level of accelerations caused by structural elasticity characteristics in the aircraft model from the total level of accelerations he/she perceives during the simulation. In other words, the level of accelerations perceived is attributed by a pilot to the aircraft considered.

The effect of the structural mode amplitude is demonstrated by time traces in Figure 73 and Figure 74. The pilot ratings given by the pilot for different amplitudes are quite different. For example (Figure 73), an increase of the amplitude by factor 2.6 leads to pilot rating degradation by 3.5 point, this would automatically shift aircraft HQ to Level 2. Though the pilot rating degradation is caused by simulator imperfection rather than aircraft model, the considered aircraft could be wrongly declared unacceptable for the serial production.

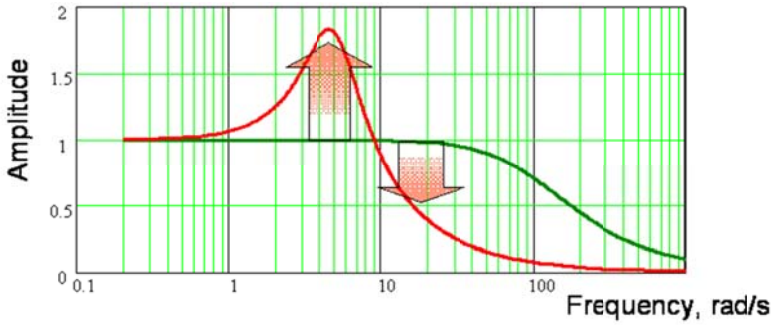

Figure 77 Possible amplitude distortions of simulator frequency response.

The local drop of the amplitude of the simulator frequency response can lead to overestimation of the aircraft HQ. This case is even more dangerous than previous, since the aircraft HQ peculiarities would be discovered only in in-flight tests, which would be followed by time and cost consuming procedure for their "treatment".

Thus, amplitude distortions can considerably affect pilot opinion of the aircraft HQ and result in incorrect conclusions being drawn.

There are two ways to proceed. One of them is the correction of amplitude by correction of the input signal. The type of amplitude distortion shown in Figure 77, can be approximated by the filter of the second order:

$$Y(s) = \frac{1}{T^2 s^2 + 2\varsigma T s + 1}$$

To implement it, we used the first and second input derivatives, which are the outputs of the respective drive algorithm filters. In this case, signal S_{contr}, which controls the cockpit lateral displacement actuators, is obtained as follows:

$$S_{contr} = S + 2\varsigma T\dot{S} + T^2\ddot{S}$$

where S is the given cockpit lateral displacement, which is output of the respective drive algorithm filter, T and ς are parameters of the second-order describing function $Y(s)$ approximating simulator frequency responses in sway.

Another method to correct simulator frequency response is to correct frequency response amplitude at the given frequencies corresponding to certain structural elasticity modes. This is done by adjusting the gain of each elastic mode component according to the value of frequency response amplitude at the given elastic mode frequencies.

It means that when the amplitude of frequency response manifests amplifying at a certain elastic mode frequency, the corresponding elastic mode component has to be decreased, and, vice versa.

Nevertheless, this method of correction is not perfect. First, each variation of elastic lateral acceleration frequencies leads to the necessity of adjusting the gain coefficient of the corresponding elastic mode, which is not very convenient. But the most important fact is that this method cannot be applied to the continuous spectrum signals, typical of rigid aircraft motion. Second, this method does not allow phase response correction.

Phase distortions

The phase lag at high frequencies in the simulator frequency response is natural, but its excessive values can be the reason for instability in the pilot-aircraft system. That is why this kind of distortion is the subject of a special interest in our 2nd test campaign (ref. 4).

A single-mode structural elasticity was considered, corresponded to the first and third mode of the basic structural elasticity configuration. The experiments were conducted for a sidestick.
The additional phase was modeled by introduction of the pure delay $e^{-p\tau}$ into the motion system drive algorithms, as shown in Figure 78.

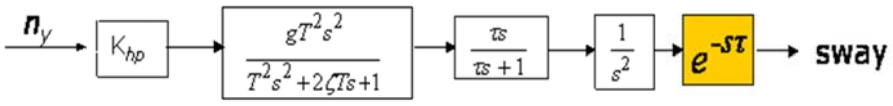

Figure 78 The method by which the phase lag was introduced in sway.

The data obtained during the course of experiments are shown in Figure 79.

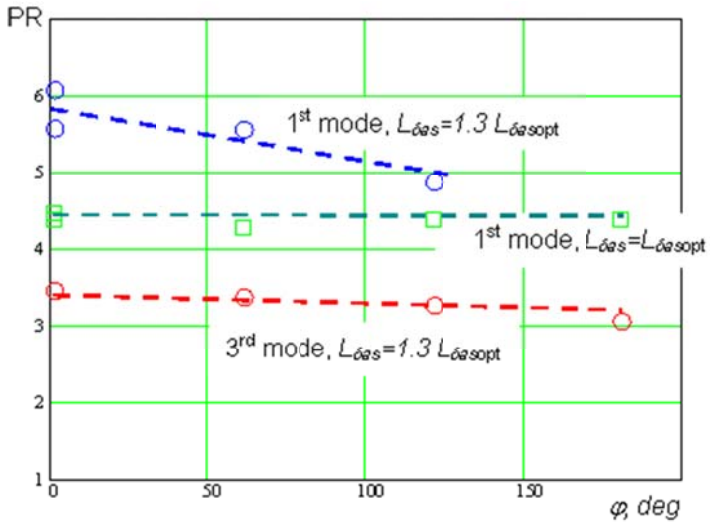

Figure 79 Effect of phase distortion on pilot ratings for the elastic aircraft.

It is seen that the effect of simulator phase distortion depends on the aircraft control sensitivity ($L_{\delta as}$) and structural elasticity characteristics. If the level of the lateral accelerations σ_{ny} is not great (see red line for the 3rd mode in Figure 20), the effect of phase distortion is not noticeable even if the roll control sensitivity is 30% greater than optimum; if the level of the lateral accelerations is great (see blue line for the 1st mode in Figure 79), the effect of phase distortion is more noticeable for roll control sensitivity greater than optimum.

The fact the phase distortion leads to better pilot ratings is due to the fact that, according to pilots' comments, the phase distortion "put off" the accelerations onset, i.e. aircraft response is not so abrupt, and pilots interpret the accelerations as a high-frequency disturbance, and do not connect them with their control activity.

3.2.4 Requirements for Motion System Drive Algorithms

Usually, reproduction of the lateral accelerations are made by using high-pass filters to reproduce high-frequency acceleration components with the help of simulator linear displacements in sway, and low-pass filters to reproduce low-frequency acceleration components with the help of cockpit tilting in roll. The total lateral accelerations reproduced by the two filters look as shown in Figure 80 (green line).

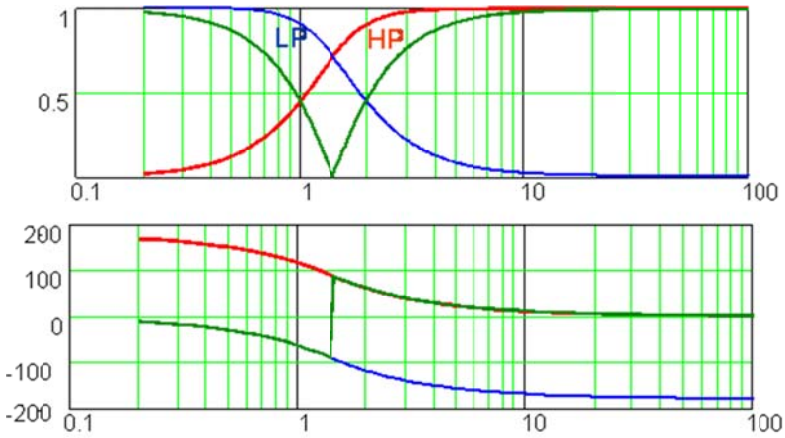

Figure 80 Frequency response of the low-pass (LP), high-pass (HP) filters and their sum (green line).

Reproduction of lateral accelerations to study the effect of aircraft structural elasticity may differ from that used for another handling qualities research, since for the rigid-body aircraft, reproduction of lateral accelerations affects piloting beneficially. In our case, lateral accelerations due to structural elasticity affect piloting negatively and the pilot rating depends on the acceleration intensity. Thus the main rule to follow while simulating structural elasticity effect is to be close to real flight. This means that we cannot scale down lateral accelerations. Lateral accelerations should be reproduced full-scale, as we did in the course of our experiments.

On the other hand, pilot's perception of high-frequency accelerations depends on the level of low-frequency components of the lateral accelerations. Thus we need to take this fact into account as well. Experiments conducted in the European project SUPRA (see Ref. 16) showed that the perception of high-frequency acceleration depends on the level of background low-frequency acceleration, and this regularity depends on the frequency of the acceleration imposed. It is seen from Figure 81 that as the frequency of the imposed accelerations increase, the pilot's sensitivity to their perception increases as well. This regularity depends also on the frequency of the background accelerations. In the experiments, the background acceleration frequency was 1 rad/s. In our case the background accelerations are accelerations at the center of gravity, and their frequency is even lower. The imposed accelerations, i.e. accelerations due to structural elasticity, are of frequencies above 1.5 Hz, and their values are much above their threshold value. In other words, in our case the pilot perception of the elastic oscillations does not practically depend on the rigid-body lateral accelerations.

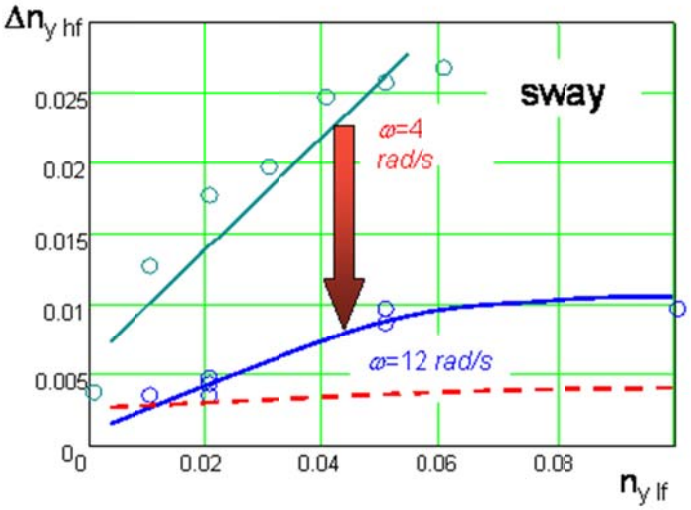

Figure 81 Thresholds of high-frequency lateral acceleration perception as a function of the low-frequency lateral acceleration

It means that the pilot perceives high-frequency component of lateral acceleration only, and we can recommend reproduction of the high-frequency acceleration component only, i.e. accelerations from the structural oscillations ($n_{y\ eb}$). In PSPK-102 it was done as shown in Figure 82. It is seen from the frequency responses shown in Figure 83, that in this case the high-frequency accelerations due to structural elasticity (i.e. accelerations above 1 Hz) can be reproduced full-scale.

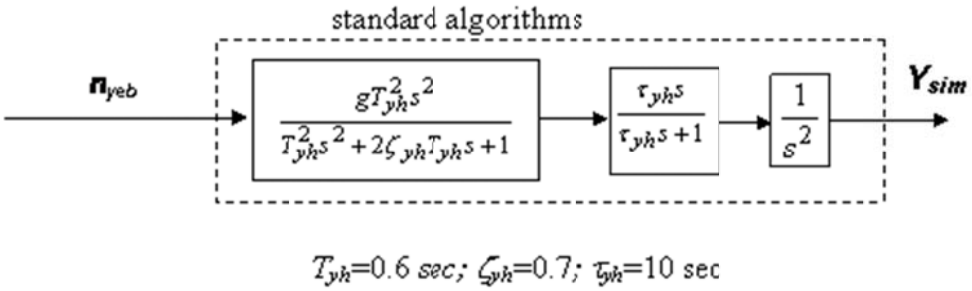

Figure 82 Block-diagram of acceleration reproduction in sway.

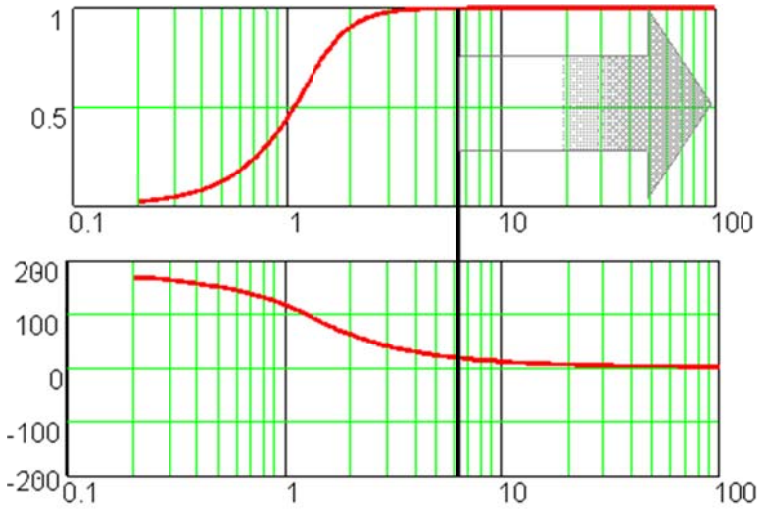

Figure 83 High-pass filter frequency response to reproduce high-frequency disturbing lateral accelerations.

3.2.5 Requirements for Inceptor Loading Characteristics

It was shown during biodynamic tests (shaking without piloting) and simulator tests (piloting the aircraft model) that the type of control inceptor can be the reason for the biodynamical interaction and lead to dramatic HQ degradation. The time traces recorded during one of the APC cases are shown in Figure 84.

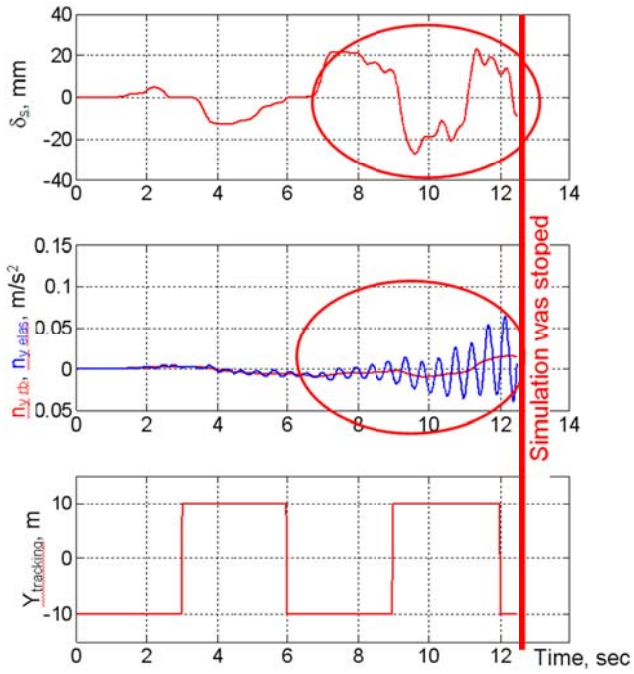

Figure 84 Time traces of one of the APC cases obtained during experiments with a sides stick. Feel system characteristics and control sensitivity corresponded to their optimum. Single 2nd structural mode, A=2A. ΔPR=7.

As the biodynamic tests showed (see Ref. 17), the biodynamic interaction is especially pronounced for the centre and side sticks. It should be mentioned as well that in the piloted experiments, APC cases were observed only for

the control system with a side stick; no one case of APC with a traditional wheel was observed in the experiments.

As it was shown in experiments of the 2nd test campaign (see Ref. 4), the introduction of the additional damping into the inceptor loading system can improve pilot ratings (see Figure 85) by reducing the level of the disturbing lateral accelerations, and, thus, reducing the APC tendency.

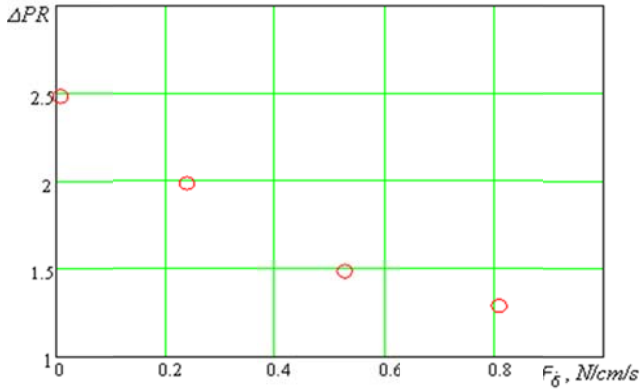

Figure 85 Beneficial effect of sidestick damping on pilot rating of elastic aircraft.

Thus, designers of the control systems with side sticks or center sticks must pay a due attention to selection of the inceptor feel system characteristics. To select them properly, the inceptor loading system must allow variation of the parameters (damping, in particular) with a wide range.

4 Training protocols for unmasking A/RPC in simulator

Improving the performance of pilots within A/RPC exercises in a simulator is discussed in the present Section. It should be mentioned from the beginning of this Chapter that the highest emphasis can be set on exposing the pilots to those mission tasks that are most appropriate to trigger A/RPCs. In this sense, in previous Sections and in Refs. [3, 4], the task guidelines were identified that the engineer can use in the simulator in order to trigger A/RPCs. How to deal with these as a pilot when flying these tasks is discussed in the present Section.

4.1 Training protocols for RPC

The example below relates to helicopters as these are more PIO prone. The same discussion can be applied as well to APC. It is well known that the hovering task is already difficult, especially for student pilots, and is one that can trigger RPC problems. Ref. 1 gave an insight into this, the helicopter's most basic exercise. Consider a helicopter hovering in calm air when suddenly a gust moves its nose slightly down. If the pilot (or an artificial stability augmentation system) doesn't stop this motion, the helicopter will go back and forth across its starting point with an ever-increasing swinging motion. This is characteristic to the so-called helicopter "hover instability" in which the helicopter motion in pitch attitude and velocity will increase in time even after the disturbance stopped. Figure 86 illustrates the physical background in the event of a disturbance of the hover condition. Looking at this Figure it follows that the instability is in fact due to the property of flapping motion to always damp the fuselage motion resulting in a perturbation in the opposite direction with increased amplitude. This is essentially the phugoid motion with an exchange of energy between speed and altitude with a typical period for helicopters of 20 seconds. For aircraft, one can consider that roll motion behaviour is analogous to helicopter's longitudinal behaviour.

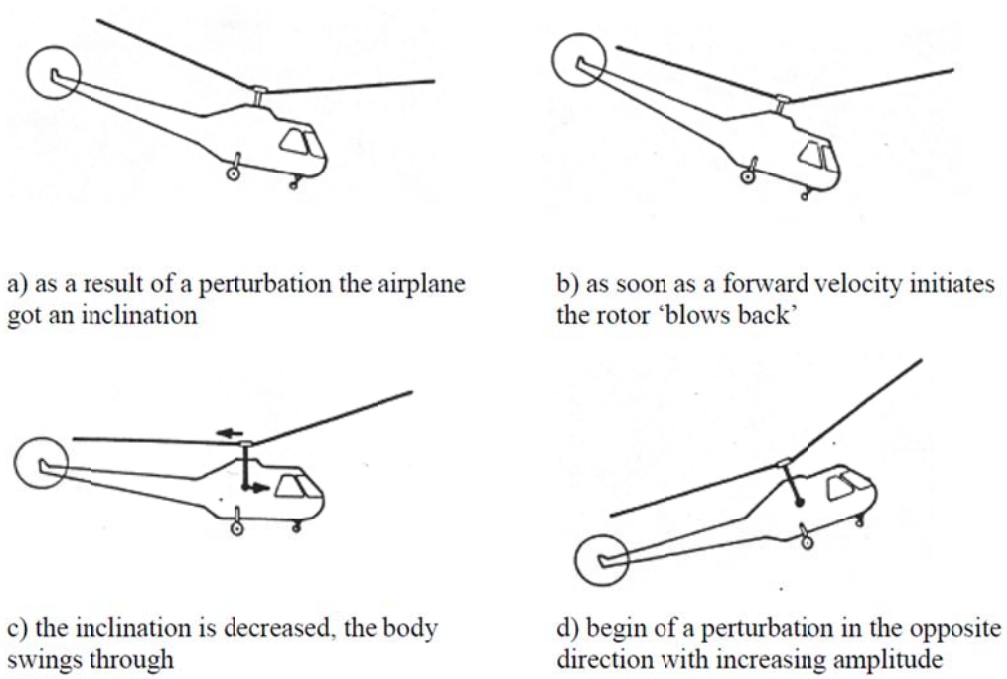

Figure 86 Cause of dynamic instability of a helicopter in hover (source Ref.2)

To be able to stop this swinging motion, the pilot must constantly move the controls. In developing the ability to do this, he/she must learn: 1) to put in just enough control without overreacting and 2) to anticipate the motion. However, before learning these skills the pilot student will overreact in his controls, among others because the helicopter is unable to react instantaneously to pilot commands. Therefore, there is a time lag between the control input and the helicopter response and this lag encourages the "impatient" pilot student to use too much control – with the resulting overshoot and panic correction. This over-controlling coupled with the poor stability characteristics and the requirement to control altitude and heading as well gets the pilot immediately into trouble. The situation changes quickly from that of the pilot driving the oscillation into the pilot driven by the oscillation, exactly as in a "real" RPC.

Reference 5 explains the first experience that a pilot may have when learning to fly helicopters: "*The first thing that will probably happen after you say, " I have control," is nothing. If the aircraft is trimmed up properly for straight-and-level flight, it will pretty much stay that way and fly by itself without pilot input. This will continue for several seconds, which will seem like minutes, and just when you think you're starting to get the hang of it, you'll notice you've started to turn off from the selected cardinal heading. This is natural and to be expected because most of us (before we become helicopter pilots) are not too precise with our feet. What has happened is that in resting your feet on the pedals, you've inadvertently put a bit more pressure on one of them. This very correctly will cause the helicopter to yaw in that direction. Your initial deviations probably won't occur with the cyclic or collective controls because you'll be concentrating much more on these. Actually, with a comfortable amount of friction on the collective and throttle, you can probably ignore your left hand. The cyclic will require the most attention and you've be trying very hard not to change its position in the slightest from where your instructor left it. Eventually, no matter how much you initially try not to, you'll forget about your feet. Next, you will try to correct for the change in heading. You'll probably do two things (if you've read this book, listened to your instructor, and are thinking at all sensibly). First, you'll push harder on one of the pedals and if lucky, it will be the one that turns you back toward the heading. Second, you'll try to help the machine back by adding cyclic in the direction you want to go. I f the first action doesn't create problems, the second one will. If you push the correct pedal, you'll probably push too hard. Well, what do you expect? You've never done this before. This initiates the turn back toward the heading too quickly and then you'll push too hard on the other pedal and then too hard on the first one again and back and forth until everything is totally out of whack and the instructor takes over. Believe me, by the time he says, " I have control," you'll want to give him the controls so quickly you'll forget to visually check that he really does have them before you release them. If you make a cyclic input, you'll start rolling as well. And, because most people tend to pull back on the cyclic a little when they try to move it from one side or the other, you'll start some pitching movements, too. Pitching movements are when the nose starts to bob up and down. As it goes up—because you unintentionally pulled back on the cyclic—you'll try to counter this by moving the cyclic forward, probably too much. As the nose dips below the horizon, you'll counter*

again with back cyclic. And every time you try to correct pitch, you'll be adding more and more roll inputs to correct the first one you made to counteract the pedal movement you didn't mean to make in the first place."[ref. 5]

An explanation of the pilot encountering an RPC is given also in reference 5. In pilot's jargon RPC is called "Pilot Induced Turbulence (pit)". "*Everybody has experienced over-controlling or pilot induced oscillations and everybody does it. (Some pilots say "pit," for pilot induced turbulence). Even experienced, professional pilots over-control when they check out in a new aircraft. It's almost impossible not to because every aircraft has a different feel. The helicopter is going to be making all sorts of funny gyrations in the sky until you start to get a feel for it. Don't worry about it. It 'll come. Ten hours of stick time is a fair rule of thumb before most pilots begin to feel comfortable in a new machine. But that's only a rule of thumb and everybody's different. As a new pilot, with less experience to draw upon, it will take you longer, maybe three or four times as much, so don't worry if you don't catch on right away. Everything comes with practice. If you get discouraged, re-read the quote by President Coolidge* (A/N 30th USA President)…(A/N "*Nothing can take the place of persistence. Talent will not; nothing is more common than unsuccessful people with talent. Genius will not; unrecognized genius is almost a proverb. Education will not; the world is full of educated derelicts. Persistence and determination alone are the omnipotent*"). *So much for the pep talk, we're still trying to fly straight-and-level. When the gyrations get too bad or the instructor feels your control movements are so much out of sync that you're not learning anything, he'll take the controls. In a second or so, the aircraft will be flying straight-and-level again, steady as a rock, and you'll swear your instructor is possessed with mystical powers. Don't let this bother you. It happens to everyone and your instructor just wants to give you a chance to start from a controlled position again. One common instruction technique is to give the student only one or two controls to handle, while the instructor takes care of the other controls. This permits the student to concentrate on handling one control correctly while the other controls don't go to pieces. Because changes in one control can affect the others, it's easy to start to feel like a one-armed wallpaper hanger on a wobbly ladder until you get the feel for how much control input is needed for a given situation. Watch what your instructor does to calm things down. It'll look like black magic at first, but basically what he'll do is simply put the cyclic, collective, and tail rotor pedals back to their neutral cruise flight positions and hold them there. When he wants to make a correction to come back on altitude or heading, he'll do it by increasing finger pressure on the appropriate control, not by moving it. Flying a helicopter takes an extremely fine touch. In fact, once you have trimmed up in straight-and-level flight, added a tad friction to the collective, and equalized the pressure on the pedals, you can easily fly by using only the thumb and forefinger of your right hand. Finding the neutral positions and acquiring the necessary touch is what it's all about. It simply takes time and practice."* [Ref. 5]

To understand the characteristics of the pilot immediately before and after an A/RPC, ARISTOTEL conducted identification experiments in two rotorcraft research simulators (SIMONA simulator (SRS) at Delft University and HELIFLIGHT-R simulator at Liverpool University) to determine the pilot control strategy during a time delay triggered 'possible' RPC event for a hover stabilization task of a Bolkow Bo-105 rotorcraft simulation model (see ref. [6]) For this, a roll disturbance compensatory manual control task was flown in the two simulators. The duration of each experiment consisted of two phases as presented in Figure 87: Phase I before applying a time delay and Phase II after applying a time delay of 300 milliseconds in order to trigger the RPC. In each phase, 81.92 seconds of measurement data (Tm_I and Tm_{II} in Figure 87) were used for Linear Time Invariant (LTI) identification of pilot control behaviour. Between the measurement partitions of these two phases, the so-called "pilot Post-Transition Retention phase" exists, in which the pilots still believe that they are controlling the vehicle operated prior to the change of control element dynamics before adapting to the time delay applied in the controls. The disturbance forcing function was given to pilots as a sum of ten sinusoids between 0.061 Hz and 2.76 Hz. Four test pilots (A, B, C and D) were used in these experiments and the mean measured frequency response (Hp_m) was determined in Phase I and Phase II. It was observed that for example, in Phase I Pilot B and C showed almost same frequency responses whereas pilot A and D showed higher visual gains. Pilot D showed a noticeable distinct higher phase margin.

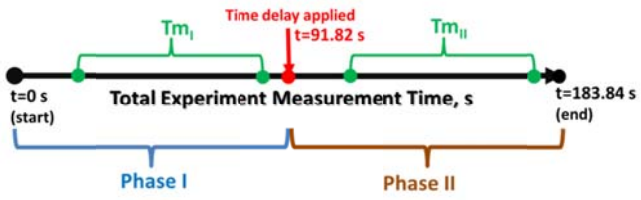

Figure 87 Understanding pilot behaviour in RPC

The results in Phase II show the adaptation of the pilots to the RPC event (the RPC was introduced by adding time delay in the control path). It was observed that all pilots matched almost the same low frequency (up to 3 rad/s) magnitude response except Pilot D, who responded with the highest visual gain which implies a higher compensatory task performance with a high crossover frequency than other pilots. All pilots showed an increased lead generation during Phase II. Another result is the reduction of pilots' neuromuscular natural frequency, such that the frequency of the magnitude peak has lower values in Phase than Phase I. This shows that the pilot's physical adaptation to RPC is to gain more phase while coping with added time delay. Akin to neuromuscular resonance frequency, pilots also showed lower neuromuscular damping (for example pilot A showed signs of a significant under-damped neuromuscular activation when compared to Phase I results). The pilot adaptation when exposed to RPC triggered time delay could be summarized as:

- There is a reduction in pilots' visual gains during RPC, especially at low frequencies, this in order to increase the vehicle stability;
- There is an increase in the pilots lead equalization (equalization can be defined as the pilots capacity to adapt their control behaviour according to the vehicle dynamics, in other words to equalize what the aircraft is doing. It is generally accepted that the pilot equalization consists of one lead term and one lag term) of the pilots in order to overcome the additional time delay introduced in the control path;
- There is a decrease in the pilot neuromuscular frequency and neuromuscular damping;

One of the lessons learned from this identification exercise showing the pilot strategy as exposed to RPC demonstrates how important the human reaction time is in A/RPCs and one can be trained for improving this reaction time in A/RPCs. Another lesson is that when exposed to a time delay in the control system, a professional pilot is backs off from the control loop trying to calm the aircraft oscillations.

Discussing human reaction time, this can be defined as the time elapsing between the onset of a stimulus and the onset of a response to that stimulus. Simple Reaction Time is generally accepted to be around 220 milliseconds [ref. 7]. In simple reaction time experiments, there is only one stimulus and one response. Simple reaction time can be gauged in a variety of ways but basically a person is asked to place their finger on a button or a switch and told to manipulate that button or switch in response to a light or a sound. In this case the person is reacting to a "Known Stimulus" during the observe step and using a pre-determined response during the decide step. It should be noted here that many researchers have found that reaction to Auditory Stimulus is faster than reaction to Visual Stimulus. Perhaps this is because an Auditory Stimulus only takes 8-10 Milliseconds to reach the brain, but a visual stimulus takes 20-40 milliseconds to reach the brain [ref. 8]. A more familiar example of simple reaction time is the "Brake Light Theory" "*You are driving down the road and you "Observe" the brake lights of the car in front of you come on. This is a "Known Stimulus" because you expect while driving to have this happen and because you expect this, you already have a predetermined response, which is to remove your foot from the accelerator and apply the brake. From the time we Observe the brake light (Onset of Stimulus) to the time we begin to remove our foot from the accelerator, (Onset of a reaction to Stimulus) less time has elapsed than if we were responding to an Unknown Stimulus, which brings us to the Flash Bang Theory. Our reaction time is slower when we are responding to "Unknown Stimulus…"*.(from Boyd's O.O.D.A Loop and How We Use It By: Tracy A. Hightower, www.tacticalresponses.com)

There are other factors that can affect the human reaction time, some of which can be overcome with training. In 1952 Hick [ref 9] confirmed that by going from one response choice (Decision Step) to two, response time increased by 58%. This is widely known as "Hick's Law" or "Hick–Hyman" Law [ref. 10] and describes the time it takes for a person to make a decision as a result of the possible choices he or she has. According to this law, increasing the number of choices will increase the decision time logarithmically. The Hick–Hyman law assesses cognitive information capacity in choice reaction experiments. The Hick-Hayman law has been repeatedly confirmed by subsequent research. For a pilot, if the vehicle does not react how it should, the more choices the pilot has to choose from, the slower he/she will react. As an example if a student through training has learned that at any given time his/her vehicle may experience a type one malfunction and he/she has trained to have a single response then as in the "Brake Light" example, through training and experience the malfunction has become a "Known Stimulus" and the solution has become a predetermined response and reaction time is faster.

Other factors that affect the human reaction time are Denial and Emotional Filter. Denial is when you refuse to accept or Deny that this is happening to you. Emotional Filter is a lot like Denial except that you wish that this were not happening to you. Both of these things can and will affect your reaction time but fortunately they can be overcome with training as this commonly happens with people who have little or no training.

In 1960, Henry and Rogers [ref. 11] found that not only does increasing the number of responses affect human reaction time, but also by increasing the complexity of the tasks, induces stress that can adversely affect your reaction time. In their experiment, while doing simple reaction time test, the participants were instructed to place their finger next to a switch and when they hear a certain sound, they are to flip the switch. After each subject's time was registered and recorded they used the same group and did the same test but added another task to do after flipping the switch. The subjects were told to flip a second switch after completing the second task. In both tests, the only time recorded was the time it took to push the first button and the researchers found that the added stress of having a more complex task to perform caused each subject's reaction time to increase by an average of 31%.

Fighter pilots know that Fatigue is also an important factor affecting pilot reaction time. Colonel Boyd, the initiator of the OODA concept in training in the 1950's (Observe, Orient, Decide and Act), observed that in a dogfight between F-86 and Mig-15, the pilots flying the F-86 were winning although it was known that F-86 aircraft was slower and less manoeuvrable when compared to Mig-15. The reason for this was that the F-86 was fully hydraulically controlled and the MIG-15 was only hydraulically assisted. This meant that Boyd's pilots could operate their aircraft with easy and gentle manipulation of the controls, while the MIG pilots had to work harder to manoeuvre their aircraft. Boyd found that the more his pilots manoeuvred and the longer a dogfight persisted the more fatigued the MIG pilots became and the slower their reaction time became until the F-86 pilots were able to manoeuvre their aircraft into a position of dominance. Discussing on the O.O.D.A. Loop mentioned above, one can conclude that this concept can apply also to pilot training in an A/RPC. This loop is a way of explaining how the pilots go through the process of reacting to stimulus. First, one observes or gets information (although we process approximately 80% of the information we receive with our sense of sight, we can and do make observations with our other senses).The next step is the Orient step in which he/she determines what it means to him/her and what he/she can do about it. In the Orient stage one is focusing his/her attention on what he/she has just observed. The next step is the Decide step in which one has to make a decision on what to do about what he/she has just observed and focused his/her attention on. Once one has made his/her decision, finally the last step comes, that is to Act upon that decision. The O.O.D.A loop is what happens between the onset of a stimulus and the onset of a reaction to that stimulus and this can be trained. In a pilot training protocol for RPC, the first and last stage of the OODA loop, i.e. Observe and Act are important (see also the APC recommendations below)

4.2 Training protocols for APC

The experiments conducted and analysis made in the previous chapters allow us to make the following recommendations for training organizations to demonstrate aeroelastic APC events to pilots and to train them to recognize and avoid these dangerous and unpleasant events.

Since the work done in the project dealt with roll control axis, the recommendations given here, are for aeroelastic APC known as "roll ratchet".

Types of simulated flight tasks.

The APC is a non-regular, accidental event. Among the triggers which can provoke APC to arise, is pilot "tight" control activity. That is why the flight tasks should force the pilots to apply such style of control. Three types of flight tasks are recommended:

1. Gust landing
2. Tracking the "jumping" runway
3. Roll tracking task

The description of the tasks is given in Section 3.2.1.

The pilots are instructed to make sharp inceptor deflections to counteract the wind gust, or to track the visual signal. The sharp control activity would provoke structural elasticity oscillations which can lead to APC event.

If there is no possibility on the training simulators to vary aircraft characteristics to demonstrate the APC tendency, the modern inceptor loading systems can allow variation of feel system characteristics, for example damping. The damping variation is an effective way to demonstrate APC tendency changing.

How to identify that an APC event is in the progress

The aeroelastic APC characterizes itself by sustained accelerations at the frequencies corresponding to the dominant structural elasticity mode. The auto-oscillations can make further task fulfillment difficult or impossible at all, and lead to dramatic pilot rating degradation.

Figure 84 above demonstrates APC in progress. As this and other recordings made during APC cases show, the aeroelastic APC grows very quickly. At the beginning the pilot can feel a certain small-amplitude "beating", which within 2-4 seconds can develop into serious sustained accelerations with rather large amplitude (up to 0.1 g). The accelerations cause abrupt body and limb-manipulator system displacements, which interfere with the voluntary pilot activities and lead to the accelerations intensification.

Piloting techniques to avoid APC and to cope with it in flight

The aeroelastic APC is an accidental event, which can occur even if structural elasticity characteristics and inceptor feel system characteristics are optimum (as it was observed in experiments in the ARISTOTEL 2nd test campaign). The trigger can be pilot sharp control activity. Thus, the general recommendation for the pilots to avoid aeroelastic APC in flight is to avoid the sharp inceptor deflections.

The introduction of the additional inceptor damping is the implementation of the idea. The damping does increase the total inceptor forces at the frequencies typical of the active control activity, but prevents the sharp control inputs leading to APC.

The control systems with side sticks and centre sticks are more prone to aeroelastic APC. If the APC occurs with such types of inceptors, the only recommendation is to release the stick until the oscillations stop. If the pilot continues to struggle with APC trying to stop it with a tighter grip, the accelerations can become even worse.

The control systems with traditional wheel are not so prone to the high-frequency APCs. Nevertheless, the APC for such type of inceptor cannot be totally excluded, for example, when the pilot controls the wheel with one hand on (the other hand is on the engine levers). In the project we did not consider this case in detail, but can assume that if wheel is deflected more than 45°, then an APC is possible.
If the APC occurs with a wheel, the recommendation to the pilot is to apply the other hand: two-hand control provides APC's reduction and disappearance.

4.3 Training Protocols for A/RPC: Pilot Guidelines

During the ARISTOTEL project, 6 professional pilots were used for investigations. Furthermore, some non-professional pilots were used. An important element of all test campaigns was the correct briefing, and engagement of pilots. It was important for the pilot to know what is expected of them during the test campaign, and the requirements for testing. This is very important for ensuring that standardized test procedures are in place. Below are some of the key requirements when conducting trials;

Task Performance Aspects

It is important that the pilot is fully aware what is expected from their completion of any tasks. Given the chance, the pilot will most likely not do the task as it was originally designed. Therefore, it is very important that the pilot is aware of what is expected, and for the engineer to carefully monitor what the pilot is achieving. RPCs only materialize in certain, possibly rare, circumstances. One pilots operation of the vehicle may be very different from the next. This is why it is important that all pilots are required to excerpt the same levels of task aggression. The tasks used in this project, performance tolerances have been carefully engineered to ensure that the required levels of aggression are met. If the pilot does not perform the task to these tolerances, it is likely they will not expose the same A/RPC tendencies as the next. In terms of standardization, it is really important that all pilots complete the task as it was designed. Furthermore, it is not acceptable for the pilot to estimate what will occur if they increase their performance to meet requirements. Occasionally, the pilot will comment "If I kept doing this, I would award a rating of ….". This is sometimes common in HQ investigations, where the rating is very dependent on the task performance. As pilots become more proficient with tasks, their confidence and performance is likely to improve. In A/RPC investigations, the dynamic nature of couplings could change as the pilot becomes more proficient with the task. The result may be that the tendency for A/RPC increases.

Awareness of what constitutes A/RPC

The test pilot is always willing to investigate performance aspects of the aircraft. However, the pilot must be able to recognize what they are looking for in the investigations. Furthermore, they must be aware of all definitions,

and the understanding of various terms. If not correctly instructed, pilots will usually try and apply their opinions, which may not necessarily agree with the opinions of those conducting the flight test. In order for pilot comments, any subjective ratings, and any opinions of the flight test team to correlate, both must have an understanding of the others views.

Therefore, in the briefing process, it is important that all pilots are made familiar with what constitutes an un-commanded oscillation, an un-demanded motion. Furthermore, it is important that pilots understand what they are assessing, and when the assessment takes place.

Observation of pilot performance

During the test process, pilots may be experienced to unfamiliar and undesirable vehicle characteristics (These are of course what the test team likely wants to see). However, these experiences may be slightly alien to the pilot, and may leave them less than happy. There could be a number of implications from this that the assessing engineer must be aware of. The first is pilot reluctance; it must be observed whether pilots are exerting consistent performance, throughout their flight tests. Ideally, at the end of day, the pilot should be performing in the same manner they performed at the start of the day. If the pilot feels any discomfort or sickness, it is likely that they will dramatically change the way in which they fly the task to compensate. The second aspect is pilot tiredness. If pilots are tired, it is likely that there performance would suffer alongside their ability to convey what they felt during the task completion. This will lead to both spurious pilot ratings and the comments, and also likely lead to a reduction in task performance.

Pilot Comments

The most important aspect of any piloted investigation is collection of their comments. Subjective ratings are taken in order to guide the pilots comment process. Questionnaires or other measures may be employed to also assist. After each test case, the pilots should give comments on their experiences which they had during completion of the task maneuver. When presenting results or discussing performance with pilots, their comments should always be used.

5 Conclusions

Concerning the **Simulation Task Recommendations** it was proved that **for helicopters,** piloting tasks that force high gain, closed-loop pilot control should be selected. These tasks must have well defined, and well justified performance parameters, to force consistent pilot control strategy. However, tasks are expected to expose performance beyond that expected for normal operation of the vehicle. Suitability of tasks can be assessed using Handling Qualities Ratings.

ADS-33 manoeuvres are a suitable baseline for RPC investigations. Tasks designed to assess vehicle handling qualities can unmask RPC tendencies, when flown using a certain piloting strategy. However, tasks do not necessarily expose deficiencies for all pilots. Pilots who are cautious, or use an ‘open-loop’ control strategy, were shown to complete ADS-33 manoeuvres without exposing deficiencies due to RPC triggers. As a result, \ high scatter in pilot subjective ratings was observed. Therefore, tasks must be modified to ensure consistent performance between pilots. Modifications should create a task that is operationally relevant, but pushes the vehicle beyond the normal operational range.

Moving the reference pole of the Precision Hover course has the desired effect of decreasing pilot variability, and increasing consistency amongst results. Furthermore, more dynamic and dangerous PIOs were observed, exposing the possible oscillations that may occur in the vehicle. Moving the pole closer to the pilot also increased the emphasis on the forward cue during completion of the manoeuvre. This was found to increase task performance consistency, and reduce differences in performance attributed to differences in the simulation cueing environment.

Changes in performance to the Roll Step did not show a large difference in subjective ratings awarded. However, increasing the task speed did show a difference in results obtained. It is recommended that the task performance requirements are again revisited. Very limited investigations with narrower gates showed a large increase in PIO susceptibility. It is envisaged that changing task performance in this way will increase the success of the manoeuvre in exposing PIOs.

A range of pilots, of different experience and backgrounds should be used for completion of Mission Tasks. Eventually, the aircraft will be flown by inexperienced pilots, who will have very different flying abilities to experienced test pilots. In the investigations, it was found that operationally current pilots are less likely to expose RPC tendencies whilst completing ADS-33 style manoeuvres. This is as they are more used to flying the manoeuvre in an environment where safety is paramount. These pilots will be more likely to back-out or abandon task as soon as they experience any problems. Test pilots who are less current, or more 'experimental' will give less consideration for safety, and will likely try and push the vehicle to its performance limitations. Changes in performance tolerances should reduce the variability offered with regards to pilot control strategy.

For aircraft, determined are the requirements to all elements important to ensure adequate fidelity of aeroelastic APC simulation (flight tasks, aircraft model, simulator dynamics, motion system drive algorithms, inceptor loading system), based on the extensive simulator experiments and the basic knowledge on the pilot's motion cues perception:
Three flight tasks are recommended to use simultaneously: gust landing, tracking the "jumping" runway, roll tracking task. The tasks force the pilot to make step-wise control inputs, which provoke high-frequency structural elasticity oscillations and can lead to APC.
The model of structural elasticity must be accurately presented. The level of accelerations determines the pilot opinion of the aircraft handling qualities and is one of the main factors leading to APC tendency.
Flight simulator must have good dynamic performance. Amplitude distortions can lead to the distortions of accelerations intensity reproduction and, as a consequence, to APC tendency overestimation or underestimation. The effect of phase distortion depends on the structural elasticity characteristics, but in any case lead to APC tendency underestimation, due to the fact the aircraft response becomes not so abrupt, and pilots interpret the accelerations as a high-frequency disturbance rather than consequences of their control activity. The recommendations in this guideline are given to improve the flight simulator dynamic performance by introduction of the special correction filters.
Lateral accelerations should be reproduced full-scale. Scaling down would reduce the accelerations' effect and distort pilot opinion of the elastic aircraft handling qualities or pilot training. Since the perception of accelerations at the frequencies typical of structural elasticity does not practically depends on the low-frequency accelerations caused by rigid-body aircraft motion, only high-frequency filters can be used to reproduce the lateral motion.
Inceptor loading system must allow variation of the feel system characteristics in a wide range in order to help designers to properly select them and to demonstrate to the pilots the APC tendency caused by inadequate inceptor characteristics. Special attention should be paid to the control systems with sidesticks and center sticks, as they are the most prone to APC.
These set of recommendations for fixed-wing flight control system developmental testing can also be applied for accurate pilot training for aeroelastic APCs, which include types of simulated flight tasks, identification of the APC in progress, piloting techniques to avoid APC and to cope with it in flight.

6 References

1. De Groot, S., Pavel MD, New Insights Into Pilot Behaviour During Hazardous Rotorcraft Pilot Induced Oscillations", American Helicopter Society 62nd Annual Forum, Phoenix, Arizona, May 9-11, 2006
2. Fay, J., 'The Helicopter; History, Piloting and how it Flies, Newton Abbot, David and Charles, 1976
3. ARISTOTEL Consortium, Deliverable No. D4.6 Simulator test data analysis of the 1st test campaign, 2012
4. ARISTOTEL Consortium, Deliverable No. D4.8 Simulator test data analysis of the 2nd test campaign, 2013
5. Padfield Randall R., Learning to fly Helicopters, TAB Books, 1992
6. Pavel M.D., Yilmaz, D., Dang Vu, B., Jump M., Lu, L., Jones, M., Adverse Rotorcraft-Pilot Couplings – Modelling and Prediction of Rigid Body RPC Sketches from the Work of European Project ARISTOTEL, 39th European Rotorcraft Forum, Moscow, Russia, September 3-6, 2013. Paper No.125
7. Laming, DR, Information theory of choice-reaction times, Academic P., 1968
8. Tapani N. Liukkonen, Human Reaction Times as a Response to Delays in Control Systems - Notes in vehicular context, www.measurepolis.fi, 2009
9. Hick, William E.; On the rate of gain of information. Quarterly Journal of Experimental Psychology, 4:11–26, 1952.

10. Hyman, Ray; Stimulus information as a determinant of reaction time. Journal of Experimental Psychology, 45:188–196, 1953
11. Schmidt, RA and Wrisberg CA, Motor Learning and Performance: A Situation-based Learning Approach, Human Kinetics, 4th Edition, 2008
12. AGARD, "Motion system dynamic performance of flight simulators." AGARD-AR-144, 1979.
13. MOOG, ECoL 8000 User Manual. Report No. CL_GMP_1U. Fokker Control Systems, 2000.
14. ARISTOTEL Consortium, "Aircraft and rotorcraft modelling for aero-servo-elastic A/RPC". ARISTOTEL Deliverable D3.4, March 2012.
15. Johnston, D.E. and McRuer, D.T. "Investigation of Limb-Sidestick Dynamic Interaction with Roll Control", AIAA Paper No.85-1853.
16. Zaichik, L.E., Yashin, Y.P. and Birukov, V.V., "Peculiarities of Motion Cues Perception Against G-load," *Conference Proceedings of the 4th European Conference for Aerospace Science*, Saint Petersburg, Russia, 2011.
17. ARISTOTEL Consortium, "Pilot modeling for aero-servo-elastic A/RPC". ARISTOTEL Deliverable D3.6, February 2013.
18. ARISTOTEL Consortium, "Design Guidelines for A/RPC Prevention". ARISTOTEL Deliverable D5.1, September 2013.
19. Grant, P. R., and Reid, L. D., Motion Washout Filter Tuning: Rules and Requirements, Journal of Aircraft, Vol. 34, (2), March-April 1997.
20. Cameron, Neil; Padfield, Gareth; "Tilt-rotor pitch/flight handling qualities", American Helicopter Society Annual Forum 63, Virginia Beach, 2007
21. McRuer, D.T., et al., "AVIATION SAFETY AND PILOT CONTROL. Understanding and Preventing Unfavorable Pilot-Vehicle Interactions", ASEB National Research Council, National Academy Press, Washington D.C., 1997
22. Anon (2003). Manual of Criteria for the Qualification of Flight Simulators. ICAO Doc.9625, AN/938. International Civil Aviation Organization, Montreal, Canada.